

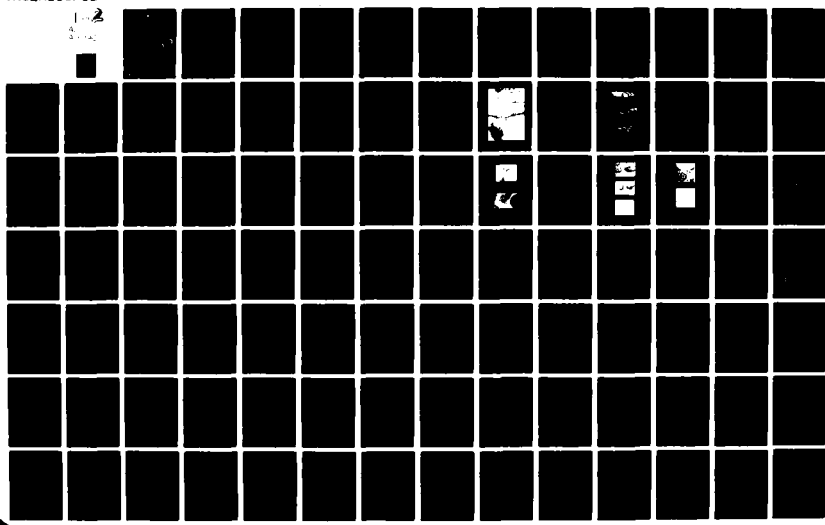
AD-A101 902

COASTAL ENGINEERING RESEARCH CENTER FORT BELVOIR VA  
HYDRAULICS AND STABILITY OF FIVE TEXAS INLETS. (U)  
JAN 81 C MASON  
CERC-MR-81-1

F/G 8/8

UNCLASSIFIED

NL



AD A101902

LEVEL

102

# Hydraulics and Stability of Five Texas Inlets

by

Curtis Mason

MISCELLANEOUS REPORT NO. 81-1

JANUARY 1981



Approved for public release;  
distribution unlimited

U.S. ARMY, CORPS OF ENGINEERS  
COASTAL ENGINEERING  
RESEARCH CENTER

Kingman Building  
Fort Belvoir, Va. 22060

81 7 23 040

DMC FILE COPY

1. The following is a list of the names of the members of the Board of Education of the City of New York, and the date of their election:

2. The following is a list of the names of the members of the Board of Education of the City of New York, and the date of their election:

3. The following is a list of the names of the members of the Board of Education of the City of New York, and the date of their election:

4. The following is a list of the names of the members of the Board of Education of the City of New York, and the date of their election:

5. The following is a list of the names of the members of the Board of Education of the City of New York, and the date of their election:

UNCLASSIFIED

SECURITY CLASSIFICATION OF THIS PAGE (When Data Entered)

(14)

CERC-MR-81-1

REPORT DOCUMENTATION PAGE		READ INSTRUCTIONS BEFORE COMPLETING FORM
1. REPORT NUMBER MR 81-1	2. GOVT ACCESSION NO. AD-A101902	3. RECIPIENT'S CATALOG NUMBER (9)
4. TITLE (and Subtitle) HYDRAULICS AND STABILITY OF FIVE TEXAS INLETS	5. TYPE OF REPORT & PERIOD COVERED Miscellaneous Report	
7. AUTHOR(s) Curtis Mason	6. PERFORMING ORG. REPORT NUMBER	
9. PERFORMING ORGANIZATION NAME AND ADDRESS Department of the Army Coastal Engineering Research Center (CERRE-FR) Kingman Building, Fort Belvoir, Virginia 22060	10. PROGRAM ELEMENT, PROJECT, TASK AREA & WORK UNIT NUMBERS F31232	
11. CONTROLLING OFFICE NAME AND ADDRESS Department of the Army Coastal Engineering Research Center Kingman Building, Fort Belvoir, Virginia 22060	12. REPORT DATE January 1981	
14. MONITORING AGENCY NAME & ADDRESS (if different from Controlling Office)	13. NUMBER OF PAGES 105	
16. DISTRIBUTION STATEMENT (of this Report)	15. SECURITY CLASS. (of this report) UNCLASSIFIED	
17. DISTRIBUTION STATEMENT (of the abstract entered in Block 20, if different from Report)		
18. SUPPLEMENTARY NOTES		
19. KEY WORDS (Continue on reverse side if necessary and identify by block number) Hydraulics Inlet-bay systems Inlet stability Texas Tidal inlets		
20. ABSTRACT (Continue on reverse side if necessary and identify by block number) Existing data on tides and currents of five Texas inlets (Freeport Harbor entrance, San Luis Pass, Galveston Bay entrance, Rollover Pass, and Sabine Pass) are analyzed to determine the hydraulics of the inlet-bay systems. The effects of the hydraulics and other factors on inlet stability are also examined. Variability in mean tidal ranges and water levels occurs on several time scales. Significant increases in both range and level will occur through 1986, when maximum values may cause inundation of areas which		
(continued)		

UNCLASSIFIED

SECURITY CLASSIFICATION OF THIS PAGE(When Data Entered)

have only recently subsided. Due to the small tidal prism of Freeport Harbor entrance, frequent dredging is required, with shoaling rates up to 1,450,000 cubic yards per year.

San Luis Pass is stable geographically, although it has been increasing slowly in size over the past hundred years. The volume of the ebb and flood tidal deltas has remained almost constant in recent years, and parts of these deltas would be good sources for beach-fill material. Such sources are also found at Galveston Bay entrance, where jetty construction produced extensive areas of accretion on the adjacent beaches. Historically, increasing cross-sectional area at Galveston resulted in corresponding increases in Galveston Bay tidal range, and ebb discharges during "northerns" contributed significantly to natural scouring of the channel.

Although small, Rollover Pass affected adjacent bay and beach characteristics in a pattern similar to that found at large inlets with manmade improvements. Complex patterns of flow occur within the Sabine Pass inlet-bay system, but strong ebb discharges during winter northerns undoubtedly enhance channel maintenance. Although bottom sediments at the pass are much finer than at other Texas inlets, changes in response to jetty construction closely parallel those at Galveston Bay entrance.

UNCLASSIFIED

SECURITY CLASSIFICATION OF THIS PAGE(When Data Entered)

## PREFACE

This report is published to provide coastal engineers with improved planning and design information on the hydraulic characteristics, stability, and effect on the longshore transport regime and adjacent beaches of the upper Texas coast inlet-bay systems. The work was in response to the needs of the U.S. Army Engineer District, Galveston, which is currently conducting the Galveston County Shoreline Erosion Study, and was carried out under the coastal processes program of the U.S. Army Coastal Engineering Research Center (CERC).

The report was prepared by Curtis Mason, Chief, Field Research Facility Group, under the general supervision of R.P. Savage, Chief, Research Division, CERC. The author appreciates the assistance of J.M. Hemsley for his extensive efforts in preparing the report for publication. The advice and encouragement of Dr. J.R. Weggel, Chief, Evaluation Branch, Engineering Development Division, CERC, are greatly appreciated.

Comments on this publication are invited.

Approved for publication in accordance with Public Law 166, 79th Congress, approved 31 July 1945, as supplemented by Public Law 172, 88th Congress, approved 7 November 1963.

  
TED E. BISHOP  
Colonel, Corps of Engineers  
Commander and Director

Accession For	
NTIS CRA&I	<input type="checkbox"/>
DTIC TAB	<input type="checkbox"/>
Unannounced	<input type="checkbox"/>
Justification	
By _____	
Distribution/	
Availability Codes	
Dist	Avail and/or Special
	

## CONTENTS

	Page
CONVERSION FACTORS, U.S. CUSTOMARY TO METRIC (SI).....	8
SYMBOLS AND DEFINITIONS.....	9
I INTRODUCTION.....	11
1. Objectives.....	11
2. Previous Reporting on Texas Coast Inlets.....	11
3. Summary of Factors Affecting Texas Coast Inlets.....	12
II TIDAL CHARACTERISTICS.....	13
1. Definitions of Tide Variations.....	13
2. Seasonal Variability in Tidal Range and Level.....	13
3. Annual Variability in Tidal Range and Level.....	15
III HYDRAULICS AND STABILITY OF SPECIFIC INLETS.....	15
1. Brazos River-Freeport Harbor Entrance.....	15
2. San Luis Pass.....	28
3. Galveston Bay Entrance.....	49
4. Rollover Pass.....	66
5. Sabine Pass.....	77
IV SUMMARY.....	90
1. Tide Characteristics.....	90
2. Freeport Entrance.....	91
3. San Luis Pass.....	92
4. Galveston Bay Entrance.....	92
5. Rollover Pass.....	93
6. Sabine Pass.....	93
LITERATURE CITED.....	95
APPENDIX MONTHLY TIDAL RANGE DISTRIBUTION, GALVESTON BAY, 1974.....	99
TABLES	
1 Amplification factors for long waves.....	27
2 San Luis Pass tidal ranges.....	41
3 Tidal lags in San Luis Pass system.....	41
4 San Luis Pass hydraulic characteristics.....	43
5 Mean tidal prisms in San Luis Pass, July and August 1969.....	44
6 Galveston Bay entrance hydraulic characteristics.....	65
7 Tidal ranges and tidal lags, Rollover Pass.....	70
8 Tidal lags, Rollover Pass.....	70
9 Summary of Rollover Pass hydraulic data.....	73
10 Tidal ranges, Sabine Pass, Texas.....	81
11 Tidal lags in Sabine Pass system, 23 July-5 August 1962.....	83
12 Discharges through Sabine Pass ranges, 18-23 July 1962.....	85

## CONTENTS

### TABLES--Continued

	Page
13 Tidal prisms through Sabine Pass, 18-23 July 1962.....	85
14 Tidal prisms at Sabine Lake and Port Arthur Canal entrances.....	89

### FIGURES

1 Longshore current and sediment transport rates, based on visual observations.....	11
2 Long-term monthly mean tidal range variability.....	13
3 Long-term monthly mean water level variability.....	14
4 Upper Texas coast monthly mean tide level variability, 1974.....	16
5 Upper Texas coast monthly mean tidal range variability, 1974.....	17
6 Historical variation in mean water level.....	17
7 Historical variation in mean diurnal tidal range.....	18
8 Variation of annual mean water level, Galveston Channel, Texas.....	18
9 Variation of annual mean tidal range, Galveston Channel, Texas.....	18
10 Freeport Harbor entrance, Texas.....	19
11 Freeport entrance charts .....	21
12 Depth changes, Freeport Harbor, Texas, 1966-75.....	22
13 Depth changes, Freeport Harbor, Texas, 1970-75.....	22
14 Positions of 12-, 20-, and 29-foot contours in 1966, 1970, and 1975, Freeport entrance, Texas.....	23
15 Nearshore changes, Freeport Harbor.....	24
16 Shoaling rates at Freeport entrance, Texas.....	29
17 Cumulative dredged volumes, Freeport, Texas, 1910-75.....	29
18 San Luis Pass, 1853.....	30
19 San Luis Pass, 1867.....	30
20 San Luis Pass, 1933.....	31
21 San Luis Pass historical variation in inlet width, area, and hydraulic radius.....	32
22 Minimum-width cross-sectional profiles, San Luis Pass, Texas.....	32
23 San Luis Pass, 1938.....	33
24 San Luis Pass, 1952.....	33
25 San Luis Pass, 1954.....	35
26 San Luis Pass, 1957.....	35
27 San Luis Pass, 1961.....	35
28 San Luis Pass, 1962.....	36

## CONTENTS

### FIGURES--Continued

	Page
29 San Luis Pass, 1965.....	36
30 San Luis Pass thalwegs.....	37
31 San Luis Pass depth changes, 1853-1933.....	38
32 San Luis Pass tide gage locations.....	39
33 Illustration of tide distortion into West Bay.....	42
34 San Luis Pass tides and discharge, 24 June 1976.....	43
35 Discharge and water level time histories, 20-23 July 1976.....	45
36 Discharge and water level time histories, 3-6 May 1965.....	45
37 Variation of dimensionless parameters with Keulegan's repletion coefficient, K.....	47
38 $V_{max}$ versus $A_c$ stability curves, San Luis Pass, Texas.....	48
39 Shoreline change rates, upper Texas coast.....	49
40 Galveston entrance minimum-width cross-sectional area profiles, 1851-1908.....	50
41 Galveston entrance minimum-width cross-sectional area profiles, 1908-75.....	50
42 Time history of minimum inlet width, area, and hydraulic radius, Galveston entrance, Texas.....	51
43 Galveston Island shorelines, 1851-89.....	51
44 Tide observations, Galveston Bay, 1852-1940.....	52
45 Galveston Island shorelines, 1889-1975.....	54
46 Galveston entrance bathymetric changes, 1867-88.....	54
47 Galveston entrance bathymetric changes, 1867-1908.....	55
48 Galveston entrance bathymetric changes, 1908-33.....	55
49 Galveston entrance bathymetric changes, 1933-65.....	56
50 Galveston entrance bathymetric changes, 1968-75.....	56
51 Bathymetry and nearshore changes, Galveston Harbor.....	58
52 Galveston entrance channel bathymetric changes, 1890 to 1940-41.....	60
53 Tide observations, Galveston Bay, 1940-78.....	61
54 Galveston Bay tidal range distribution, November 1936.....	62
55 Galveston Bay tidal range distribution, June 1937.....	62
56 Galveston Bay tidal range ratio distribution, average annual, 1974....	63
57 Galveston Bay monthly mean tidal range variability, 1974.....	63
58 Galveston Bay monthly mean water level variability, 1974.....	64

## CONTENTS

### FIGURES--Continued

	Page
59 Average maximum velocity versus minimum cross-sectional area, Galveston Bay entrance, Texas.....	65
60 Comparison of beach profile and aerial photo erosion rates.....	68
61 Tidal lags versus water level, 16 July-9 September 1974.....	71
62 Rollover Pass monthly mean tide level variability.....	71
63 Rollover Pass monthly mean tidal range variability.....	72
64 Tides and currents at Rollover Pass, 4 and 5 May 1965.....	72
65 Relationship between average velocity and head difference, Rollover Pass .....	74
66 Time history of cross-sectional area changes, Rollover Pass, 1957-74..	75
67 Depth changes, Rollover Pass, Texas, July 1968-winter 1971-72.....	75
68 Average maximum velocity versus cross-sectional area, Rollover Pass, Texas.....	76
69 Longshore and shore-normal components of monthly resultant wind, Sabine Pass (Port Arthur), Texas, 1973.....	77
70 Bathymetry, Sabine Pass.....	79
71 Nearshore changes, Sabine Pass.....	79
72 Sabine Pass fill and scour, 1966-74.....	80
73 Tide gage location, Sabine Pass, Texas.....	80
74 Sabine Lake monthly mean tidal range variability, 1973.....	82
75 Mean monthly highs, lows, and ranges, Port Arthur canal SWG GAGE, 1936.....	82
76 Sabine Lake monthly mean tide level variability, 1973.....	83
77 Tides and surface currents, Sabine Pass, Texas, 19-21 July 1962.....	84
78 Sabine Pass discharges, 10-12 September 1974.....	87
79 Sabine Pass stage, 10-12 September 1974.....	87
80 Sabine Pass discharges, 22-24 July 1975.....	88
81 Sabine Pass stage, 22-24 July 1975.....	88
82 $V_{max}$ versus $A_c$ stability curves, Sabine Pass, Texas.....	90

CONVERSION FACTORS, U.S. CUSTOMARY TO METRIC (SI) UNITS OF MEASUREMENT

U.S. customary units of measurement used in this report can be converted to metric (SI) units as follows:

Multiply	by	To obtain
inches	25.4	millimeters
	2.54	centimeters
square inches	6.452	square centimeters
cubic inches	16.39	cubic centimeters
feet	30.48	centimeters
	0.3048	meters
square feet	0.0929	square meters
cubic feet	0.0283	cubic meters
yards	0.9144	meters
square yards	0.836	square meters
cubic yards	0.7646	cubic meters
miles	1.6093	kilometers
square miles	259.0	hectares
knots	1.852	kilometers per hour
acres	0.4047	hectares
foot-pounds	1.3558	newton meters
millibars	$1.0197 \times 10^{-3}$	kilograms per square centimeter
ounces	28.35	grams
pounds	453.6	grams
	0.4536	kilograms
ton, long	1.0160	metric tons
ton, short	0.9072	metric tons
degrees (angle)	0.01745	radians
Fahrenheit degrees	5/9	Celsius degrees or Kelvins <sup>1</sup>

<sup>1</sup>To obtain Celsius (C) temperature readings from Fahrenheit (F) readings, use formula:  $C = (5/9) (F - 32)$ .

To obtain Kelvin (K) readings, use formula:  $K = (5/9) (F - 32) + 273.15$ .

#### SYMBOLS AND DEFINITIONS

$A_b$	bay area
$A_c$	inlet cross-sectional area
$A_{cb}$	area of Chocolate Bayou
$A_{ce}$	equilibrium cross-sectional area
$A_{c+b}$	area of Christmas and Bastrop Bays
$A_n$	difference between postdredging and subsequent predredging cross-channel profile
$A_{wb}$	area of West Bay (to Carancahua Reef only)
$a_o$	mean diurnal tidal amplitude
$D$	distance between stations
$d$	water depth
$f$	Darcy Weisbach friction coefficient
$g$	acceleration of gravity
$K$	Keulegan repletion coefficient
$k$	wave number
$L$	channel length
$L_e$	effective channel length
$n$	Manning's coefficient
$P$	tidal prism
$Q$	instantaneous tidal discharge
$R$	hydraulic radius at inlet minimum cross-sectional area
$R_g$	hydraulic radius of gorge
$R_s$	hydraulic radius of shallow section
$R_{wb}$	tidal range at Alligator Point in West Bay
$S_n$	shoaling rate
$T$	tidal period
$T_s$	time between surveys

SYMBOLS AND DEFINITIONS--Continued

$u_{\max}$	maximum wave orbital velocity
$\bar{V}$	average current speed
$\bar{V}_c$	average current speed at gorge centerline
$\bar{V}_g$	average current speed in gorge
$\bar{V}_{\max}$	maximum average current speed
$\bar{V}_s$	average current speed in shallow section
$\bar{V}_T$	average current speed through pass
$\bar{V}_{T\max}$	maximum average current speed through pass
$v^1$	dimensionless velocity coefficient
$W_n$	width over which deposition occurred at station n
$\Delta H$	head differential

## HYDRAULICS AND STABILITY OF FIVE TEXAS INLETS

by  
Curtis Mason

### I. INTRODUCTION

#### 1. Objectives.

The objectives of this study were to (a) define the hydraulic characteristics of the upper Texas coast inlet-bay systems (Fig. 1), (b) quantitatively analyze the observed and predicted stability of these inlets, and (c) assess their effect on the longshore transport regime and adjacent beaches. The results are intended to provide improved planning and design information for the Galveston County Shoreline Erosion Study being conducted by the U.S. Army Engineer District, Galveston.

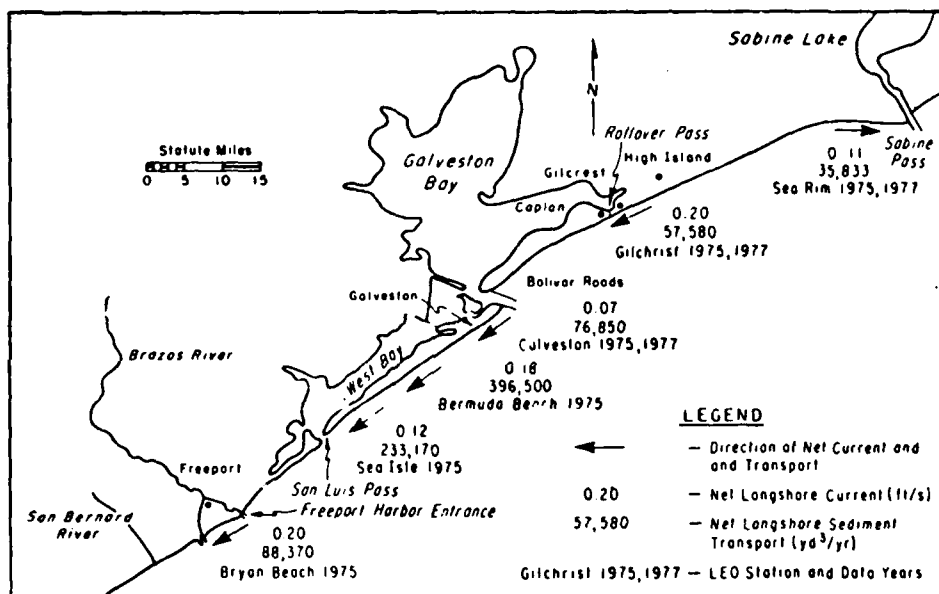


Figure 1. Longshore current and sediment transport rates, based on visual observations.

The report reviews previous reports, provides a general discussion of factors influencing the stability of Texas inlets, and analyzes the tidal characteristics of the gulf and major bays in the study area. Discussions on the hydraulics and stability of each specific inlet, beginning with the southwesternmost (Freeport Harbor entrance) and progressing sequentially to the easternmost (Sabine Pass), include a historical review, sediment volume changes, tidal characteristics, tidal hydraulics, and inlet stability.

#### 2. Previous Reporting on Texas Coast Inlets.

Most reporting on specific inlets along the upper Texas coast has been by the Corps of Engineers. However, several Texas universities have published results of field and in-house research on San Luis Pass (Herbich and Hales, 1970), Freeport Harbor entrance (Seelig and Sorensen, 1973), and Rollover Pass

(Prather and Sorensen, 1972); Morton (1977) summarized long-term changes occurring after jetty construction at Freeport Harbor and Galveston Bay entrances and Sabine Pass. Price (1947, 1951, 1963) also published extensively on inlet processes along the Texas coast. Hydraulic data have been documented primarily by the Corps of Engineers and the Texas Water Development Board (usually under contract), although the National Ocean Survey (NOS) and the U.S. Geological Survey (USGS) have extensive unpublished data.

### 3. Summary of Factors Affecting Texas Coast Inlets.

The significant environmental factors controlling the size, shape, and stability of a tidal inlet are the astronomical tide characteristics, the wave climate and related longshore sediment transport rates, bottom sediment type and size, and storm-induced water level changes, whether by wind effects or increases in freshwater flow into the bays.

a. Tides. The average diurnal gulf tidal range of about 2 feet produces maximum currents between 3 and 4 feet per second through most inlets on the Texas coast. Monthly and seasonal variations in tide level and range have been found to affect the stability of Corpus Christi Pass (Behrens, Watson, and Mason, 1977) and probably most other inlets as well. Deposition usually occurs during low mean tide levels in the winter and summer, and erosion during high levels in the fall and spring. There is also correlation between deposition and decreasing tidal ranges and erosion and increasing ranges.

b. Wave Climate. The wave climate along the Texas coast is generally mild with an annual average significant height of about 1.5 feet and a mean period of about 6 seconds at Galveston (Thompson, 1977). Estimates of 1974-77 longshore sediment transport rates, based on visual observations of wave height, period, and direction (Fig. 1), indicate net southwestward transport throughout the study area and agree with the direction of net longshore currents measured concurrently, as well as with historical conclusions on net transport direction.

c. Sediment Type and Size. Sand along the Texas coast is finer than on other U.S. coasts, ranging generally between 0.15 and 0.20 millimeter, and is the primary sediment found at San Luis, Galveston, and Rollover Pass. However, muds and silts predominate at Sabine entrance and, to some extent, at Freeport; large-scale depositional features are significantly different.

d. Storms. During the winter, strong frontal systems (northerns) significantly influence the stability of most Texas coast inlets. Before the arrival of the front, strong southerly winds usually produce larger than average waves. Upon arrival, north winds rapidly drive large volumes of water south or southwestward along the bays and out of the inlets, causing extensive channel scouring. Price (1951) noted that stable inlets are usually at the southwestern ends of the Texas bays and attributed this stable position to the norther-induced ebb flows described above. However, the net southwesterly longshore sediment transport could also contribute to this preferential location.

Hurricanes are perhaps the single most important factor controlling the Texas inlet and beach changes, but the lack of quantitative hydraulic data and prestorm and poststorm inlet and beach bathymetries prohibits a detailed assessment of their effect.

## II. TIDE CHARACTERISTICS

### 1. Definitions of Tide Variations.

Tides in the Gulf of Mexico control the daily exchange of water through the many Texas passes, enhancing the quality of the water in the bays and estuaries. The exchange also provides a means of transport for larval and adult animal populations, and transports sediment into and out of the passes, significantly affecting their stability. Knowledge of the variability in gulf tides is important to understand the variability in bay tides and the hydraulic characteristics of the Texas passes. This section presents the results of an analysis defining the short- and long-term variations in gulf tides, using data collected from the U.S. Army Engineer District, Galveston (SWG) and NOS (formerly U.S. Coast and Geodetic Survey) tide gages. The following definitions are used: (a) Diurnal tidal range, daily higher high water minus lower low water; (b) diurnal tide level, average of higher high water and lower low water; and (c) mean water level, average of hourly water levels over some time period.

In analyzing tide data collected simultaneously from the NOS and SWG gages at about the same location, it was found that mean water levels often differed significantly with respect to stated mean low water (MLW) datums. Whether this was caused by a difference in the MLW datums or by errors in the gage elevations is unknown. Regardless of the cause, quantitative level comparisons between the gages of the two agencies could not be made. Therefore, much of the level data are presented as the difference between selected values and a long-term mean computed from those values.

### 2. Seasonal Variability in Tidal Range and Level.

Behrens, Watson, and Mason (1977) found that seasonal variability in monthly mean diurnal tidal ranges and levels affects the stability of tidal inlets on the Texas coast. Therefore, data from the NOS gages at Freeport Harbor, Galveston Pleasure Pier, and Sabine Pass were used to examine seasonal fluctuations between 1955 and 1975. Figures 2 and 3 show the mean deviation

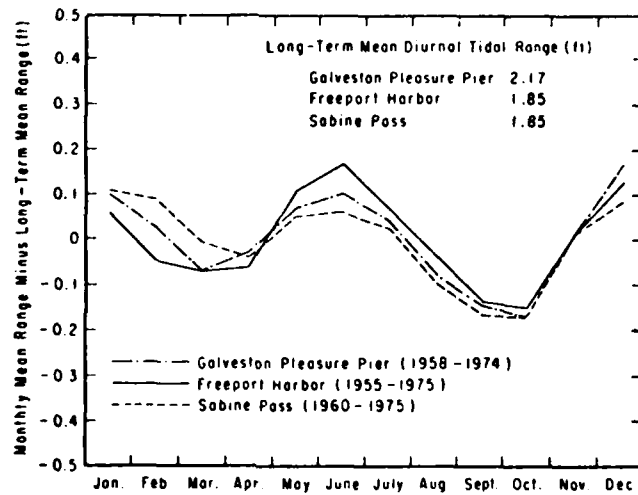


Figure 2. Long-term monthly mean tidal range variability.

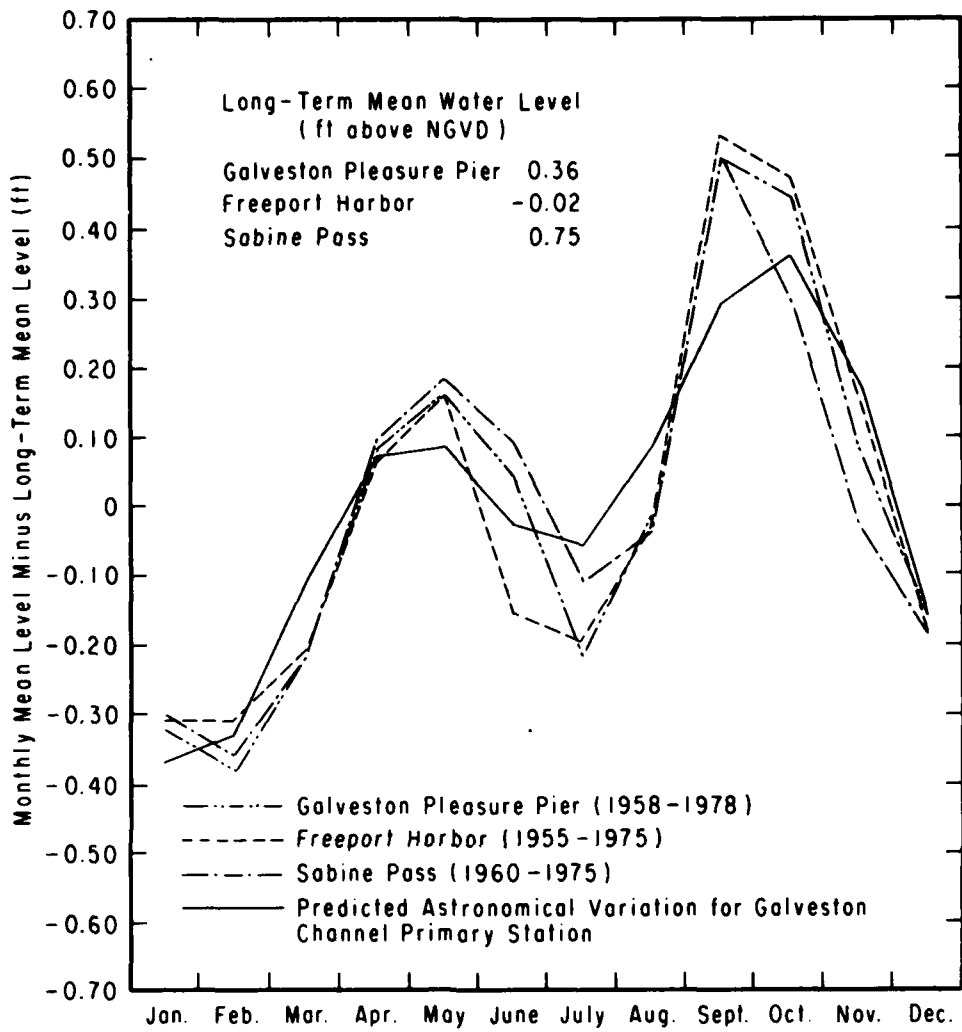


Figure 3. Long-term monthly mean water level variability.

of monthly mean values of the tidal range and the water level from the long-term average. Good agreement exists among the three stations, indicating relatively uniform long-term behavior of the gulf tides throughout the study area. Figure 3 also includes the mean levels at Galveston due solely to astronomical forces, which were predicted using a computer program developed at CERC (Dr. D.L. Harris, Oceanographer, personal communication, 1978).

Maximum monthly ranges occur at the summer and winter solstices (June and December) when the sun's gravitational vector is more nearly parallel to the Earth's in subtropical and higher latitudes (Fig. 2). Minimum ranges occur at the equinoxes (September and March) when the sun's gravitational vector is smallest. The tidal range fluctuations shown in Figure 2 include the effects of winds.

The seasonal cycle in tidal range is not in phase with a similar cycle in water level, which results primarily from astronomical forces, modified

somewhat by meteorological and steric effects. Maximum water levels occur in September when onshore winds combine with warmest (least dense) water. A secondary maximum associated with onshore winds and astronomical forces occurs in May. Minimum levels occur in February, when the water is coldest (most dense) and astronomical influences produce a near-minimum level, and in July.

Figure 4 illustrates the variability in diurnal tide level and range for a representative year (1974), using data from a number of NOS and SWG gages throughout the study area. Note the typical pattern of tide level variation at stations from Freeport to Sabine Pass, although deviations from the mean are much larger than the long-term data in Figure 3. Figure 5 shows greater scatter in the range variation, probably due to meteorological effects.

### 3. Annual Variability in Tidal Range and Level.

In analyzing the data, it became apparent that another type of variability, the difference between mean annual ranges and levels and their long-term means, could be important. Available data from 1955 to 1975 for three NOS gulf coast tide stations are plotted in Figures 6 and 7. The NOS Galveston channel gage records, which began in 1909, provide perspective to the trends shown at the three stations in Figures 6 and 7. Plots of the historical variation in level and range at this site are shown in Figures 8 and 9. Figures 6 and 8 illustrate a recent rapid increase in mean annual water levels at all stations; the average rate of rise was rather gradual between 1955 and 1970, then increased drastically between 1970 and 1975. The last time such a rapid increase occurred was in 1940. Most of the recent rise may be due to increased subsidence, since the pattern of relative water level rise, which had been similar for the three stations between 1960 and 1970, shows considerably different trends in the last 5 years of record (Fig. 6). Marmer (1951) analyzed long-term records from a number of gulf coast stations and found the average rate of rise was not constant throughout the gulf. He assumed this difference was due to localized subsidence. The importance of mean water elevation changes to beach and inlet stability cannot be neglected and is discussed later in this report.

The historical record of annual mean diurnal tidal range at Galveston (Fig. 9) clearly shows the 19-year-cycle characteristic of ocean tides. This results from interference of shorter period astronomical tide components; therefore, the pattern also holds for Freeport Harbor and Galveston Pleasure Pier, where the mean annual diurnal range varied as much as 0.34 foot between 1955 and 1975 (Fig. 7). The Sabine Pass range variation did not follow this pattern, perhaps due to the effects of freshwater flow on the midpass water levels. The predicted values shown in Figure 7 result from the computer program developed at CERC (Dr. D.L. Harris).

## III. HYDRAULICS AND STABILITY OF SPECIFIC INLETS

### 1. Brazos River-Freeport Harbor Entrance.

a. Historical Review. Freeport Harbor (the old Brazos River Estuary) is the southernmost entrance studied (Fig. 10). Before the existence of Freeport Harbor, the Brazos River was a major sediment contributor to this area of the Texas coast; the harbor is under consideration as a site for a deep-draft port. Construction activities in this area have been extensive and varied, and interesting effects of such activities on the littoral regime have developed.

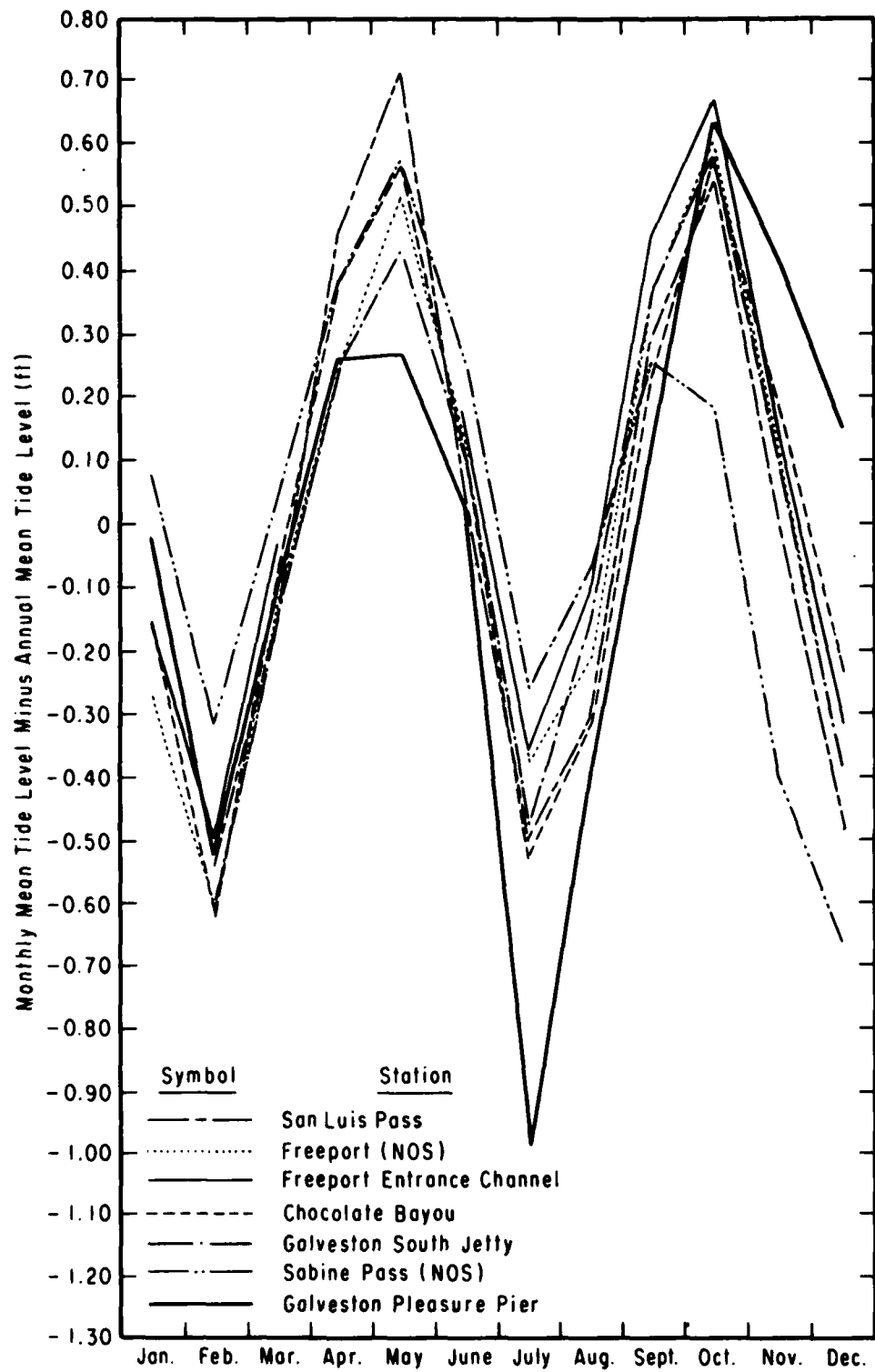


Figure 4. Upper Texas coast monthly mean tide level variability, 1974.

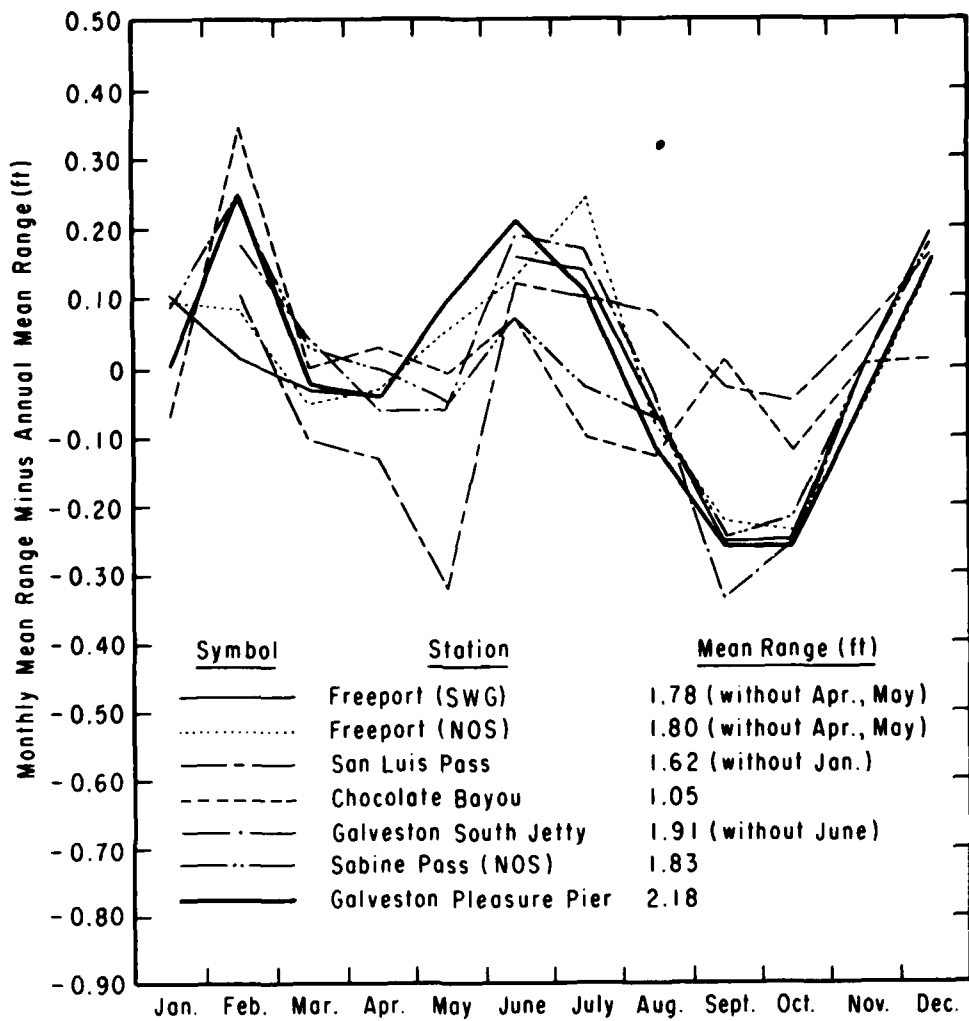


Figure 5. Upper Texas coast monthly mean tidal range variability, 1974.

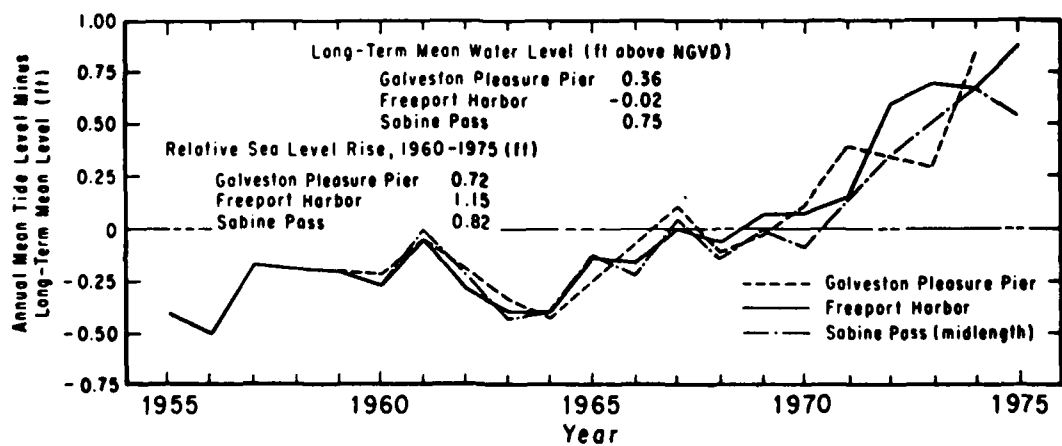


Figure 6. Historical variation in mean water level.

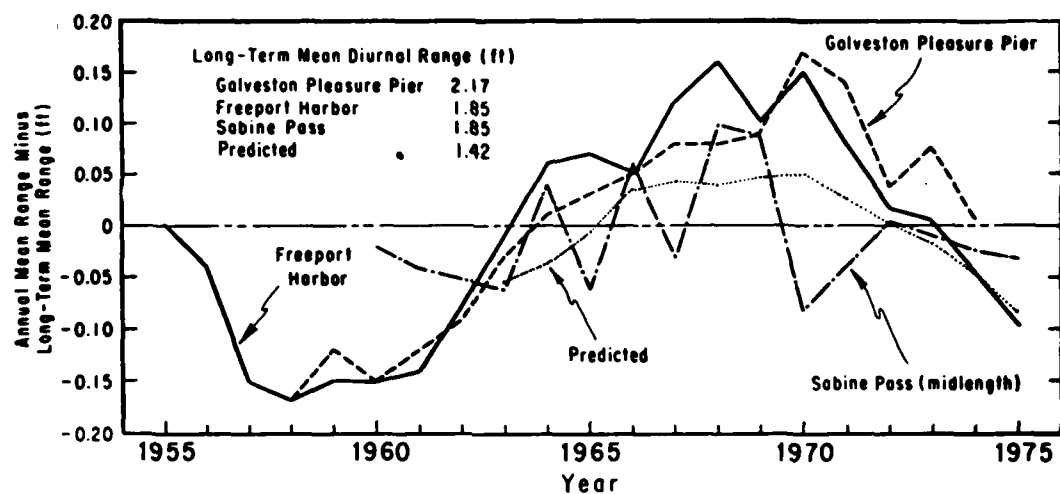


Figure 7. Historical variation in mean diurnal tidal range.

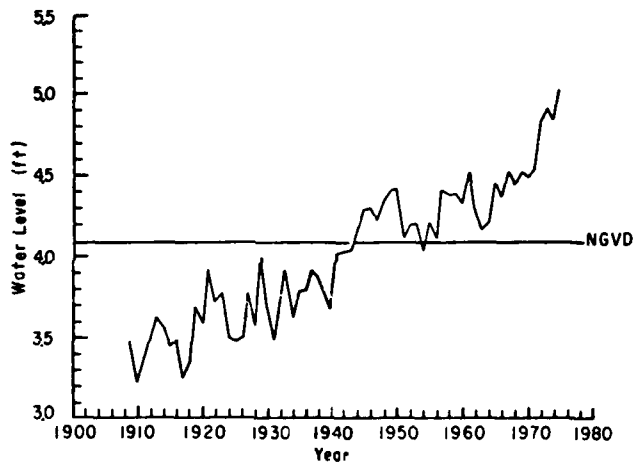


Figure 8. Variation of annual mean water level, Galveston Channel, Texas.

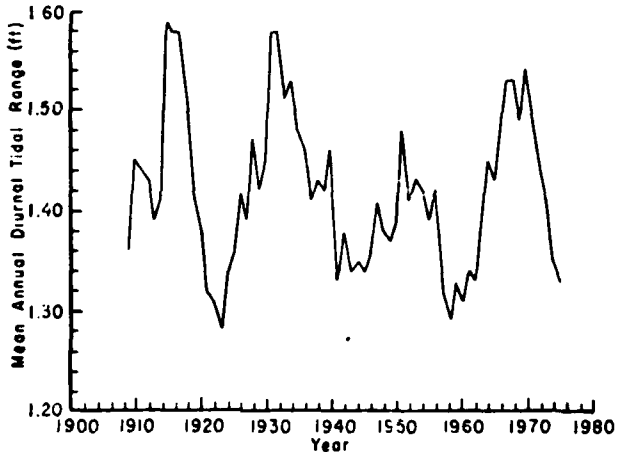


Figure 9. Variation of annual mean tidal range, Galveston Channel, Texas.

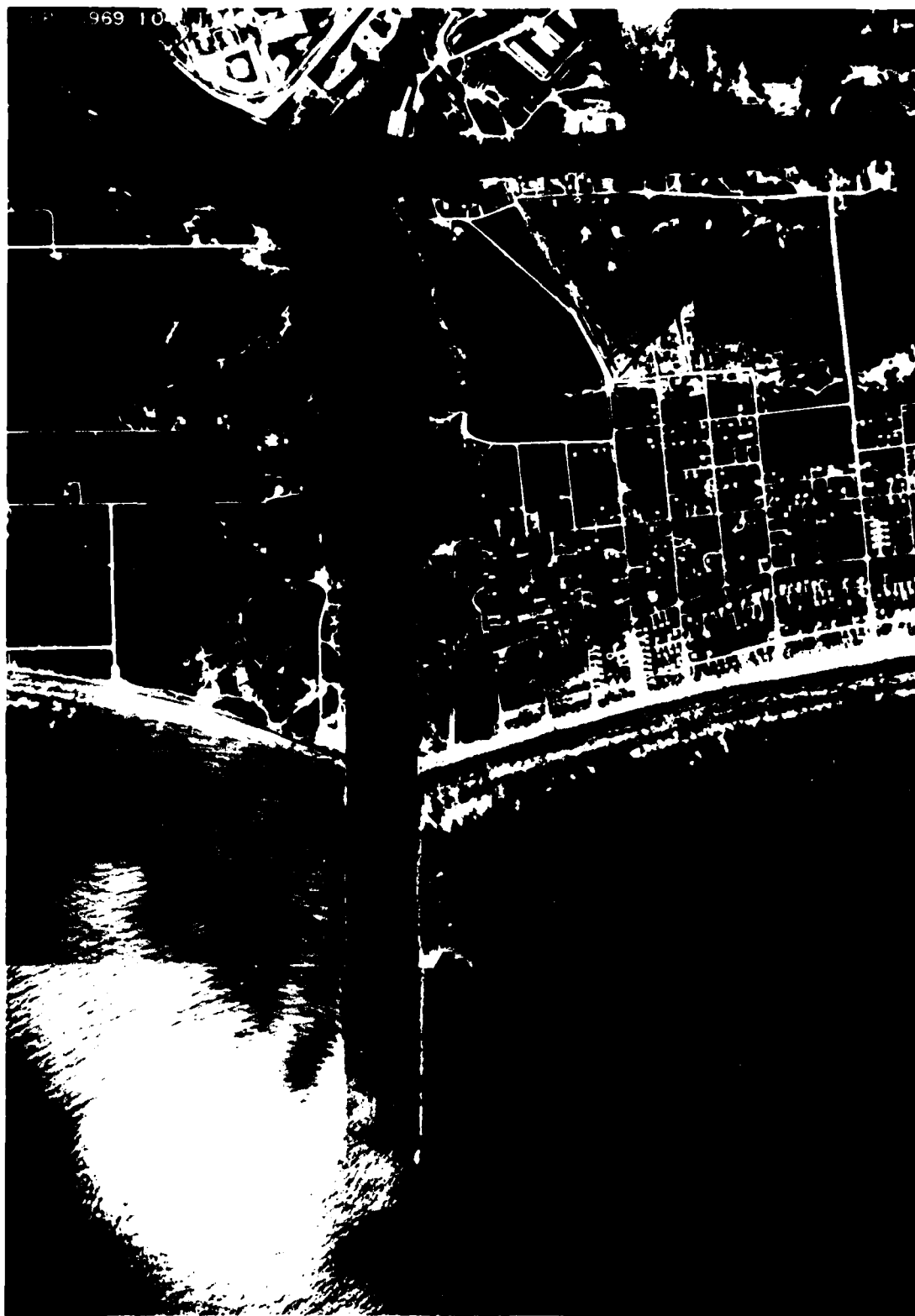


Figure 10. Freeport Harbor entrance, Texas.

Before 1881, the river mouth was natural, and ships visiting the ports of Quintana and Velasco, on either side of the river, probably had to contend with a shallow, frequently shifting channel through the ebb tidal delta. The earliest available charts of the Freeport area show that in 1852 the Brazos River mouth was flanked on the west side by a relatively small subaerial delta, but the subaqueous part of the delta extended some distance into the gulf and slightly eastward (Fig. 11,a). An initial attempt by the Federal government to stabilize the entrance with jetties in 1881 resulted in rapid accretion on the west side and lesser accretion adjacent to the east jetty (Fig. 11,b). Accumulation on the west side of this significant sediment source indicated net westward longshore sediment transport. The jetties were completed in 1899, and by 1909 extensive accretion (particularly on the west side) had occurred and a large ebb tidal delta existed (Fig. 11,c). The diversion of the Brazos River to a new location 6 miles west of Freeport in 1929 eliminated the source of material to the surf zone, and the beaches both downdrift (west) and updrift (east) of Freeport began eroding. At the new Brazos outlet, a delta rapidly formed, reaching its maximum seaward extent by 1948. Again, the maximum accumulation was on the downdrift (west) side. Some material in the new delta was probably derived from erosion of the large accumulation west of the Freeport entrance; most of this bulge had been obliterated by 1948.

Dam construction on the Brazos River in the 1940's greatly reduced the peak flows, drastically reducing the sediment supply at the mouth (Mathewson and Minter, 1976). This caused recession of the new Brazos River delta after 1948. Seelig and Sorensen (1973) estimated that only one-third of the pre-1940 sediment supply was available after 1950. The major change in the bathymetry offshore of Freeport entrance between 1946 and 1966 was a general deepening of the entire area (Seelig and Sorensen, 1973). To determine recent volumetric changes in the nearshore bathymetry adjacent to Freeport, SWG surveys from 1966, 1970, and 1975 were used to construct Figures 12 and 13. A planimeter was used to determine areas within selected contours, which were multiplied by the average depth change within that area to yield volumetric changes. Positions of the 12-, 20-, and 29-foot contours are plotted in Figure 14.

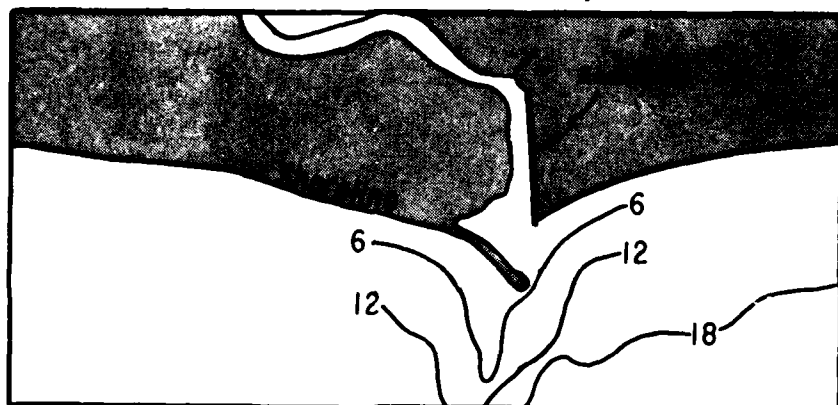
Within the survey limits on the east side of the entrance, a loss of  $3.3 \times 10^6$  cubic yards occurred between 1966 and 1975, mostly in a zone centered about 4,000 feet east of the jetties. Some material accumulated in a localized area between this erosion zone and the jetties, and about 4,000 feet offshore. These zones of deposition and erosion were formed primarily between 1970 and 1975. Within the scour zone, the 12- and 20-foot contours moved inshore. This erosion may have contributed to the current increased shoreline recession rates east of the jetties by allowing larger waves to reach the foreshore, particularly at the apex of the zone where recent MSL retreat rates have been about 33 feet per year. However, subsidence is also a possible contributing factor.

On the west side of the entrance, an accretion zone occurred between 1966 and 1975 in the same relative position with respect to the jetties as on the east side: 4,000 feet offshore and 4,000 feet west of the jetties. However, a net erosion of  $2.1 \times 10^6$  cubic yards occurred between 1966 and 1975. Along the offshore limits of the control area, extensive erosion occurred between 1966 and 1970, with some accretion immediately adjacent to the west jetty.

a. Chart 206 dated April 1858 (survey date 1852)



b. Chart 206 dated January 1881



c. Chart 206 dated March 1909

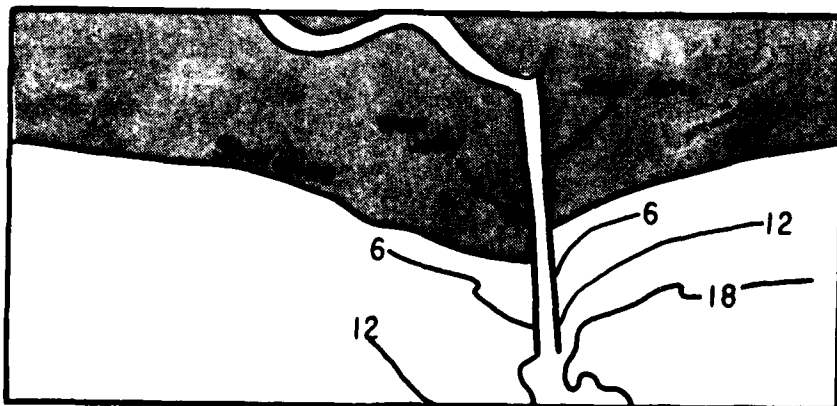


Figure 11. Freeport entrance charts with depth contours in feet below MLW (after Seelig and Sorensen, 1973)

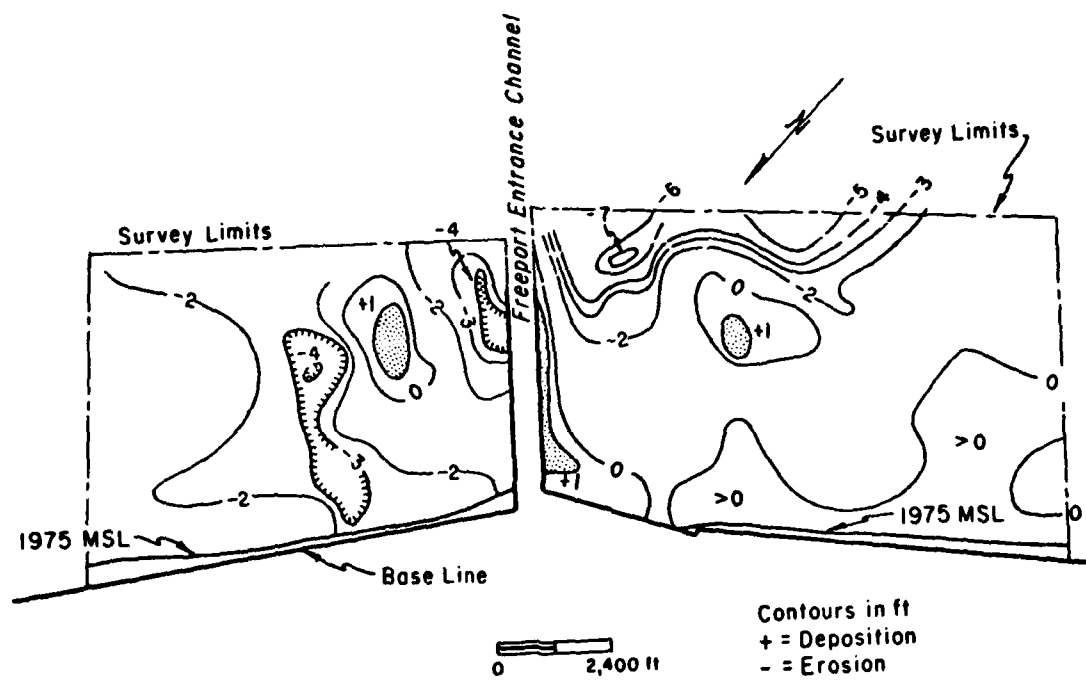


Figure 12. Depth changes, Freeport Harbor, Texas, 1966-75.

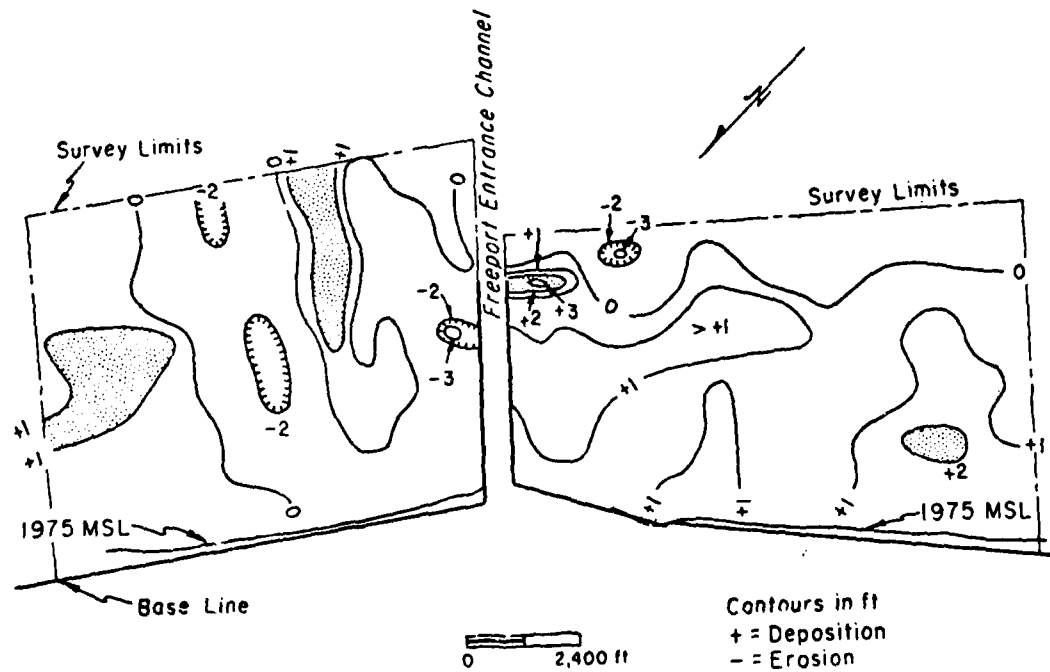


Figure 13. Depth changes, Freeport Harbor, Texas, 1970-75.

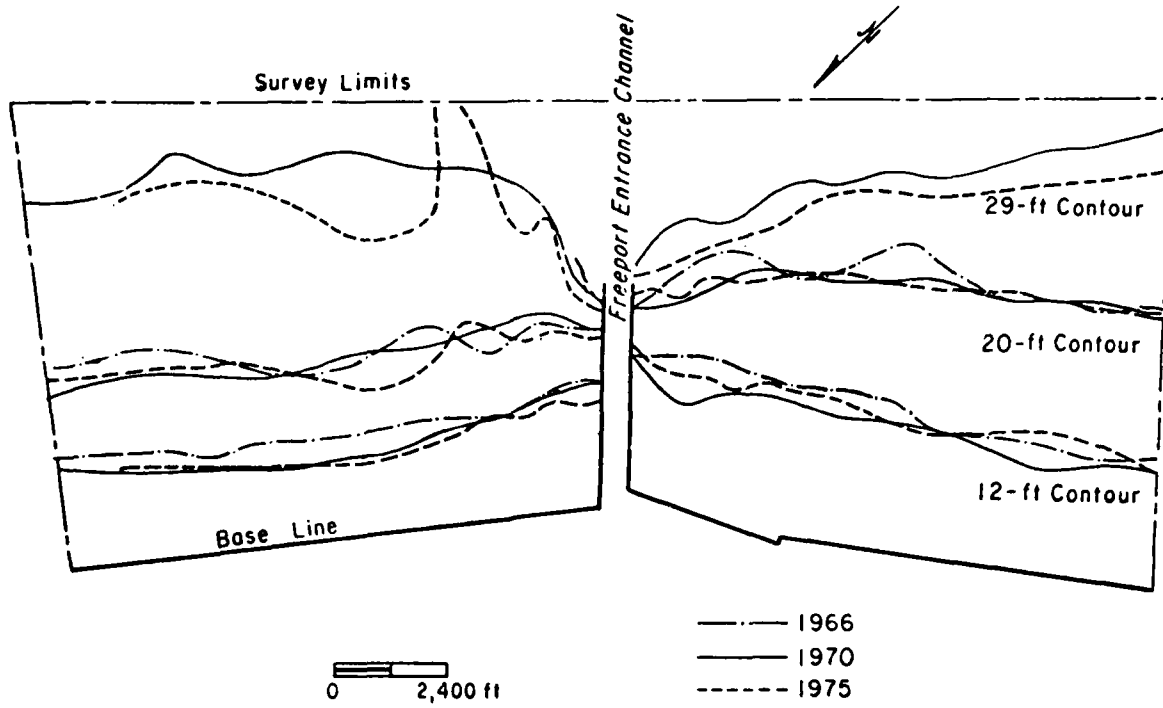


Figure 14. Positions of 12-, 20-, and 29-foot contours in 1966, 1970, and 1975, Freeport entrance, Texas.

The 29-foot contour moved landward near the dredged channel; away from the channel the contour moved offshore. The 20-foot contour, located in the offshore erosion zone, migrated landward in two locations between 1966 and 1970. However, the 12-foot contour, which moved inshore between 1966 and 1970, showed extensive offshore movement in later years, corresponding to the deposition zone shown in Figure 13.

This concurrent erosion in the area of the 20-foot water depth and the deposition near the 12-foot contour led to an examination of beach profiles taken between 1966 and 1975 within 6,000 feet west of the jetties. The profiles showed a zone of anomalously steep offshore slope between the 18- and 30-foot water depths which eroded rapidly during that period. It is speculated that this is the slipface of the old Brazos River delta which is eroding and supplying sediment to the shallower areas near the 12-foot contour. If this is the case, then rapid beach recession west of the jetty may occur in the future as the offshore zone reaches equilibrium. Morton (1977) documented erosion of the delta between 1937 and 1974 (Fig. 15). Over the long term (1855 to 1974), Morton showed net nearshore deposition with offshore and downdrift erosion.

b. Tide Characteristics. Two tide gages have been in continuous operation at Freeport (see Fig. 10): an NOS control station near the Dow barge canal since May 1954, and an SWG gage between the jetties since June 1965. The tide characteristics at these locations were determined by calculating the mean monthly diurnal tidal ranges and levels, and the annual means, for the representative year (1974). Unfortunately, some days in April and May were missing from the SWG gage, so these months were not included. The 1974 mean

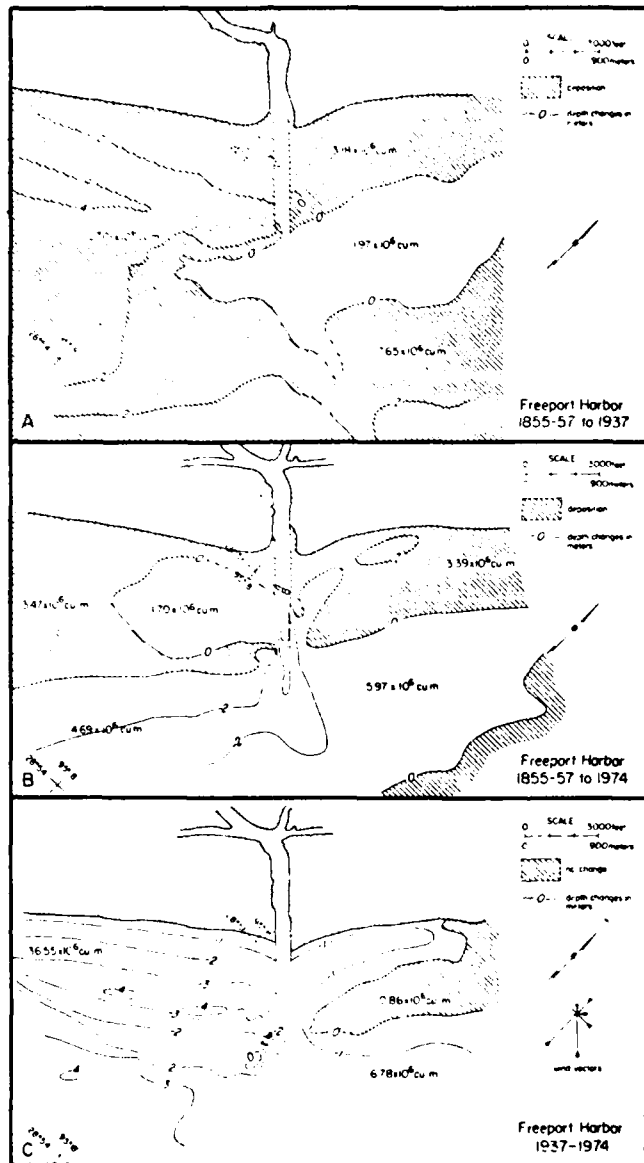


Figure 15. Nearshore changes, Freeport Harbor (after Morton, 1977).

ranges differed little between stations: 1.80 feet for the NOS gage and 1.78 feet for the SWG gage. However, the annual mean diurnal levels differed significantly--0.50 foot above the National Geodetic Vertical Datum (NGVD) of 1929 or 1.90 feet above MLW for the NOS gage, and 0.80 foot above SWG MSL datum or 2.36 feet above SWG MLW. This exemplifies the datum problem discussed previously. Figures 4 and 5 show almost identical monthly variations in level and range for the two gages.

c. Tidal Hydraulics. Unlike the other passes analyzed, the Freeport Harbor system has a very small tidal prism. No tidal current data were found; therefore, several theoretical approaches were taken to determine the hydraulic regime. Due to time and funding constraints, two-dimensional numerical models were not applied. The simplest method to compute inlet hydraulic characteristics is that of Keulegan (1967), but recent refinements by Seelig, Harris, and Herchenroder (1977), based on less restrictive assumptions, have been found to provide more accurate results in most cases.

(1) Keulegan Method. Keulegan (1967) defined the ability of an inlet to fill its bay in terms of a repletion coefficient,  $K$ , given by

$$K = \frac{TA_c}{\pi A_b} \sqrt{\frac{g}{2a_0 \left(1 + \frac{fL}{4R}\right)}} \quad (1)$$

where

$T$  = gulf diurnal tidal period (89,000 seconds)

$2a_0$  = mean diurnal gulf tidal range (2.17 feet) (20-year mean at Galveston Pleasure Pier)

$A_c$  = inlet cross-sectional area (square feet)

$A_b$  = bay area (square feet)

$R$  = hydraulic radius of inlet cross section (feet)

$f$  = Darcy Weisbach friction coefficient =  $116n / R^{1/3}$ ;  
where  $n$  is Manning's coefficient, and 0.025 is the average value from field data on many inlets

$L$  = channel length (feet)

$g$  = acceleration of gravity (32.2 feet per second squared)

From charts and other sources, the Freeport entrance parameters of  $A_c = 15,000$  square feet,  $A_b = 1.9 \times 10^7$  square feet,  $R = 30$  feet,  $L = 4,660$  feet, and  $f = 0.023$ :  $K = 22.4$ , indicating complete filling of the bay. However, if this were the case the tidal range in the harbor would be close to that at the Pleasure Pier. Instead, it is about 0.3 foot less, indicating either the open-coast range is less at Freeport or there is some minor loss through the entrance channel unaccounted for by the Keulegan method. Multiplying the long-term average harbor tidal range of 1.84 feet by the harbor area alone yields an average tidal prism of  $3.5 \times 10^7$  cubic feet. However, this is a minimum value, since the extent to which filling of the gulf Intracoastal

Waterway affects the hydraulics is unknown. The average current speed,  $\bar{V}$ , through the entrance is given by

$$\bar{V} = \frac{\text{tidal prism}}{\frac{T}{(2)} (A_c)} \quad (2)$$

For the values above, an average speed is 0.05 foot per second. If a sinusoidal variation is assumed, the maximum velocity is  $\pi/2(0.05)$ .

(2) Long Wave Method. Because some material has been deposited in the entrance channel, average speeds are probably higher than 0.05 foot per second. Therefore, the second approach is to consider speeds associated with propagation of the tidal wave through the entrance, rather than those produced hydraulically. From small-amplitude theory, the maximum horizontal orbital velocity,  $u_{\max}$ , of a shallow-water wave is given by

$$u_{\max} = a_o \sqrt{\frac{g}{d}} \quad (3)$$

where  $a_o$  is the amplitude of a wave whose period equals the tidal period,  $g$  is the acceleration of gravity, and  $d$  is the depth. For  $a_o = 0.9$  foot and  $d = 38$  feet:  $u_{\max} = 0.82$  foot per second, which is considerably greater than the hydraulic speed found using equation (2).

(3) Harbor Resonance Model. The effects of other long wave action in the harbor were considered by applying Ippen and Goda's (1963) harbor resonance model. Their model provides acceptable results over a large range of values of  $kd$  ( $k$  = wave number =  $2\pi/L$ ,  $L$  = wavelength,  $d$  = half of the harbor width) for relatively large values of the reflection coefficient (between 0.8 and 0.9). The theory is based on the following assumptions:

- (a) The harbor is excited by a regular wave train moving normal to the coastline.
- (b) All boundaries are perfectly reflecting.
- (c) The water depth is constant and equal, both inside and outside the harbor.
- (d) Small-amplitude wave theory is applicable.
- (e) The harbor entrance is small compared to the wavelength ( $kc/2 \leq 1$ ;  $c$  = width of the harbor entrance).

For tidal periods, no amplification of the tidal range was predicted. However, for waves of the periods shown in Table 1, significant amplification could occur. Unfortunately, the coarseness of the tidal data precluded performing a spectral analysis to determine if energy is present in the gulf at these periods.

Galveston District has proposed modifications to the harbor and entrance which roughly double the present channel width, jetty spacing, and cross-sectional area, and increase the authorized depth from 45 to 50 feet. Using

Table 1. Amplification of factors for long waves.

Incident wave period (min)	Amplification factor	
	Present geometry	Planned geometry
68.1	34	30
22.2	24	11
13.3	14	7
9.5	10	5

equation (3), it is predicted that  $u_{max}$  in the new channel reduces to about 0.7 foot per second. Ippen and Goda's program shows that amplification of any long waves will be reduced.

(4) External Effects. The hydraulics of Freeport are also influenced by a manmade factor, the Dow Chemical Company's withdrawal of water from the harbor and subsequent discharge into the Brazos River. Figures obtained from Dow (J.M. Kieslich, Galveston District, personal communication, 1977) show that the quantities of water range from about  $5.4 \times 10^9$  cubic feet per month (winter) to  $7.6 \times 10^9$  cubic feet per month (summer) or an average flow through the entrance of between 2,000 and 2,900 cubic feet per second. Thus, a landward average velocity of 0.14 to 0.10 foot per second would be superimposed on any tidal currents. These velocities will be greater if the instantaneous withdrawal rate is greater than the monthly average. This velocity component may seem small, but consider that sediment transport rate is an exponential function of velocity (assume third power). For  $u_{max} = 0.82$  foot per second (tidal only) and the maximum average artificial current, 0.19 foot per second,  $u_{max, flood} = 0.82 + 0.19 = 1.01$  feet per second and  $u_{max, ebb} = 0.82 - 0.19 = 0.63$  foot per second. The flood sediment transport capability would then be four times as great as the ebb, a factor which could be contributing to the entrance shoaling problems.

d. Stability of Freeport Entrance. Freeport Harbor entrance is atypical of other inlets in this study since currents are probably unable to transport sand size material or scour finer sediment. Therefore, the major problem at the entrance is extensive deposition of very fine silts and clays. To quantify the deposition rate of this material, dredging surveys from 1970 to 1973 were analyzed, and these rates were computed using equation (4):

$$S_n = \frac{A_n + A_{n+1}}{2} \frac{(D_{n+1} - D_n)}{\left(\frac{W_n + W_{n+1}}{2}\right) T_s} \quad (4)$$

where

$S_n$  = shoaling rate (cubic yards per month per foot) width between stations n and n+1

$A_n$  = difference between postdredging and subsequent predredging cross-channel profile (square yards) at station n

$D_{n+1} - D_n$  = distance between stations n and n+1

$W_n$  = width over which deposition occurred at station n (feet)

$T_s$  = time between surveys (months)

Values of  $S_n$  for stations 0 (the jetty heads) to -100 (the gulfward limit of dredging at the 40-foot contour 10,000 feet seaward of jetty ends) are plotted in Figure 16. Note that the area of greatest deposition in the offshore section of channel is usually 3,000 to 4,000 feet gulfward of the jetty ends, while between the jetties a slight maximum occurs 1,000 feet inside the ends. The offshore maximum may reflect material moved either from the offshore bottom or from the adjacent (5,000 feet downcoast) disposal area by wind-driven currents. Alternatively, it may be very fine material from the longshore transport regime which has been deflected gulfward by the jetties.

Channel dredging rates have generally increased over the years (Fig. 17). Between 1940 and 1957 the annual rate was about 940,000 cubic yards per year; between 1957 and 1968 about 800,000 cubic yards per year; and between 1968 and 1975 about 1,450,000 cubic yards per year. This may be attributed to increasing depths in the navigation channel (1932 to 1961, 32 feet; 1961 to present, 38 feet), but realinement of the offshore bottom adjacent to the channel may also have increased maintenance requirements.

e. Summary. Since Freeport entrance has no self-scouring capability, conventional stability analyses discussed later cannot be applied. However, due to the lack of significant water exchange between Freeport Harbor and the Gulf of Mexico, the dredged navigation channel serves as an excellent trap for deposition of fine-grained sediment. Three possible sources of this material are (1) dredged-spoil disposal too close to the channel with subsequent movement into the channel; (2) seaward deflection of the longshore currents which, when flowing over the channel, lose much of their transportive power and allow fine sediment deposition; and (3) adjustment of the offshore bottom to the artificially steep channel shape.

Two approaches can be used to possibly reduce deposition in the entrance and harbor. First, surveys indicate that hopper-dredged material, currently disposed of within 5,000 feet of the channel, is not accumulating in the disposal area. Therefore, the material *may be* returning to the navigation channel. A tracer test could be used to determine whether moving the disposal sites farther away from the entrance will reduce maintenance dredging requirements in both the offshore and jetty channels. Second, reducing the intake of Dow Chemical Company's waterflow could produce beneficial results. However, more data on inlet flow velocities and salinities should be collected before such a procedure is considered.

## 2. San Luis Pass.

a. Historical Review. San Luis Pass, which connects the Gulf of Mexico with Christmas, Bastrop, and West Bays (Fig. 1), is located at the southwest end of West Bay. Price (1951) characterized the southwest end as an equilibrium position for many Texas inlets.

The first U.S. Coast and Geodetic Survey (USC&GS) chart survey of San Luis Pass was made in 1853 (chart H389, Fig. 18), although the pass had been in existence since at least 1834 (Lee, 1966). Additional USC&GS surveys were made in 1867 (chart H931, Fig. 19) and 1933 (chart H5488, Fig. 20). There is

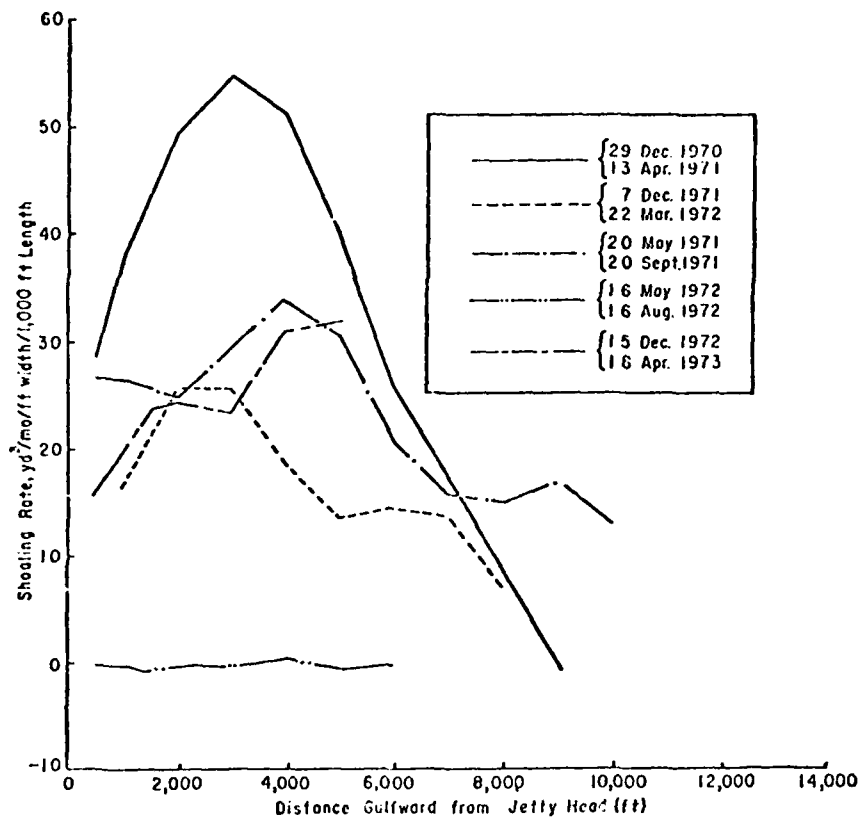


Figure 16. Shoaling rates at Freeport entrance, Texas.

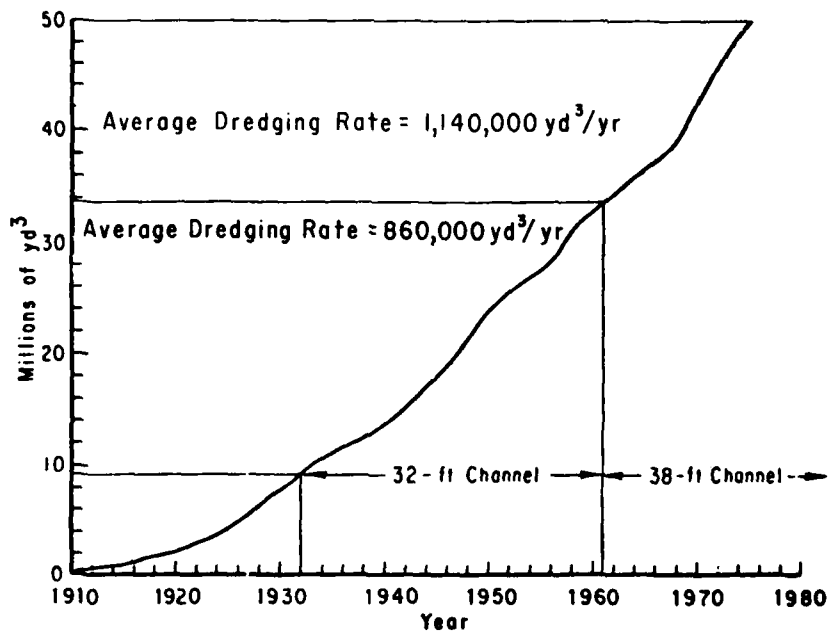


Figure 17. Cumulative dredged volumes, Freeport, Texas, 1910-75.

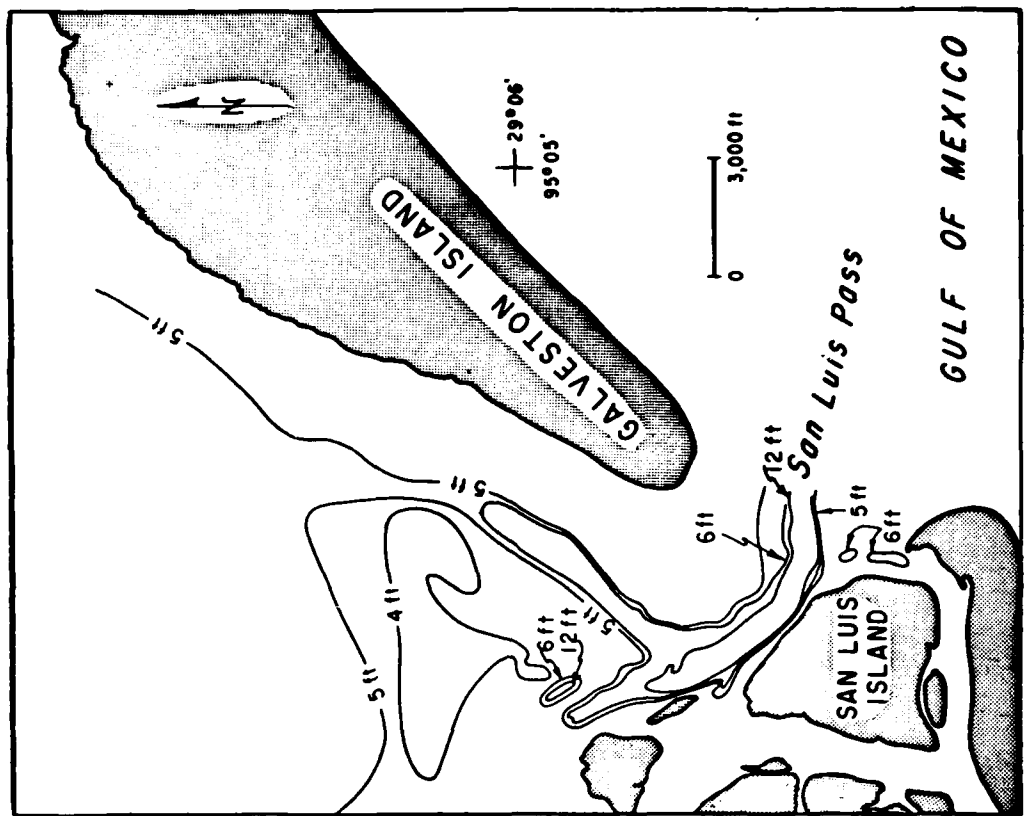


Figure 19. San Luis Pass, 1867  
(after USCGS chart H931).

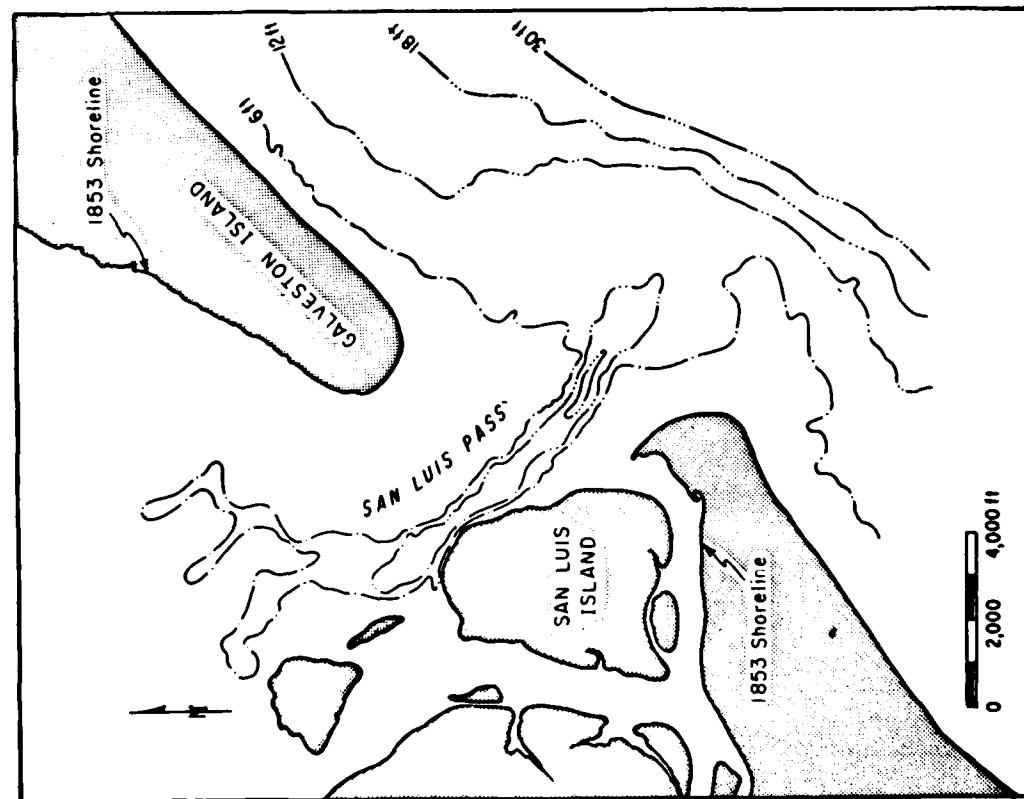


Figure 18. San Luis Pass, 1853  
(after USCGS chart H389).

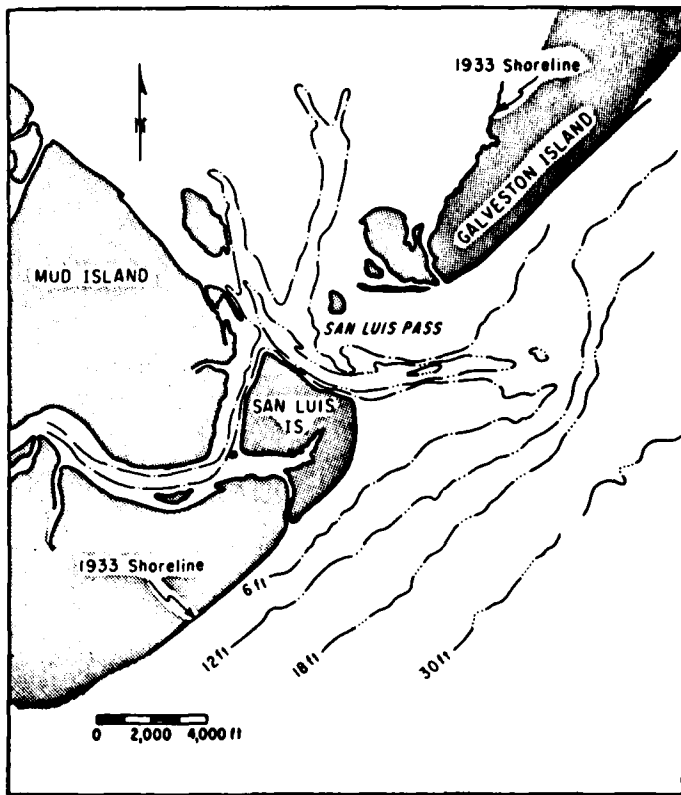


Figure 20. San Luis Pass, 1933 (after USC&GS chart H5488).

some discrepancy between the longitudes on the first two surveys and the 1933 survey. If permanent interior reference points are used, the longitude lines of the early surveys are 1,460 feet (more than  $0.4^\circ$ ) west of their counterparts on the 1933 survey. The 1867 survey is also questionable in other respects; the survey shows that the west end of Galveston Island had extended westward more than 2,000 feet in only 14 years. These surveys and numerous aerial photos were used to determine the historical variation in inlet cross-sectional area, minimum width, and hydraulic radius (Fig. 21). Widths obtained from the photos are approximately from mean high water (MHW) to MHW and are accurate to at least 10 percent. Cross-sectional profiles of the minimum-width cross section are shown in Figure 22.

The deepest part of San Luis Pass has historically been the southwest side of the inlet, very close to San Luis and Follett's Islands. Through at least 1867, San Luis Island and Follett's Island were separated by a wide and relatively deep channel known as Cold Pass which, with another channel on the north side of San Luis Island, supplied gulf water to Christmas Bay and adjacent areas. By 1933 (Fig. 20), Follett's Island extended across Cold Pass and connected with San Luis Island. By 1938 (Fig. 23), a wide platform with a high berm along the outer edge had developed gulfward of San Luis Island. Between 1938 and 1952 (Fig. 24) the width drastically decreased due to westward growth of Galveston Island. Unfortunately, no photos were available which revealed the possible causes of this event. Major hurricanes in the early 1940's and weather patterns associated with a drought in the late 1940's and early 1950's may have contributed.

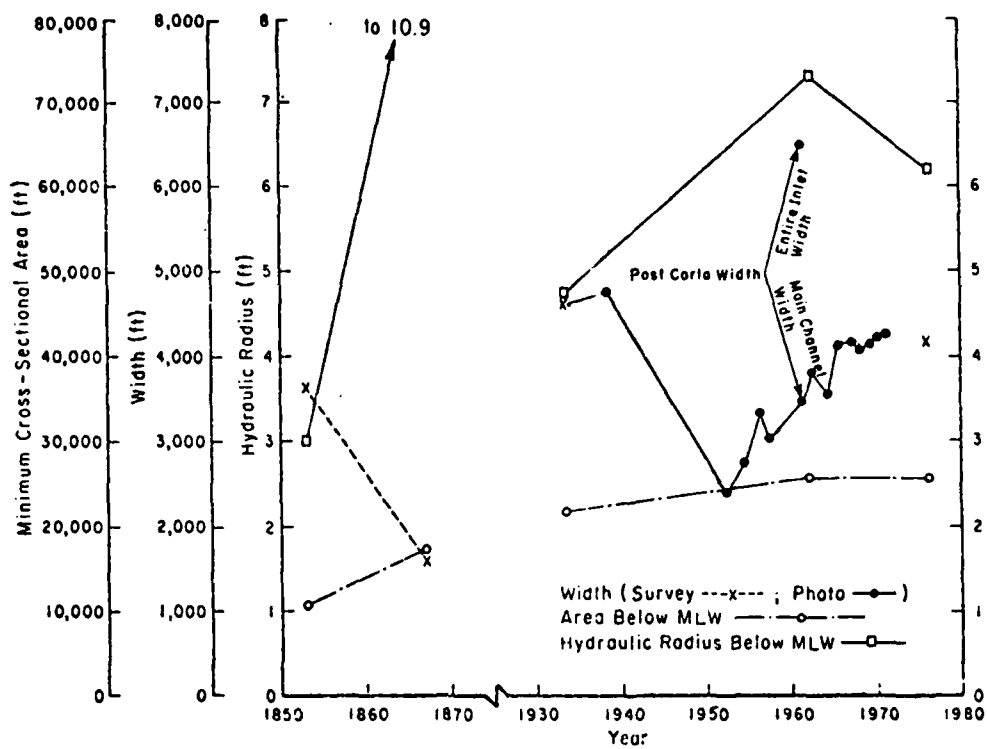


Figure 21. San Luis Pass historical variation in inlet width, area, and hydraulic radius.

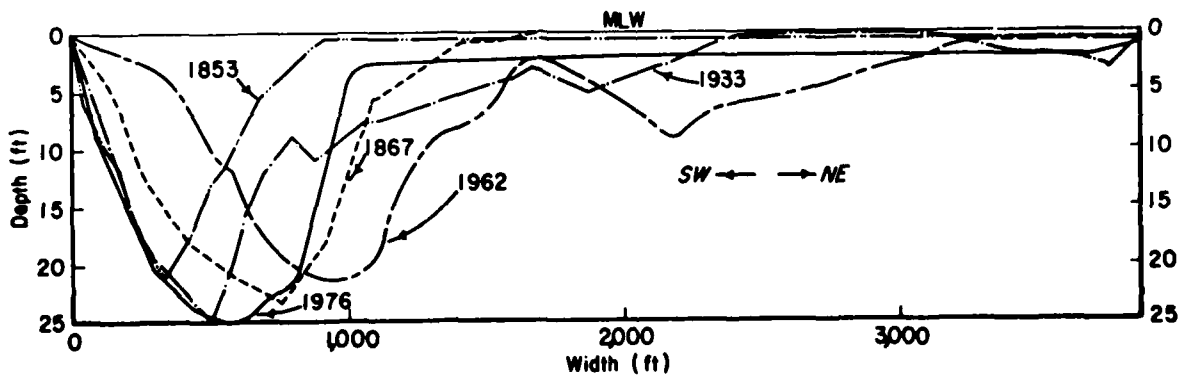


Figure 22. Minimum-width cross-sectional profiles, San Luis Pass, Texas.



Figure 23. San Luis Pass, 1938.



Figure 24. San Luis Pass, 1952.

A period of inlet widening began between 1952 and 1954. Figure 25 shows parts of the ebb tidal delta. Continued widening between 1954 and 1956 coincided with slight accretion on the southwest shoulder and minor rotation of the shoal adjacent to it. Figures 26 and 27 provide a comparison of the entire extent of the ebb tidal delta in 1957 and the posthurricane condition in 1961. During this 4-year period, the end of Cold Pass was overtapped and a large hurricane washover, with a similar breach on the east side, developed. A large bulge formed on the southwest shoulder; gulfward of the bulge the ebb tidal delta had moved about 1,700 feet southwest. These major changes were undoubtedly due to hurricanes. A hurricane in 1959 passed directly over the pass, and in 1961 Carla struck the coast at Pass Cavallo, producing unusually large waves and strong currents at San Luis Pass. Unfortunately, no photos were available between 1957 and 1961 to indicate the extent of these changes.

The 1962 photo (Fig. 28) shows continued change in the location and shape of the ebb tidal delta, but the southwest beach remained relatively constant. The first available cross section since 1933 showed an increase of about 4,000 square feet in the minimum area, with a shallower thalweg located about 500 feet east and a deeper east side (Fig. 22). Between 1962 and 1965 (Fig. 29) the southwest shoreline bulge remained exactly in line with the end of the ebb tidal delta, but both had moved away from the pass, and the inlet width had increased to more than 4,000 feet. On the northeast side, a thin spit connecting Galveston Island with the higher remnants of the island was exposed in 1962 (Fig. 23). Since 1965, the inlet width has remained almost constant at slightly more than 4,000 feet; the cross-sectional area apparently remained constant between 1962 and 1976. Beaches within 5,000 feet southwest of the pass have accreted, while those within 10,000 feet northeast have eroded, accentuating the downdrift offset typical of many Texas inlets.

b. Sediment Volume Changes.

(1) Ebb Tidal Delta. The 1853 and 1933 surveys provided enough data to quantitatively define the ebb tidal delta, and three methods were used to calculate sediment volume changes. The first method was that of Dean and Walton (1973), where the ebb tidal delta was delineated by the points at which shore-parallel bottom contours are first distorted by the influence of the inlet. These contours were then drawn shore-parallel across the inlet location to their counterparts on the opposite side. Grids were superimposed on these contours and the actual survey, and differences between the artificial and actual depths at each grid point were calculated. An average depth difference from the four corners of each grid square was calculated, and this difference was multiplied by the grid square area to arrive at a volume. The volumes were then summed over the entire ebb tidal delta to yield the total volume of sediment in the delta. Each side of the squares used in this analysis was 625 feet long.

The ebb tidal delta volume in 1853 was 4,815,000 cubic yards over an area of  $8.67 \times 10^7$  square feet. By 1933 the volume had increased to 6,070,000 cubic yards over an area of  $7.3 \times 10^7$  square feet. Between 1853 and 1933 relative sea level rose 1.4 feet or 0.0175 foot per year (Hicks, 1972), which over an area of  $7.3 \times 10^7$  square feet amounts to a volumetric increase of 3,790,000 cubic yards. Therefore, the total volume change on the ebb tidal delta between 1853 and 1933 was 5,050,000 cubic yards, with an annual accretion rate of 63,000 cubic yards per year. An area decrease of  $1.37 \times 10^7$  square feet off the tip of Follett's Island also occurred during this period.



Figure 25. San Luis Pass, 1954.



Figure 26. San Luis Pass, 1957.

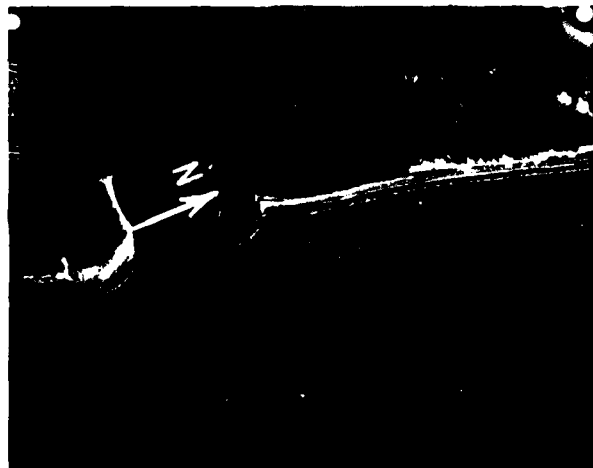


Figure 27. San Luis Pass, 1961.



Figure 28. San Luis Pass, 1962.

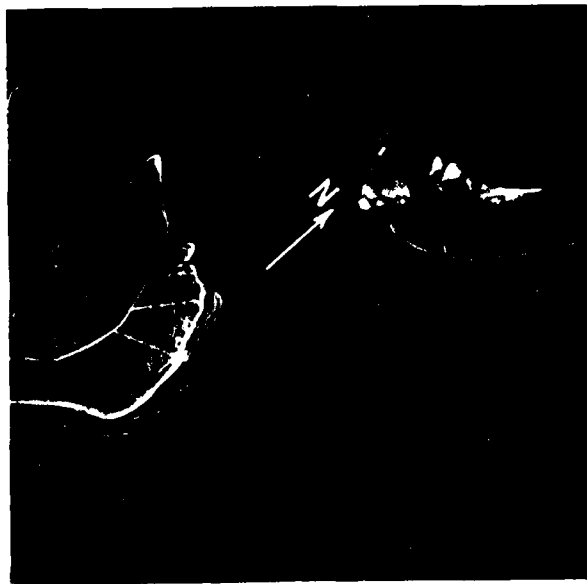


Figure 29. San Luis Pass, 1965.

In 1853, the thalweg extended south-southeast from the pass and was flanked by a large shoal to the west. By 1933, the thalweg had shifted such that the gulf end was aligned almost due east, and the shoal had been driven north and east, thus reducing the total area of the ebb tidal delta. Future shifts in the thalweg locations (Fig. 30) were obtained from aerial photos. Compared to most other inlets, the location of the San Luis Pass thalweg has remained quite stable.

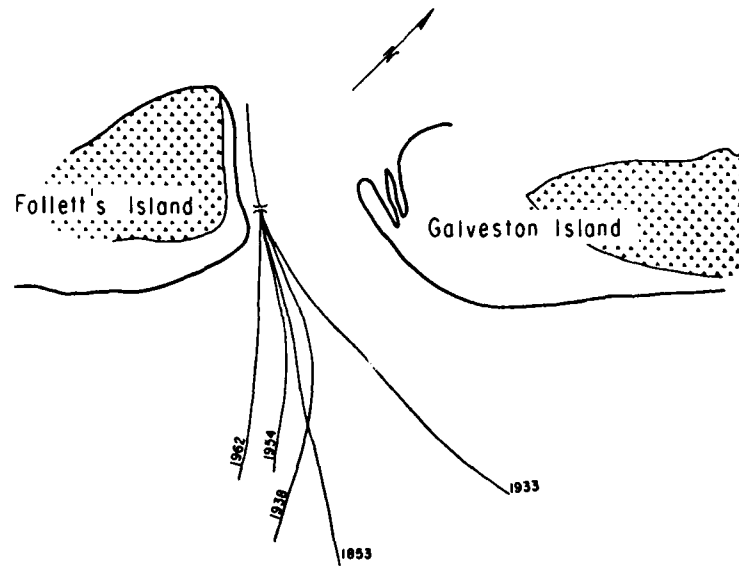


Figure 30. San Luis Pass thalwegs.

(2) Flood Tidal Delta. The boat sheets and aerial photos examined provided little quantitative data for the flood tidal delta. Only about 60 percent of the area surveyed in 1933 had been surveyed in 1853 and 1867, and then widely spaced survey lines were used. Therefore, the accuracy of the second method is not as great as the method used for the ebb tidal delta. An 833-foot grid square was superimposed on each boat sheet and the depths at each grid point were noted. The difference between the 1853 and 1933 depths at each grid point was averaged for each square. This difference was then multiplied by the grid square area to yield the volume difference. The volume difference for the flood tidal delta area (about  $8.7 \times 10^7$  square feet) was 178,000 cubic yards. However, accounting for the relative sea level rise of 1.4 feet, the total volume deposited was 4,690,000 cubic yards with an annual accretion rate of 59,000 cubic yards per year, which is about the same as the ebb tidal delta rate of 63,000 cubic yards per year. Since the sum of these rates (122,000 cubic yards per year) differed from other computed estimates, a more accurate method was then applied to both the ebb and flood tidal deltas.

(3) Ebb and Flood Tidal Deltas. The third method consisted of again using 625-foot grid squares, but this time applied over the entire area of the 1853 survey ( $2.3 \times 10^8$  square feet). At each grid point, the 1853 and 1933 depths were recorded and the 1933 value subtracted from the 1853 value. The results of the differences were then contoured (Fig. 31). To obtain the volume change, the areas within each contour line were measured, using a planimeter, and then multiplied by the average depth change within the area. These volumes were then summed, arriving at values of 2,540,000 cubic yards of deposition on the flood tidal delta and 11 million cubic yards of erosion on the ebb tidal delta. If the 1.4-foot sea level rise is multiplied by the ebb and flood delta areas, and the products added to these values, deposition was 7,700,000 cubic yards on the flood tidal delta and erosion was 4,330,000 cubic yards from the ebb tidal delta, for a net deposition of 3,370,000 cubic yards at an average annual deposition rate of 42,000 cubic yards per year. This third method was also used by Morton (1977) to estimate volume changes at other Texas inlets.

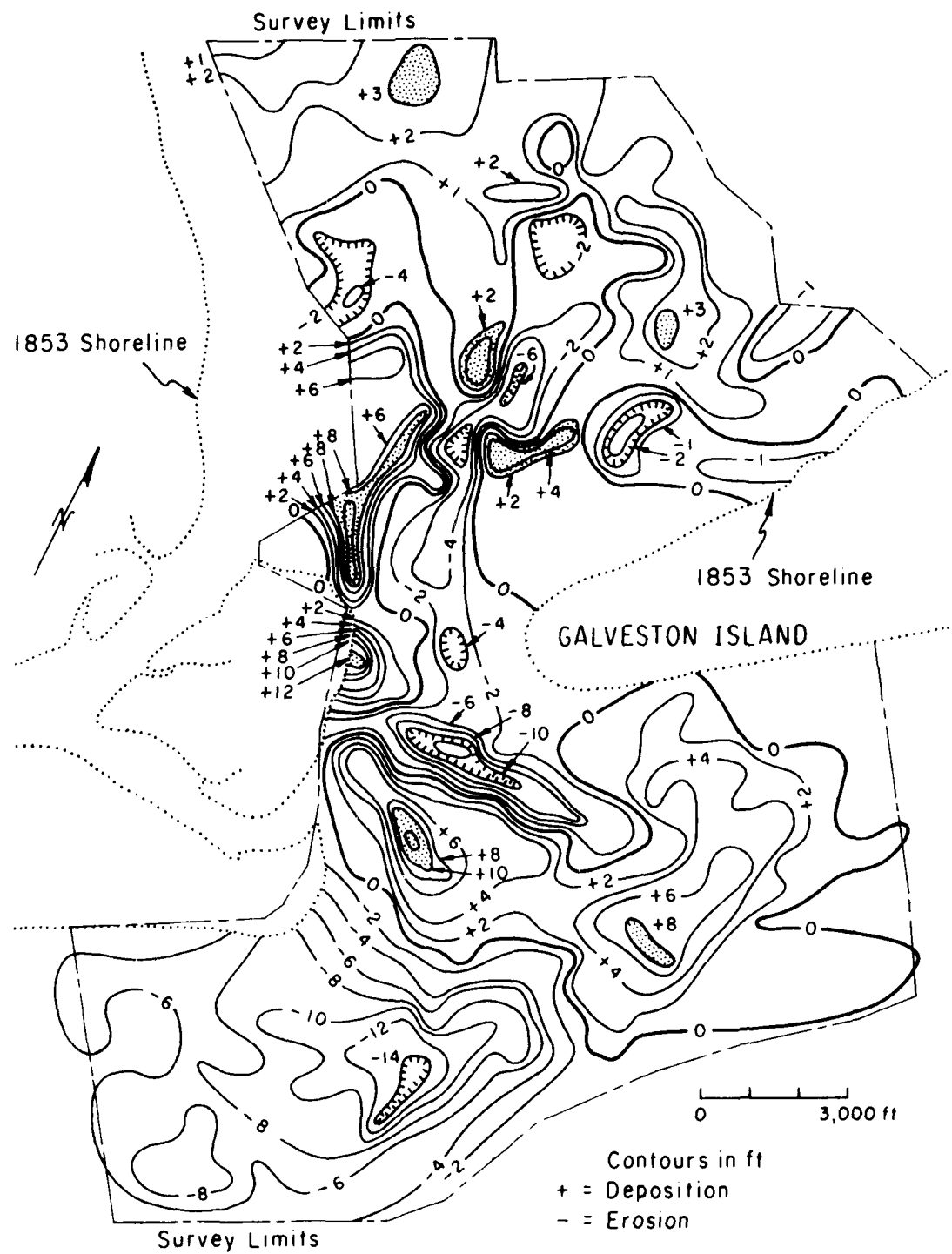


Figure 31. San Luis Pass depth changes, 1853-1933.

c. Tide Characteristics.

(1) Summary of Hydraulic Data Collection. Extensive tide and current data for the San Luis Pass system (Christmas Bay, Bastrop Bay, and West Bay) were available to analyze the hydraulics of the system. The first tide measurements were made by NOS in connection with the 1933 bathymetric survey and were obtained just inside the inlet at the site shown in Figure 32. Between October 1936 and October 1937, SWG conducted an extensive tide gaging program throughout Galveston Bay, and records for the months November 1936 and June 1937 were published (U.S. Army Engineer District, Galveston, 1942).

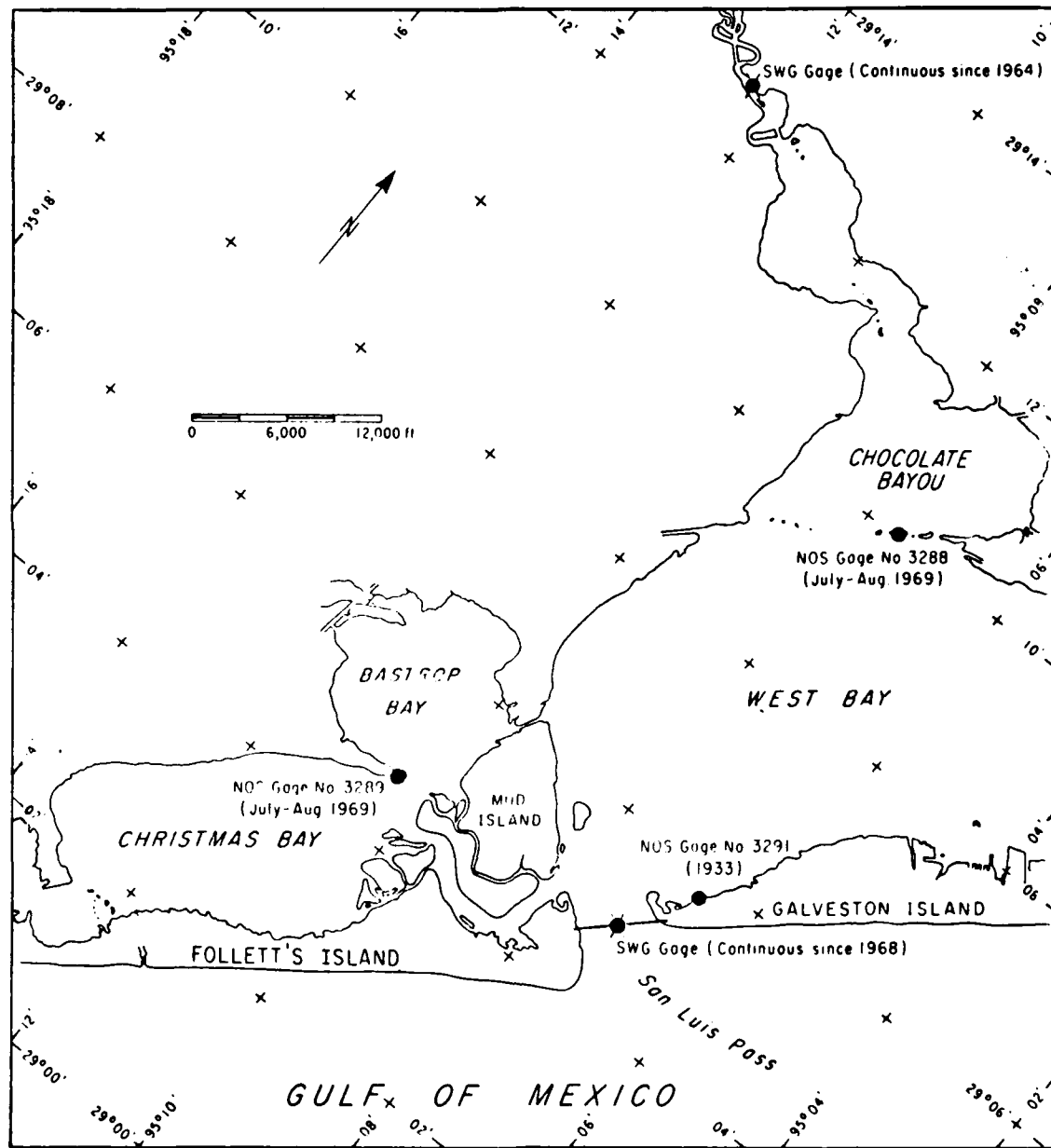


Figure 32. San Luis Pass tide gage locations (after NOS chart 11322).

Tide and current data measured over a 15-hour period were obtained by SWG in February 1962 for use in calibrating a physical model of Galveston Bay. Only two current stations in the throat were occupied; velocities were measured every half hour at three depths: usually 1, 7, and 13 feet.

Current speeds were again measured for 28 hours by SWG between 4 and 5 May 1965 for the physical model in the Texas Coast Hurricane Studies. Measurements were made at only one station in the throat at four depths: 2, 7, 12, and 18 feet. An SWG tide gage at Sea Isle Marina in West Bay was operational from 14 August 1964 to 3 January 1968, providing an analog record of the bay tide.

Several tide gages were operational between September and November 1965: NOS gage at Jamaica Beach in West Bay and the Galveston Pleasure Pier, SWG gages in Chocolate Bayou (26 August 1964 to present) and Sea Isle Marina.

In July and August 1969, tide measurements were made by NOS in Christmas Bay, West Bay (Alligator Point), and at the Pleasure Pier. Analog records for 1974 were obtained for the SWG San Luis Pass and Chocolate Bayou gages, as were tabulated highs and lows for the NOS Galveston Pleasure Pier gage.

On 24 June 1976, current measurements between 1300 and 2400 hours were made by Espey, Huston and Associates to obtain a rating curve for the pass (Johnston and Ward, 1976). Three stations were occupied in the throat of the pass. From these data, a discharge versus center velocity curve was developed for future measurements. Espey, Huston and Associates reoccupied the center station in the throat between 20 and 23 July 1976, and obtained hourly measurements, usually at five depths, with occasional readings at the bottom. Concurrent tidal data were available from the SWG gages at the pass and Chocolate Bayou.

(2) Data Analysis and Results. The objective of the hydraulic data analysis was to determine the tide characteristics, currents, and discharges, along with friction and discharge coefficients.

(a) Tidal Ranges and Levels. Table 2 summarizes the available information on tidal ranges throughout the inlet-bay system. West Bay (including Chocolate Bayou) and Christmas Bay respond similarly to the gulf tide; i.e., the tidal range in each bay is about 0.45 that at the Galveston Pleasure Pier. The 1974 average annual San Luis Pass range is about three-fourths that of the pier, indicating some energy loss over the ebb tidal delta. The pattern of 1974 monthly variability in tidal range for the San Luis Pass gage (Fig. 5) was considerably different from that of Chocolate Bayou and the Pleasure Pier, presumably the result of meteorological effects at the pass since the pattern of range variability due to astronomical causes more closely approximates the Chocolate Bayou pattern. The monthly tide level variability patterns (Fig. 4) are similar to those of other gulf coast locations.

(b) Tidal Phases. Phase information is useful in analyzing the hydraulics of an inlet bay system. Concurrent tidal data from 15 to 30 July 1969 were analyzed to determine the phase lags between high and low waters at several locations; the results are summarized in Table 3. High and low waters occur almost simultaneously at San Luis Pass and the Galveston Pleasure Pier.

Table 2. San Luis Pass tidal ranges.

Date	Location and gage	Diurnal range, R (ft)	Ratio of ranges	
			Pier	San Luis
Oct. 1933	Just inside inlet (NOS)	1.13	----	----
Nov. 1936	Just inside inlet	0.71	1.00	----
	Karancahua Reef	0.89		
June 1937	Just inside inlet	0.72	0.48	0.54
	Karancahua Reef	0.90		
Sept. to Nov. 1965	Galveston Pleasure Pier (NOS)	2.06	1.00	----
	Jamaica Beach, West Bay (NOS)	0.98	0.48	0.50
	Chocolate Bayou (SWG)	0.98	0.48	0.52
July to Aug. 1969	Galveston Pleasure Pier (NOS)	2.16	1.00	----
	San Luis bridge (SWG)	1.81	0.84	1.00
	Christmas Bay (NOS)	0.98	0.45	0.54
	Alligator Point (NOS)	0.91	0.42	0.50
	Chocolate Bayou (SWG)	0.94	0.44	0.52
1974	Galveston Pleasure Pier (NOS)	2.18	1.00	----
	San Luis Pass bridge (SWG)	1.62	0.74	1.00
	Chocolate Bayou (SWG)	1.05	0.48	0.65
July 1974	Galveston Pleasure Pier (NOS)	2.18	1.00	----
	San Luis Pass bridge (SWG)	1.72	0.79	1.00
	Chocolate Bayou (SWG)	0.95	0.44	0.55
20 to 23 July 1976	San Luis Pass bridge (SWG)	1.54	----	1.00
	Chocolate Bayou (SWG)	0.98	----	0.64

Table 3. Tidal lags in San Luis Pass system

Location	High water lag (hr)	Low water lag (hr)
San Luis Pass	0.0	0.0
Galveston Pier	0.25	0.0
Alligator Point	6.0	4.25
Christmas Bay	6.1	3.5
Chocolate Bayou	7.6	6.25

However, the high water lags in West and Christmas Bays are about 6 hours, and low water lags are substantially less. These phase lags are considerably greater than those predicted from shallow-water theory. For example, the distance from the San Luis Pass gage to the Chocolate Bayou gage is about 60,000 feet. If an average depth of 5 feet is assumed, the traveltimes for a long wave would be about 1.3 hours.

In a few cases, high water lags of as much as 15 hours occurred, due to distortion of the dual-peak gulf water level fluctuation. The second peak, which is lower on the open coast, is more readily transmitted through the inlet due to the higher water level. Consequently, the water reaches a greater amplitude in the bay than during the first peak. An example of this situation is shown in Figure 33.

d. Tidal Hydraulics. Current and discharge characteristics of San Luis Pass are summarized; the total discharge through the pass was computed as follows: When two or three current measurement stations were located in the gorge, as in 1962 and June 1976, the gorge cross section was subdivided into parts whose boundaries were equidistant (horizontally and vertically) from current meter locations. Each of these parts was then multiplied by the

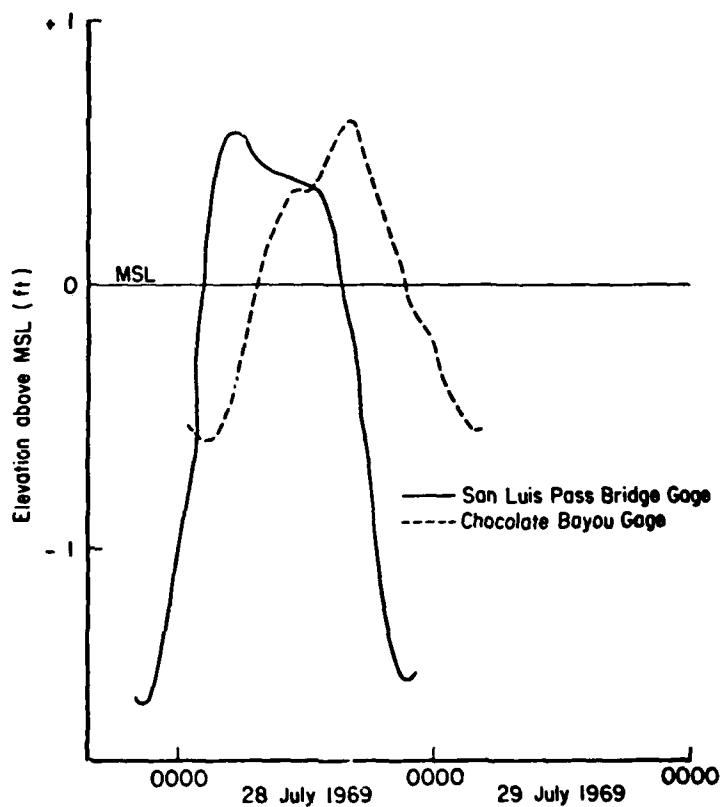


Figure 33. Illustration of tide distortion into West Bay.

instantaneous current speeds, and the products summed to provide the discharge through the gorge. Dividing this sum by the total gorge area gave the average current speed through the gorge. The total discharge through the pass must include that through the shallow east part of the profile, and no currents were measured there. Jarrett's (1976) method was used to estimate the average velocity in this section:

$$\bar{V}_s = \bar{V}_g \left( \frac{R_s}{R_g} \right)^{2/3} \quad (5)$$

where

$\bar{V}_s$  = average current speed in shallow section

$\bar{V}_g$  = average current speed in gorge

$R_s$  = hydraulic radius of shallow section

$R_g$  = hydraulic radius of gorge

Using this relationship, in 1962  $\bar{V}_s = 0.55 \bar{V}_g$ ; in 1976  $\bar{V}_s = 0.27 \bar{V}_g$ . The total discharge through the pass is the sum of the channel discharge and the section discharge, and the average current speed through the pass is  $V_T$ . A

plot of total discharge versus time for 24 June 1976 is shown in Figure 34; tidal prisms for 1962 and 1976 are given in Table 4.

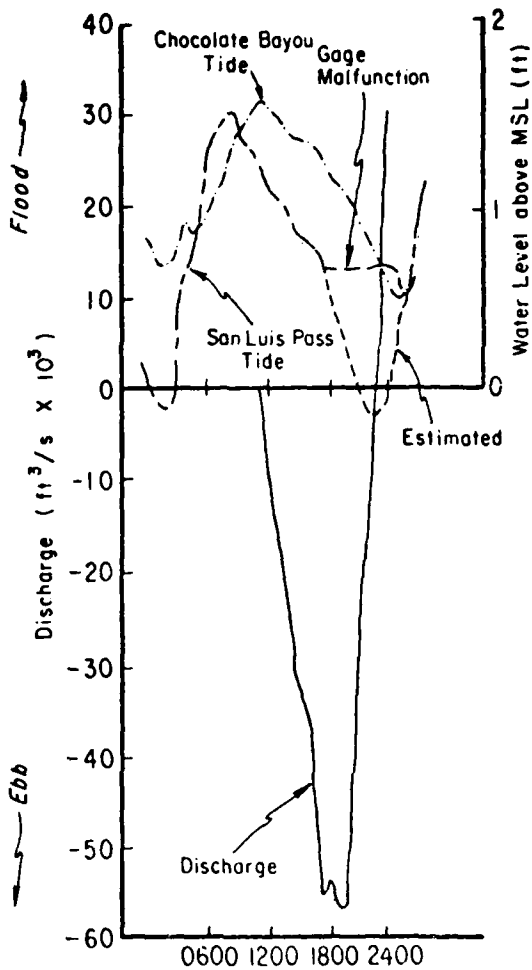


Figure 34. San Luis Pass tides and discharge 24 June 1976.

Table 4. San Luis Pass hydraulic characteristics.

Date	West Bay tidal range (ft)	Method	Prism ( $ft^3 \times 10^3$ )	Velocities (ft/s)				
				$\bar{V}_c$ <sup>1</sup>	$\bar{V}_g$	$\bar{V}_T$	$\bar{V}_{gmax}$	$\bar{V}_{Tmax}$
2 Feb. 1962	----	Discharge (one ebb)	1.51	2.18 <sup>2</sup>	2.07	1.70	3.22	2.64
3-5 May 1965	1.17	Bay range-area Discharge (two flood, one ebb)	1.85 1.59 <sup>2</sup>	----	1.89 1.80 <sup>2</sup>	1.48 <sup>2</sup>	3.23 <sup>2</sup>	2.65 <sup>2</sup>
July-Aug. 1969	0.91	Bay range-area	1.44	----	----	----	----	----
24 June 1976	0.97	Bay range-area Discharge (one ebb)	1.53 1.51	----	1.73 1.75	1.35	2.84	2.19
20-23 July 1976	0.95	Bay range-area Discharge (three flood, three ebb)	1.50 1.87 <sup>3</sup>	----	2.08 1.98 <sup>3</sup>	1.62 <sup>3</sup>	3.16 <sup>3</sup>	2.43 <sup>3</sup>

<sup>1</sup> $\bar{V}_c$  = Average current speed at the centerline of the gorge.

<sup>2</sup>Values based on 1962 discharge-velocity relationships.

<sup>3</sup>Values based on June 1976 discharge-velocity relationships.

Currents in 1965 and July 1976 were measured only in the center of the inlet throat; therefore, a relationship between total discharge through the inlet and average centerline velocity was needed to determine the tidal prisms. The June 1976 centerline measurements showed that  $Q_T = 19,050 \bar{V}_d$ , where  $Q_T$  is the instantaneous discharge through the entire pass, and  $\bar{V}_d$  is the average speed at the centerline of the gorge. This relationship was used to calculate the July discharges (Fig. 35). However, no centerline measurements were made in 1962, so a predicted centerline speed was calculated using the observed 1976 relationship  $\bar{V}_d = 1.05 \bar{V}_g$ . Using equation (5) and the appropriate flow areas, discharges for 1965<sup>g</sup> conditions were calculated (Fig. 36). Tidal prisms were obtained by integrating the area beneath the discharge curves of Figures 35 and 36 (see Table 4).

In 1969 no discharges were measured and tidal prisms were obtained by multiplying the bay tidal range by the bay area affected by that range. The mean tidal prisms for July and August 1969 in each bay (Table 5) indicate that West Bay accepts most of the flow passing through San Luis Pass.

Table 5. Mean tidal prisms in San Luis Pass, July and August 1969.

Location	Tidal prism (ft <sup>3</sup> x 10 <sup>9</sup> )	Total flow through pass (pct)	Bay area (ft <sup>2</sup> x 10 <sup>9</sup> )	Bay tidal range (ft)
West Bay (Alligator Point)	1.76	79	1.93	0.91
Chocolate Bayou	0.16	7	0.167	0.94
Christmas and Bastrop Bays	0.31	14	0.318	0.98
Total	2.23	100	2.42	0.92

For comparison purposes, prisms based on bay tidal ranges were also computed for discharge measurement periods (Table 4). Relationships between the ranges measured at the three locations in 1969 were used to arrive at the following equation for San Luis Pass tidal prism,  $P$ :

$$P = \underbrace{A_{wb} R_{wb}}_{\text{West Bay prism}} + \underbrace{\left( \frac{0.94}{0.91} R_{wb} \right) (A_{cb})}_{\text{Chocolate Bayou prism}} + \underbrace{\frac{0.98}{0.91} R_{wb} (A_{c+b})}_{\text{Christmas and Bastrop Bays prism}} \quad (6)$$

where

$R_{wb}$  = tidal range at Alligator Point in West Bay

$A_{wb}$  = area of West Bay (to Carancahua Reef only),  $1.06 \times 10^9$  square feet

$A_{cb}$  = area of Chocolate Bayou,  $0.17 \times 10^9$  square feet

$A_{c+b}$  = area of Christmas and Bastrop Bays,  $0.32 \times 10^9$  square feet

or

$$P = (1.06 R_{wb} + 0.176 R_{wb} + 0.345 R_{wb}) \times 10^9$$

and

$$P = 1.58 \times 10^9 R_{wb}$$

Using both discharge and range-area tidal prisms, the average San Luis Pass prism computed from discharge measurements is  $1.65 \times 10^9$  cubic feet; the

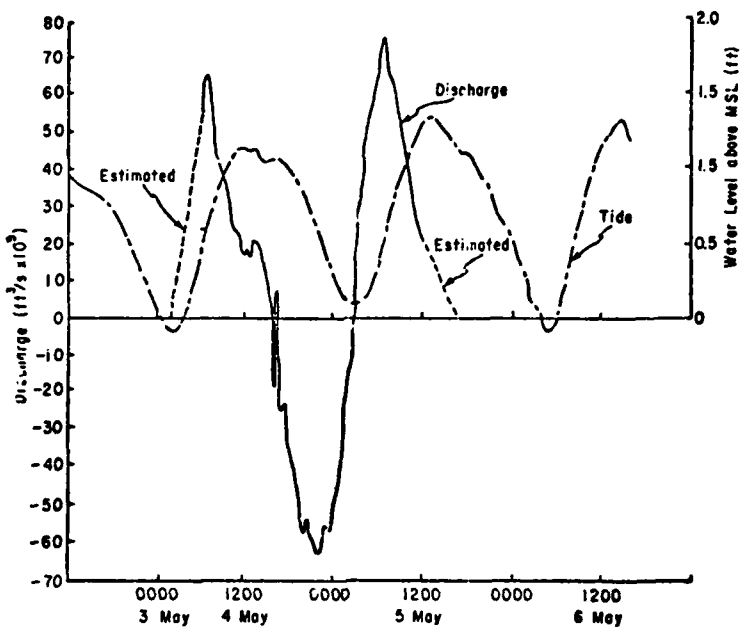


Figure 35. Discharge and water level time histories, 20-23 July 1976.

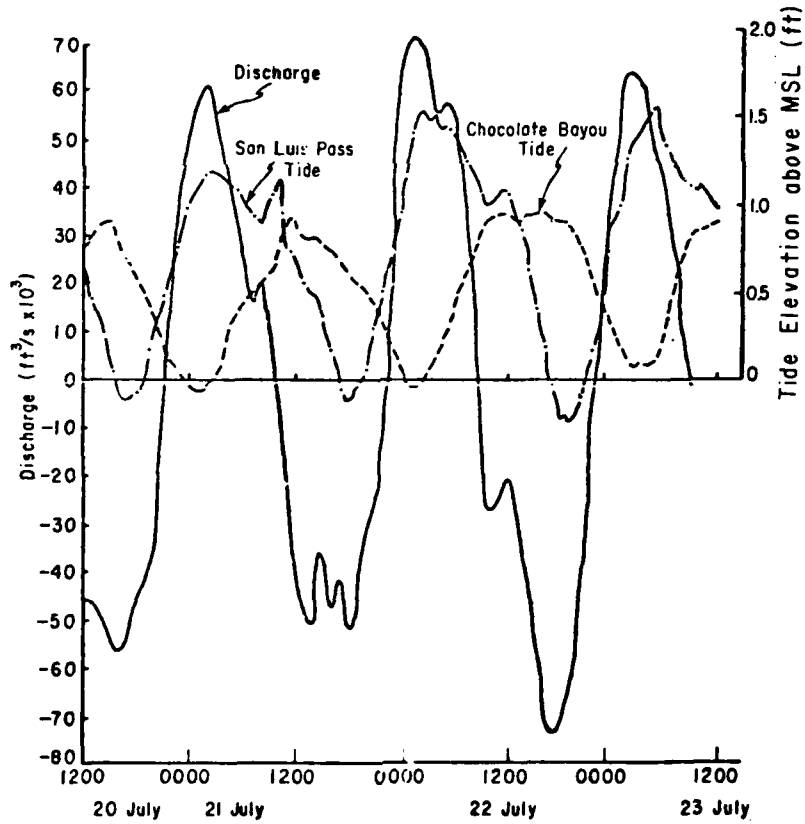


Figure 36. Discharge and water level time histories, 3-6 May 1965.

range-area method average prism is  $1.63 \times 10^9$  cubic feet, which is in remarkably close agreement considering the assumptions made in delimiting the bay areas and other possible sources of error. For the 1974 annual mean West Bay range of 1.02 feet, a mean annual prism of  $1.61 \times 10^9$  cubic feet is obtained. On the average, the July 1976 prisms showed no flood or ebb predominance, but wind effects may have been important in this regard. In addition, Figure 5 shows that some seasonal variation in the monthly mean tidal range occurs, so seasonal variations in tidal prisms can be expected, with slightly greater than average prisms in January, May, June, November, and December, and lower than average prisms in March, August, and October.

e. Stability of San Luis Pass. The stability of San Luis Pass was analyzed using O'Brien and Dean's (1972) method. This method combines a stability relationship between maximum average velocity,  $\bar{V}_{max}$ , and inlet cross-sectional area,  $A_c$ , similar to that of Escoffier (1940), with the simplified hydraulic analysis of Keulegan (1967) discussed previously. At San Luis Pass, the following constants were used:  $T = 89,000$  seconds;  $A_b = 2.42 \times 10^9$  square feet and  $2a_o = 2.17$  feet. The most difficult variable to define was the inlet length,  $L$ . This was obtained by using the recent values of  $A_c = 25,550$  square feet,  $R = 6.2$  feet,  $f = 0.042$ , and the observed long-term value of  $K$  in equation (1). The bay to gulf tidal range ratio of 0.44 was determined from the tidal data; a corresponding  $K$  value of 0.40 was determined from Figure 37(c). Solving for  $L$  yields an effective length,  $L_e = 4,325$  feet.

O'Brien and Dean's (1972) stability method is based on the fact that at the two extremes of a cross-sectional area,  $A_c = 0$  and  $A_c = \infty$ , the velocity through the inlet will be 0. For intermediate values, the relationship between  $\bar{V}_{max}$  and  $A_c$  is given by

$$\bar{V}_{max} = \frac{V' \pi 2a_o A_b}{TA_c} \quad (7)$$

where  $V'$  is a dimensionless velocity coefficient related to  $K$  by Figure 37(b). The stability curves shown in Figure 38 were developed as follows: for each value of  $A_c$ , a corresponding value of  $K$  was calculated from equation (1) using one of four lengths:  $L = L_e$ ,  $L = 432$  feet ( $0.1 L_e$ ),  $L = 1,000$  feet ( $0.23 L_e$ ), and  $L = 2,000$  feet ( $0.46 L_e$ ). Various lengths are necessary because the length over which the cross-sectional area may change will influence the hydraulic response of the inlet. O'Brien and Dean (1972) refer to "deposition lengths" (i.e., channel segments in which sand is deposited to change the cross-sectional area), and they suggest a standard length of 1,000 feet. It was found that the hydraulic radius varies with  $A_c$  as follows:  $R = 0.5 + 2.3 \times 10^{-4} A_c$ .

$K$  values were calculated for individual values of  $A_c$ ,  $R$ , and  $L$ ; the corresponding values of  $V'$  were obtained from Figure 37(b); values of  $\bar{V}_{max}$  were calculated using equation (7); and  $\bar{V}_{max}$  versus  $A_c$  was plotted in Figure 38. The peaks of each curve represent the critical cross-sectional area for that particular length. For areas less than the critical value, the inlet is unstable; i.e., an increase (decrease) in area causes an increase (decrease) in maximum velocity. For areas greater than the critical value, the inlet is stable, and an increase (decrease) in area produces a decrease

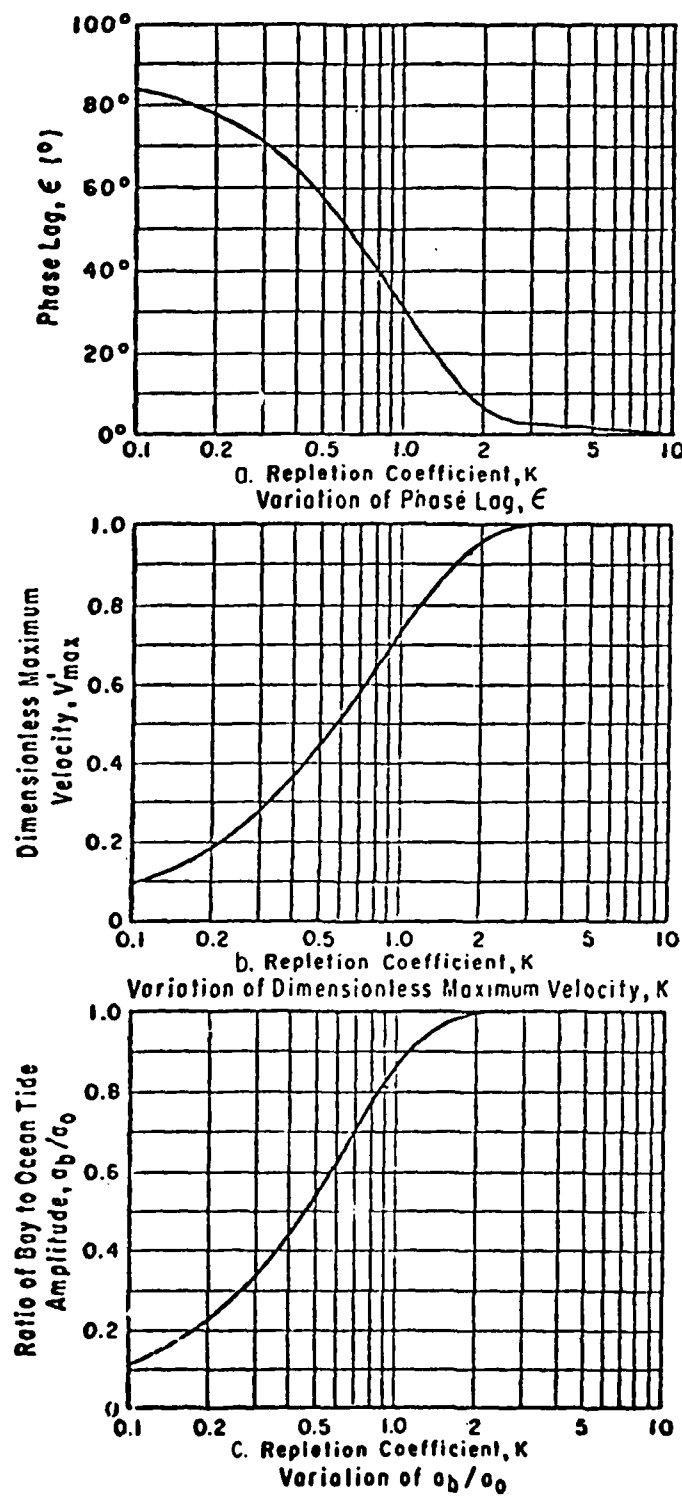


Figure 37. Variation of dimensionless parameters with Keulegan's repletion coefficient, K (after O'Brien and Dean, 1972).

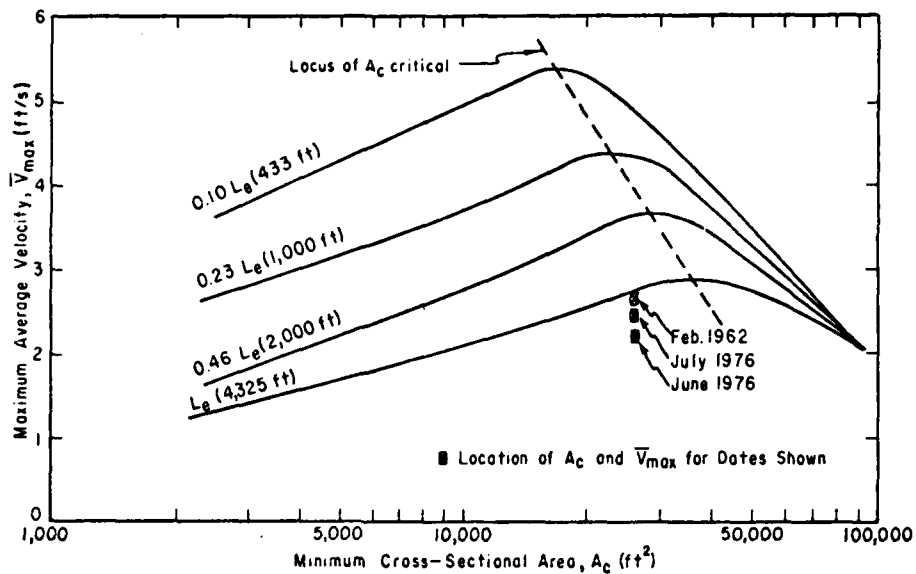


Figure 38.  $\bar{V}_{\max}$  versus  $A_c$  stability curves, San Luis Pass, Texas.

(increase) in velocity. Note that the actual values of  $A_c$  and  $\bar{V}_{\max}$  indicate that San Luis Pass is slightly below the critical area for the calculated length of 4,325 feet.

Another measure of the stability of San Luis Pass is to use Jarrett's (1976) relationship between equilibrium cross-sectional area,  $A_{ce}$  and diurnal tidal prism,  $P$ , for unjettied gulf coast inlets:

$$A_{ce} = 3.5 \times 10^{-4} P^{0.86} \quad (8)$$

For the average tidal prism of  $1.6 \times 10^9$  cubic feet, an equilibrium area of 27,490 square feet is found, which is only slightly greater than the present value of 25,790 square feet.

f. Summary. Throughout its history, San Luis Pass has been a downdrift offset inlet in the classic pattern described by Hayes, Goldsmith, and Hobbs (1970) and Galvin (1971), and has remained in the same location at the southwest end of West Bay, typifying the stable Texas Inlet (Price, 1951). Between 1853 and 1933, annual sediment volume changes within the inlet system were relatively minor, with a net erosion of the ebb tidal delta associated with a counterclockwise rotation of the delta and thalweg. The eroded material may have moved downcoast or into the bay where deposition occurred on the flood tidal delta. The minimum cross-sectional area has doubled since 1853; unfortunately, there are not enough data to determine the possible causes. Hurricane Carla apparently caused a major change in ebb tidal delta configuration in about 1961, but since then both the cross-sectional area and the inlet width have remained relatively constant. Long-term changes on the adjacent beaches indicate a relatively stable updrift area with minor erosion downdrift of the pass, probably due to sediment trapping by the pass (Fig. 39). Theoretical stability predictions agree well with the actual stability, indicating that San Luis Pass has been in an unstable scouring mode, but is predicted to

reach a stable critical area of about 35,000 square feet, which will result in maximum average velocities of about 3 feet per second.

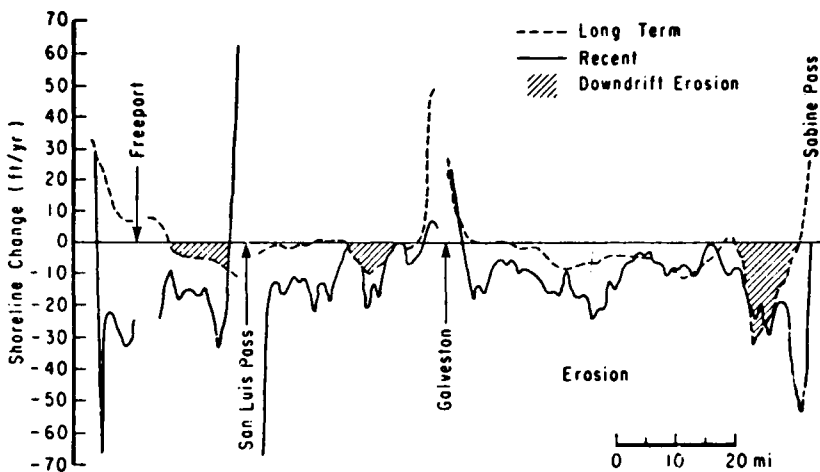


Figure 39. Shoreline change rates, upper Texas coast (after Morton, 1975).

### 3. Galveston Bay Entrance.

a. Historical Review. Galveston Bay entrance is the largest pass on the Texas coast and the best documented of the five passes studied. SWG and NOS boat sheets were analyzed to document long-term changes in cross-sectional areas of the pass and more recent changes in the adjacent beach and offshore zones resulting from jetty construction.

(1) Cross-Sectional Changes. Figures 40 and 41 show cross-sectional profiles at the minimum inlet width made from the earliest survey, 1851, through the latest available, 1975. Historical variations in minimum inlet area, width, and hydraulic radius are plotted in Figure 42.

From 1851 to 1908 (Fig. 40), the point of maximum depth in the inlet throat moved consistently westward at a rate of about 30 feet per year; the east side of the channel (Bolivar Peninsula) migrated westward at a slower rate. Construction of the south jetty by 1888 fixed the west end of the profile, and deposition on Bolivar Peninsula resulted in a constantly decreasing width to 1933 (Fig. 42). Concurrent with the width reduction was a general deepening of the profile. Postconstruction hydraulic radii were about 5 feet greater than during prejetty conditions. Note that in 1888, a deep channel began developing west of the main thalweg, and the continued growth of this channel apparently caused the increase in cross-sectional area between 1867 and 1908. This rather sudden change in profile shape could have resulted from either natural or manmade scouring action. Between 1874 and 1880, the United States constructed a submerged jetty extending northeastward from the north end of Galveston Island to the edge of the entrance channel (Fig. 43), which could have constricted the channel and increased scour.

Between 1908 and 1933 (Fig. 41) the thalweg increased its westward movement rate to about 60 feet per year, double its rate from 1867 to 1908. This movement could have been accelerated by the 1919-22 dredging projects which increased navigation channel depths to 35 feet. The major reason given for this movement is construction of the Texas City dike (Fig. 44) in 1915, which

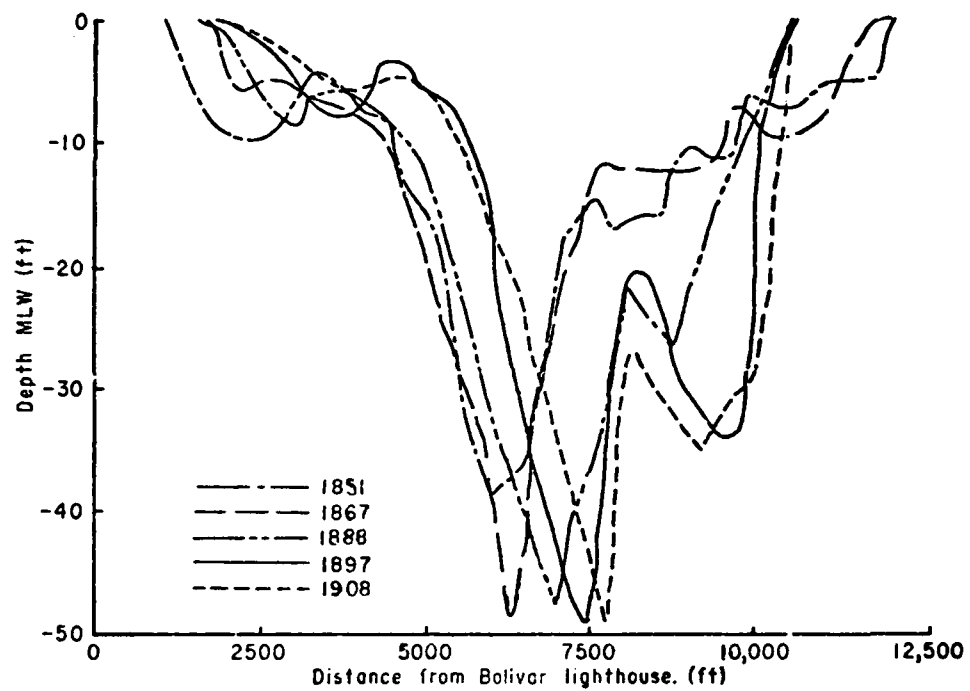


Figure 40. Galveston entrance minimum-width cross-sectional area profiles, 1851-1908.

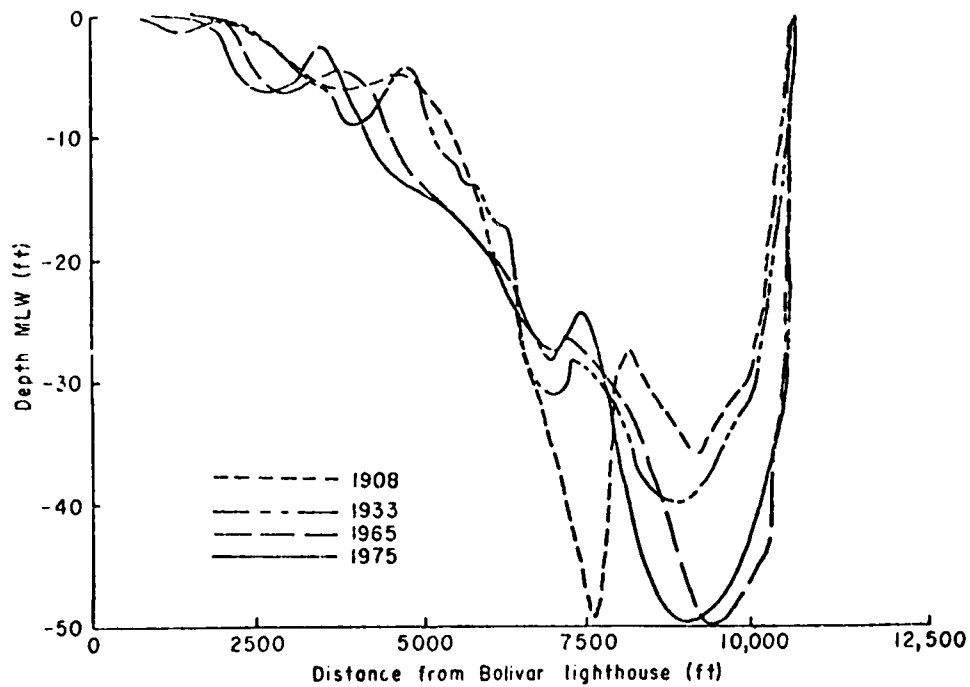


Figure 41. Galveston entrance minimum-width cross-sectional area profiles, 1908-75.

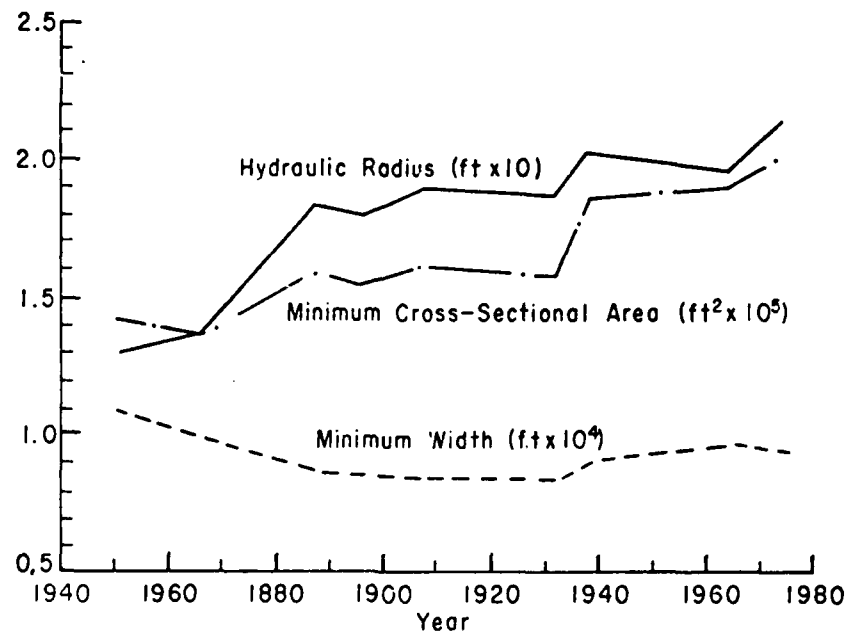


Figure 42. Time history of minimum inlet width, area, and hydraulic radius, Galveston entrance, Texas.

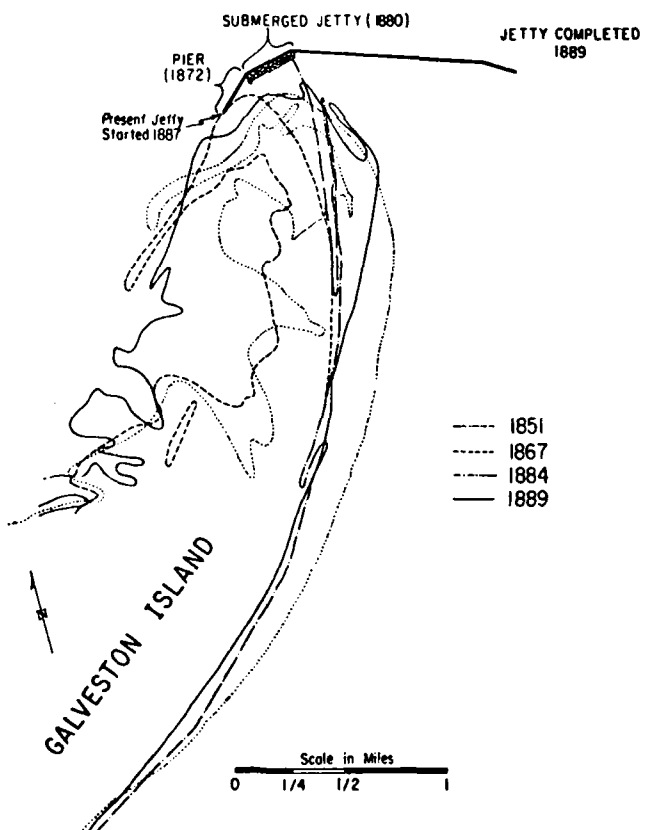


Figure 43. Galveston Island shorelines, 1851-89.

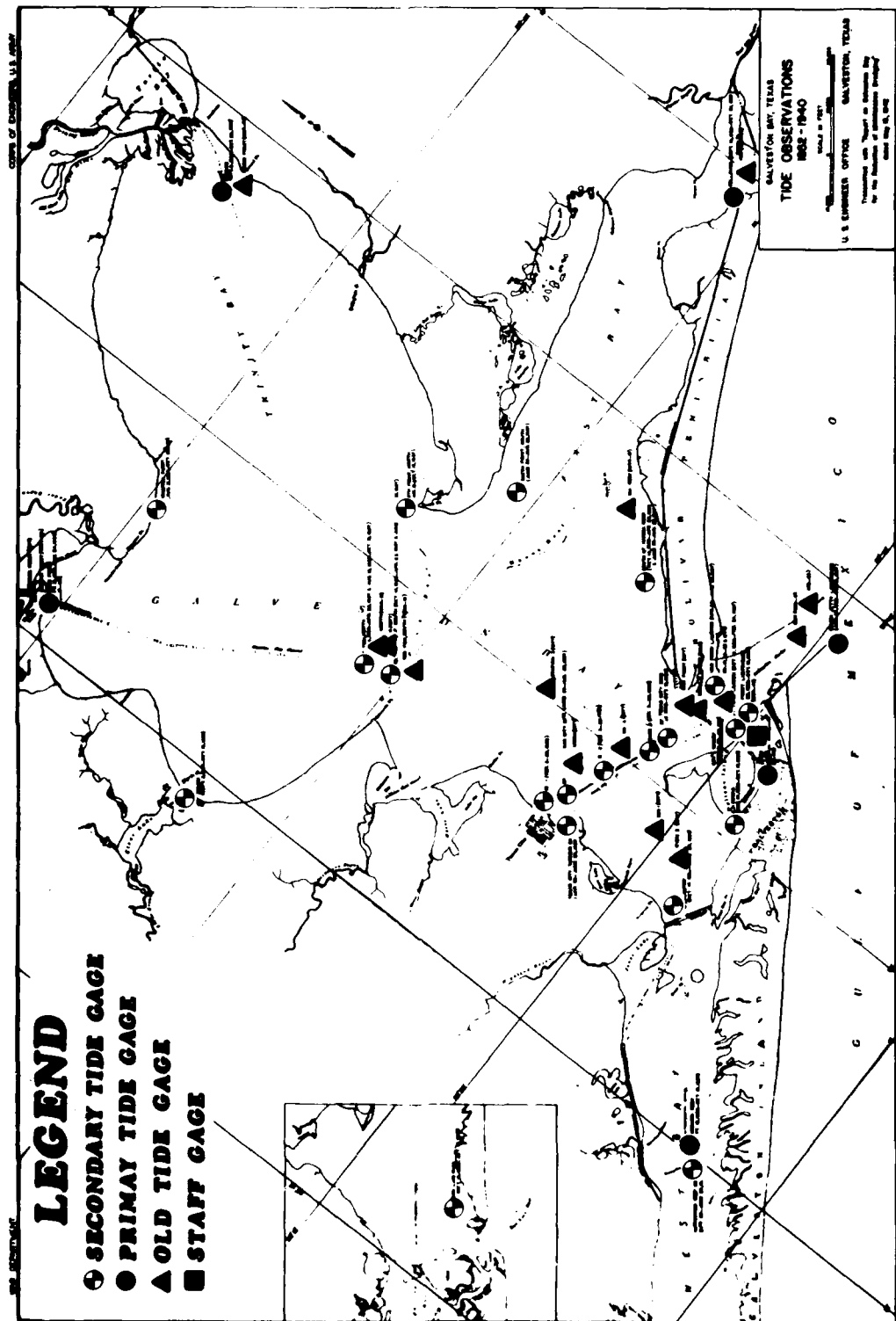


Figure 44. Tide observations, Galveston Bay, 1852-1940 (after U.S. Army Engineer District, Galveston, 1942).

directed currents toward the north end of Galveston Island (U.S. Army Engineer District, Galveston, 1942). By 1965, the channel had once again reached a 50-foot-maximum depth, though this point was westward of its 1933 position, causing a steep-sided channel adjacent to the south jetty. Increases in cross-sectional area and hydraulic radius between 1933 and 1965 (Fig. 42) may have been due to natural expansions of the profile or from the dredging to increased project depths.

(2) Changes to Adjacent Beaches and Offshore Zones. The effect of jetty construction on Galveston entrance is illustrated in the Galveston Island shorelines from 1851 to 175 (Figs. 43 and 45), and maps of bathymetric changes between survey dates (Figs. 46 to 50). The effect of a relative sea level rise of 0.02 foot per year during this century was included in all volumetric calculations (see Fig. 8).

(a) Changes Between 1851 and 1889. Between 1851 and 1867, the northern end of Galveston Island receded greatly (Fig. 43); a storm in October 1867 cut a 1,000-foot-wide channel 2 feet deep across the northern end of the island (U.S. Army Corps of Engineers, 1868). Construction of the submerged jetty in 1880 caused local accretion at the tip of the island (compare the 1867 and 1884 shorelines in Fig. 43). More extensive deposition occurred between 1884 and 1889, corresponding to construction of the shoreward part of the south jetty between 1887 and 1889. Figure 46 shows the bathymetric changes which occurred between 1867 and 1888. About 3.5 million cubic yards of sand accumulated in the fillet on the tip of Galveston Island, at an average rate of about 166,000 cubic yards per year. However, most of this accumulation may have occurred between 1884 and 1888, when the impermeable jetty probably prohibited sand movement around the tip. Extensive offshore deposition occurred on the north side, and nearshore deposition on the south side of the entrance; about twice as much was deposited on the north as on the south. The northern deposition was due to natural processes, since the south jetty had not been extended seaward in 1888 and north jetty construction did not start until 1893. An extensive zone of minor erosion existed in the offshore area on the south side.

(b) Changes Between 1888 and 1908. The north tip of Galveston Island accreted rapidly in response to jetty construction (Fig. 45). Comparing Figures 46 and 47 shows that about 14.7 million cubic yards of sand accumulated in the south fillet between 1888 and 1908. However, Figure 47 also shows a large offshore erosion zone with a deposition zone landward extending to the fillet. The volume deposited between 1867 and 1908 was about the same as the volume eroded (i.e., about 15 million cubic yards).

Between 1888 and 1908, south side erosion totaled 15.5 million cubic yards, nearshore deposition was 5.8 million cubic yards, and 14.7 million cubic yards accumulated in the fillet. Thus, total south side deposition following jetty construction was 20.5 million cubic yards and the net change was +5 million cubic yards or about 250,000 cubic yards per year. It is concluded that much of the material which comprised the fillet actually came from adjustment of the ebb tidal delta to jetty construction. With jetty construction, the erosion zone, which had previously experienced considerable tidal current action, was subjected only to waves and wave-induced currents. These tended to drive the material landward into the fillet and perhaps also through the jetty.

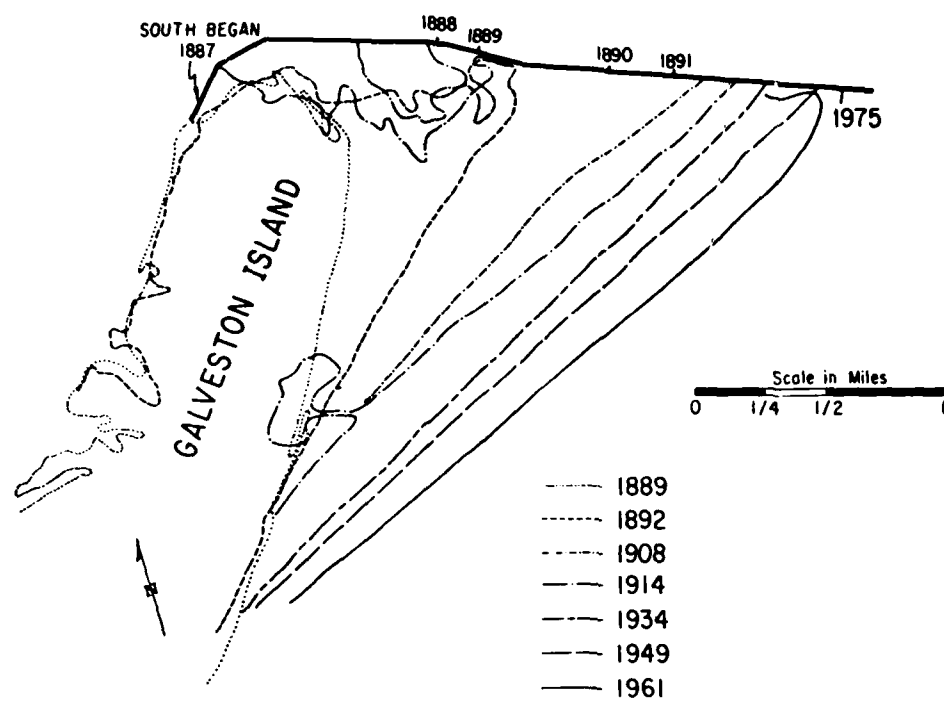


Figure 45. Galveston Island shorelines, 1889-1975.

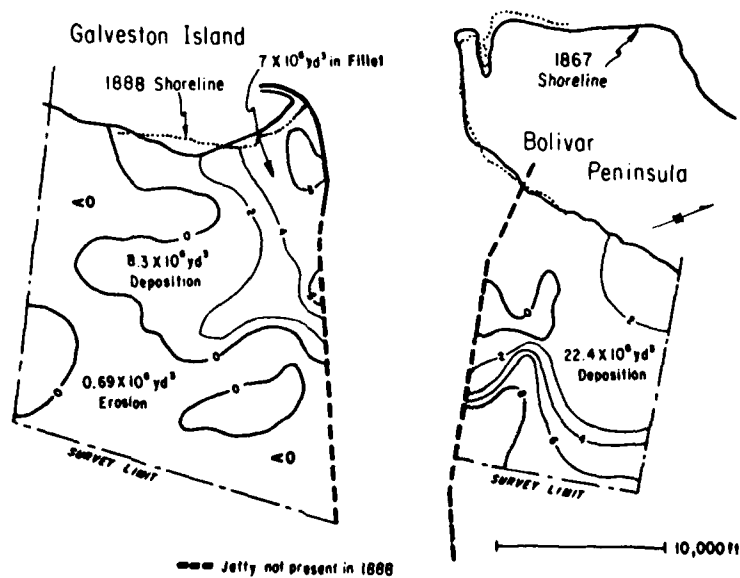


Figure 46. Galveston entrance bathymetric changes, 1867-88.

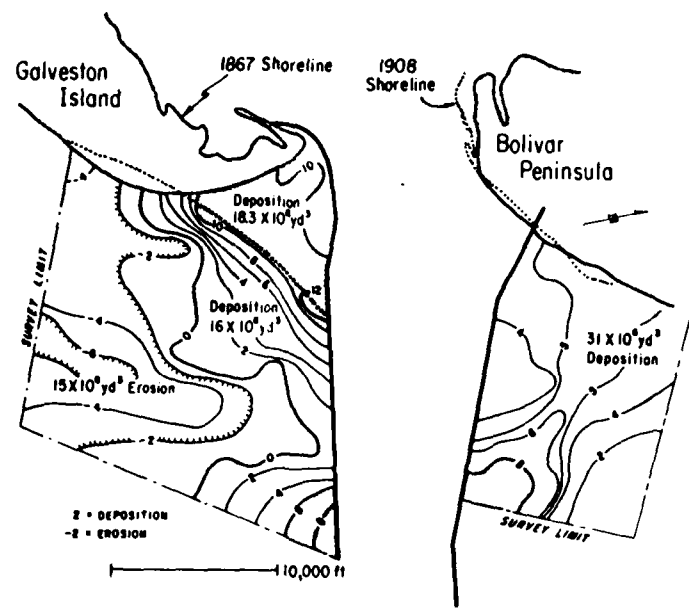


Figure 47. Galveston entrance bathymetric changes, 1867-1908.

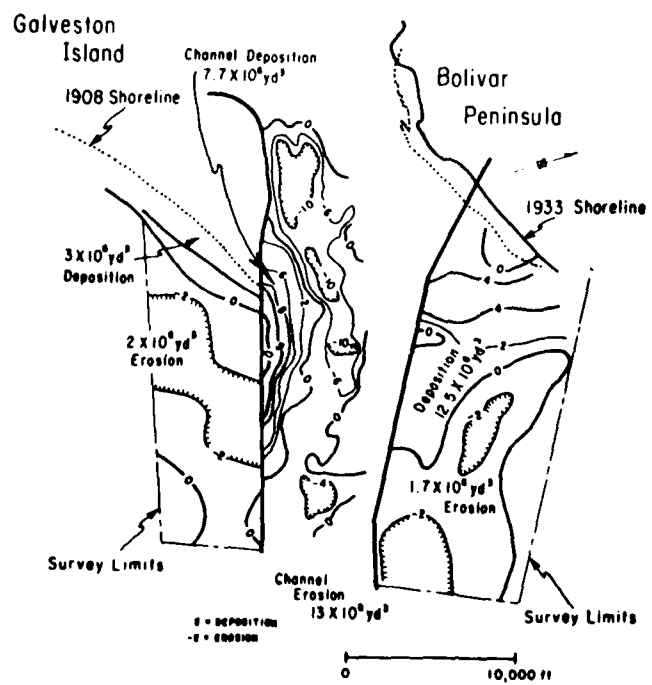


Figure 48. Galveston entrance bathymetric changes, 1908-33.

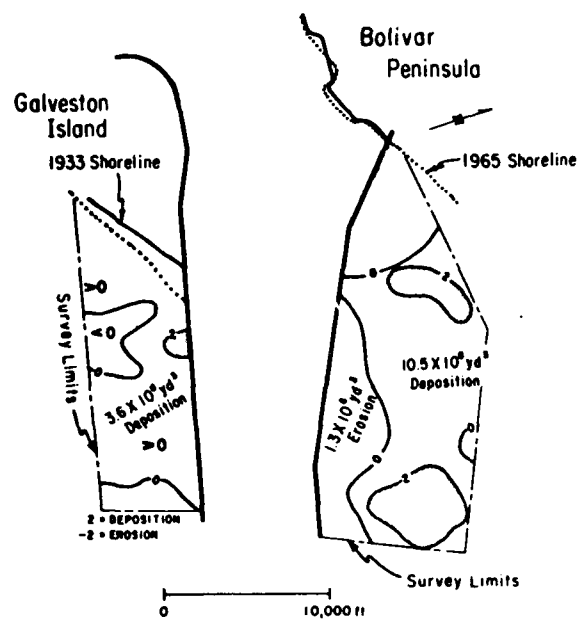


Figure 49. Galveston entrance bathymetric changes, 1933-65.

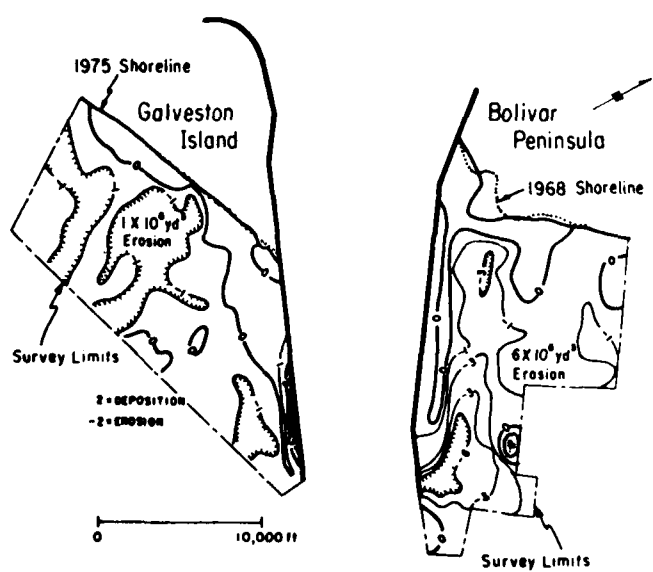


Figure 50. Galveston entrance bathymetric changes, 1968-75.

On the northeast side, deposition between 1888 and 1908 was about 8.6 million cubic yards, a rate of 430,000 cubic yards per year. How much of this occurred as a result of the north jetty is difficult to determine. The area had accreted rapidly (1,060,000 cubic yards per year) before jetty construction. The 1908 shoreline showed little change from the 1867 condition.

(c) Changes Between 1908 and 1933. The shoreline of Galveston Island continued to grow seaward during this period (Fig. 45). Next to both the north and south jetties, a similar pattern of offshore erosion and nearshore accretion occurred (Fig. 48). One million cubic yards accreted south of the jetty, at an average rate of about 40,000 cubic yards per year. However, extensive deposition occurred just north of the jetty, and much of this material may have come through or over the jetty. Some of the material could also have come from scour of the entrance channel. On the northeast side, net deposition was 10.8 million cubic yards, an annual rate of 430,000 cubic yards per year. The shape of the deposition area shown in Figure 48 indicates that the north jetty may have been impermeable, trapping most of the westward-moving longshore transport. If this was the case, and the area of deposition extended eastward beyond the limits of the available data, then the minimum westward transport rate was 500,000 cubic yards per year between 1908 and 1933.

(d) Changes Between 1933 and 1965. Figure 49 shows the 1965 shoreline intercepting the south jetty about 2,300 feet seaward of the 1933 intercept. However, offshore changes south of the jetty were relatively minor, and it is concluded that the adjustment of the ebb tidal delta to a wave-dominated environment had been completed by 1933. On the north side, however, deposition continued between 1933 and 1965 (at a rate of at least 420,000 cubic yards per year), and minor erosion occurred along the seaward section of the jetty.

(e) Changes Between 1965 and 1975. The shorelines on either side of the pass changed little between 1965 and 1975 (Fig. 45). In the offshore zone south of the south jetty, erosion totaled about 1 million cubic yards between 1968 and 1975 (Fig. 50); on the north side the erosion was about six times greater. Much of this was concentrated in a region just north of the gulf end of the jetty.

(f) Summary of Changes Between 1867 and 1975. Bathymetric and shoreline changes were previously examined at 20- to 25-year intervals. Morton (1977) analyzed changes at many Texas inlets and found those for Galveston between 1867 and 1974 (Fig. 51) to be similar to those at Sabine, Brazos-Santiago, and Freeport, i.e., a downdrift tripartite pattern of offshore deposition, nearshore erosion, fillet and beach accretion, and an updrift pattern of widespread accretion. This analysis revealed that these patterns were established shortly after the completion of the jetty construction, and that later adjustments were relatively minor compared to those occurring in the first 10 to 15 years. Estimates of westward longshore sediment transport rates based on postconstruction accumulation are between 420,000 and 500,000 cubic yards. Calculations of eastward rates were complicated by landward migration of the ebb tidal delta but averaged 170,000 cubic yards per year, for about a 2.5:1 westward-to-eastward ratio.

(g) Changes in Entrance Channel. Shoaling and scour patterns for the entrance channel between 1890 and 1940-41 were provided by U.S. Army

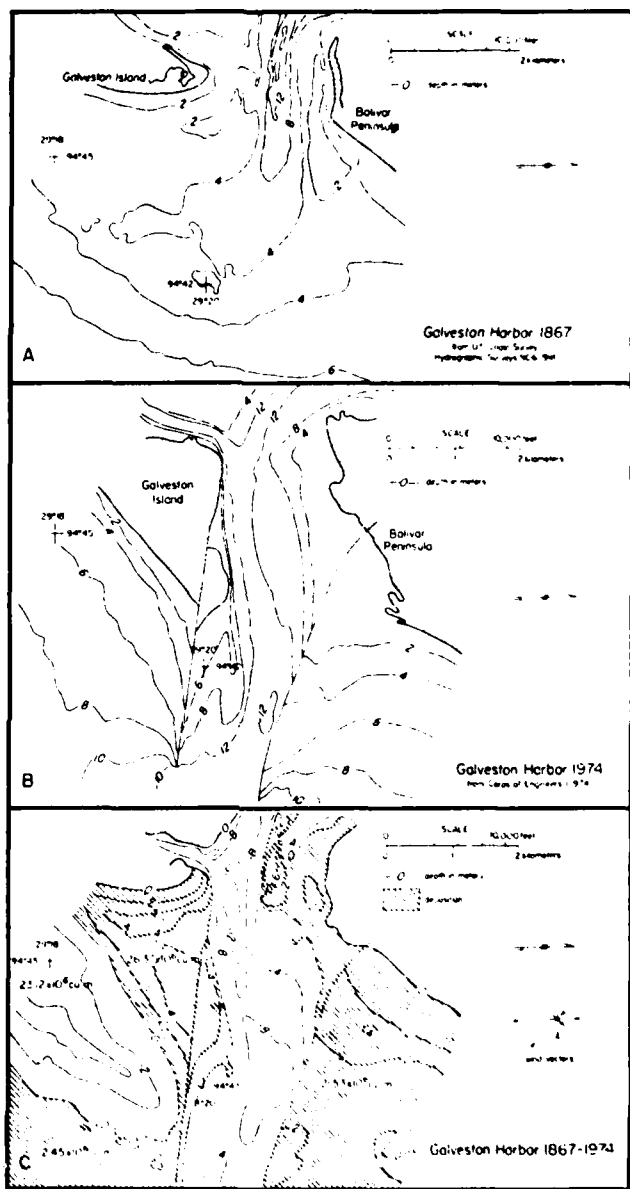


Figure 51. Bathymetry and nearshore changes, Galveston Harbor (after Morton, 1977).

Engineer District, Galveston (1942) (Fig. 52). In this time period, 6.6 million cubic yards of material was deposited between the jetties, and 28.3 million cubic yards was eroded, for a net erosion of 21.7 million cubic yards. One major zone of erosion just north of the base of the south jetty was discussed previously in connection with the cross-sectional area profiles; about 5 million cubic yards eroded from this area. The other zone was adjacent to the middle of the north jetty, where more than 10 million cubic yards eroded. Unfortunately, the effects of extensive channel dredging could not be assessed because the precise dredging limits are unknown. However, from the configuration of the changes, it appears that a natural shift in the thalweg resulted from the jetty construction and perhaps construction of the Texas City dike. This shift could have contributed to increased deposition, inside the jetties adjacent to the southwest fillet, which totaled about 2.8 million cubic yards.

b. Galveston Bay Tides and Currents.

(1) Summary of Hydraulic Data Collection. Tide measurements have been taken in Galveston Bay since 1852; a summary of the tide stations and dates of operation is given in Figure 44 for 1852-1940 and in Figure 53 for 1940-78. Current measurements from 1867 to present have been taken extensively.

(2) Data Analysis and Results. This analysis summarizes the hydraulic characteristics of Galveston entrance for selected time periods. As will be seen, these characteristics varied little over the years.

(a) Tidal Ranges and Levels. Figures 54 and 55 show the tidal range ratio distribution in Galveston Bay for November 1936 and June 1937, respectively. The values shown are the ratios between the monthly mean range at each station and the monthly mean range at the Galveston Pleasure Pier. Considering Galveston and East bays as a combined system, the average November 1936 range ratio was 0.51, and the average June range ratio was 0.49. Tidal ranges and ratios for each month in 1974 are presented in the Appendix. A plot of the annual mean ratios (Fig. 56) shows that the average bay range ratio in 1974 was 0.56, about 12 percent more than the 1936-37 range, and in qualitative agreement with the 25-percent increase in cross-sectional area during that time.

Unfortunately, stations 3, 6, and 7 were missing several months of data. Therefore, the range and level variability plots (Figs. 57 and 58) show considerably more scatter than those for a complete year of data shown in Section II. In general, however, the same trends prevail.

(b) Currents and Discharges. Table 6 summarizes the current and tidal prism data used in this study. Data for 1936 and earlier were obtained from U.S. Army Engineer District, Galveston (1942); those for 1962 were obtained from raw data supplied by the Galveston District. The average diurnal tidal prism is about  $11 \times 10^9$  cubic feet; for a mean tidal range the prism is about  $6.5 \times 10^9$  cubic feet.

c. Theoretical Stability Analysis. O'Brien and Dean's (1972) stability method was used to predict the response of Galveston entrance to sedimentation. However, since Manning's  $n$  value could not be determined due to the lack of appropriate tidal data, curves of  $\bar{V}_{max}$  versus  $A_c$  were plotted in Figure 59 for various values of  $n^2 L$ . Thus, using a representative

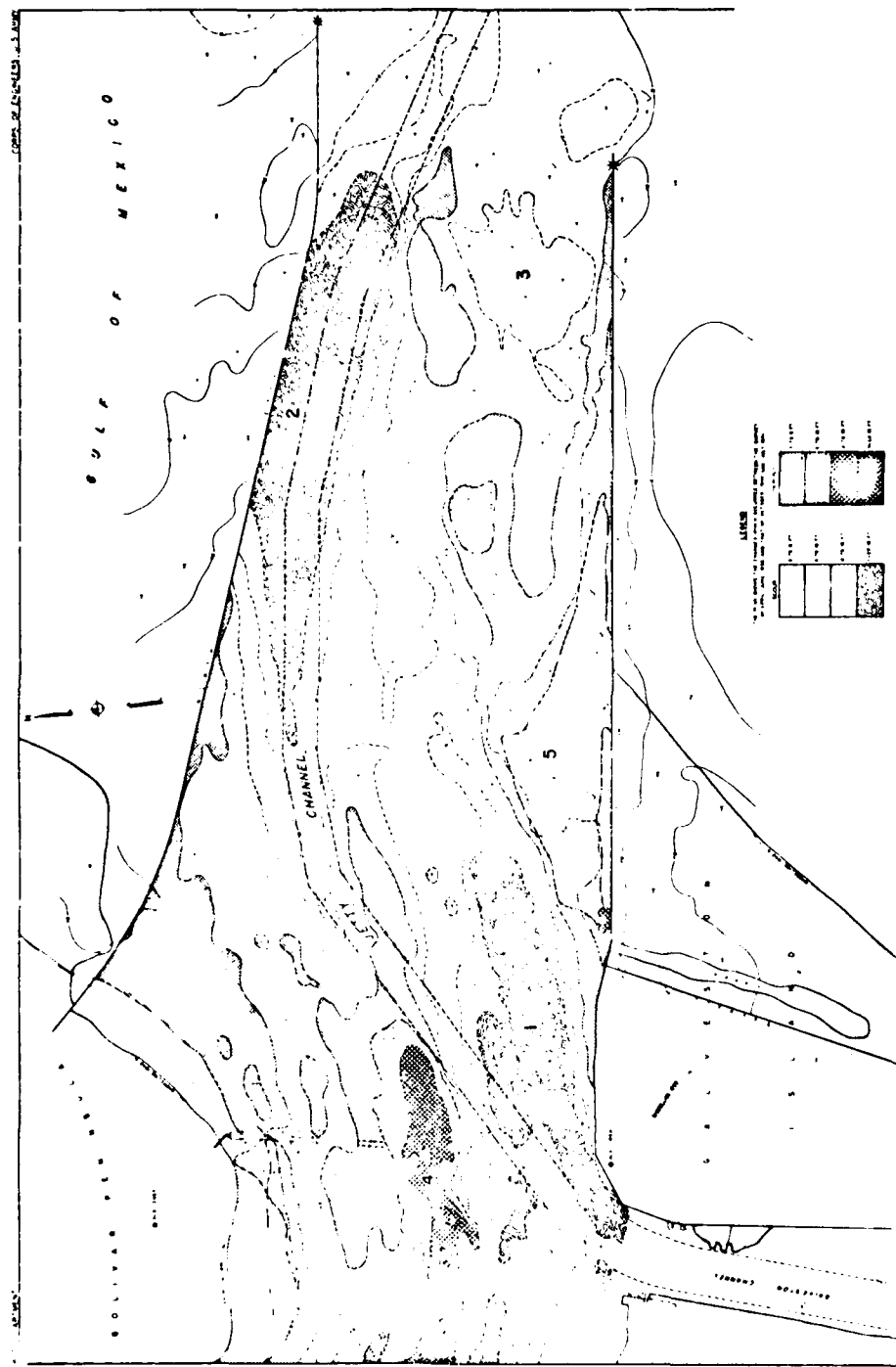


Figure 52. Galveston entrance channel bathymetric changes, 1890 to 1940-41.  
 (after U.S. Army Engineer District, Galveston, 1942).

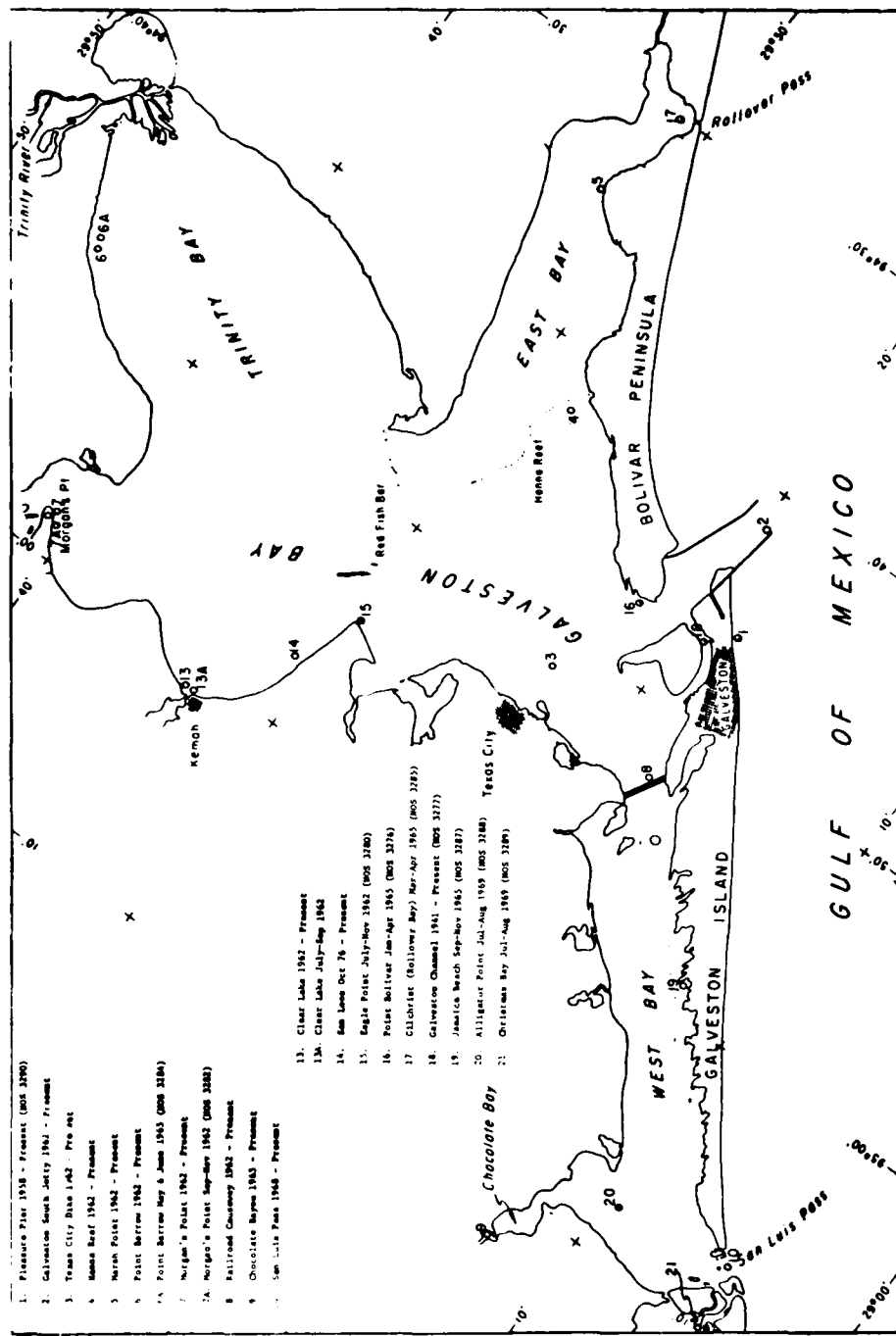


Figure 53. Tide observations, Galveston Bay, 1940-78.

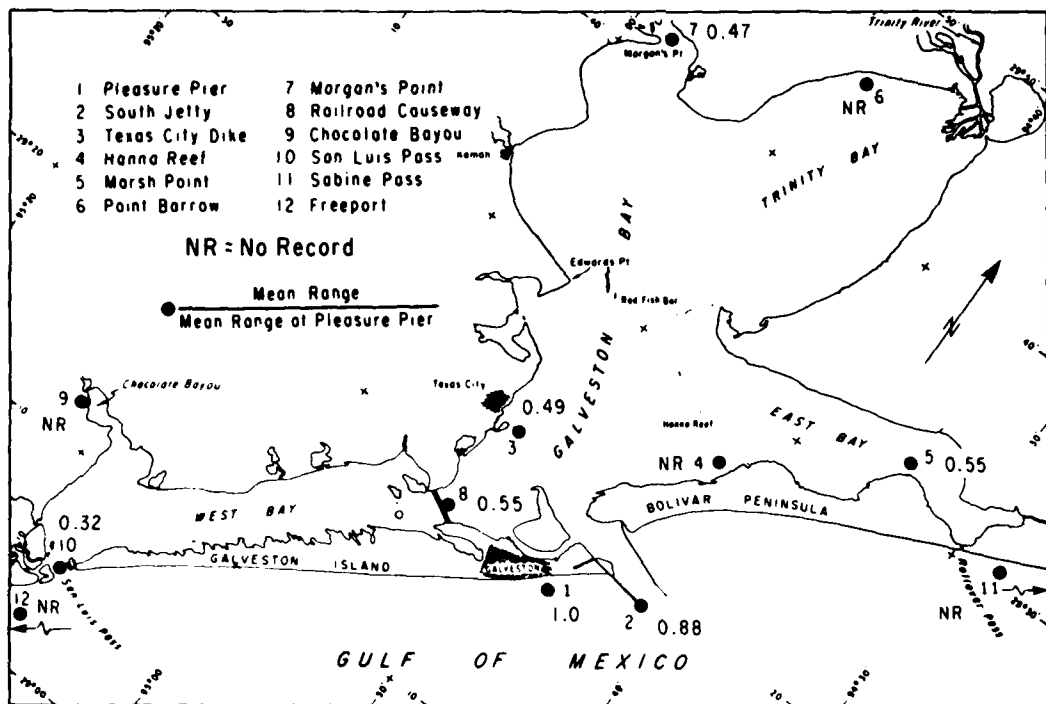


Figure 54. Galveston Bay tidal range distribution, November 1936.

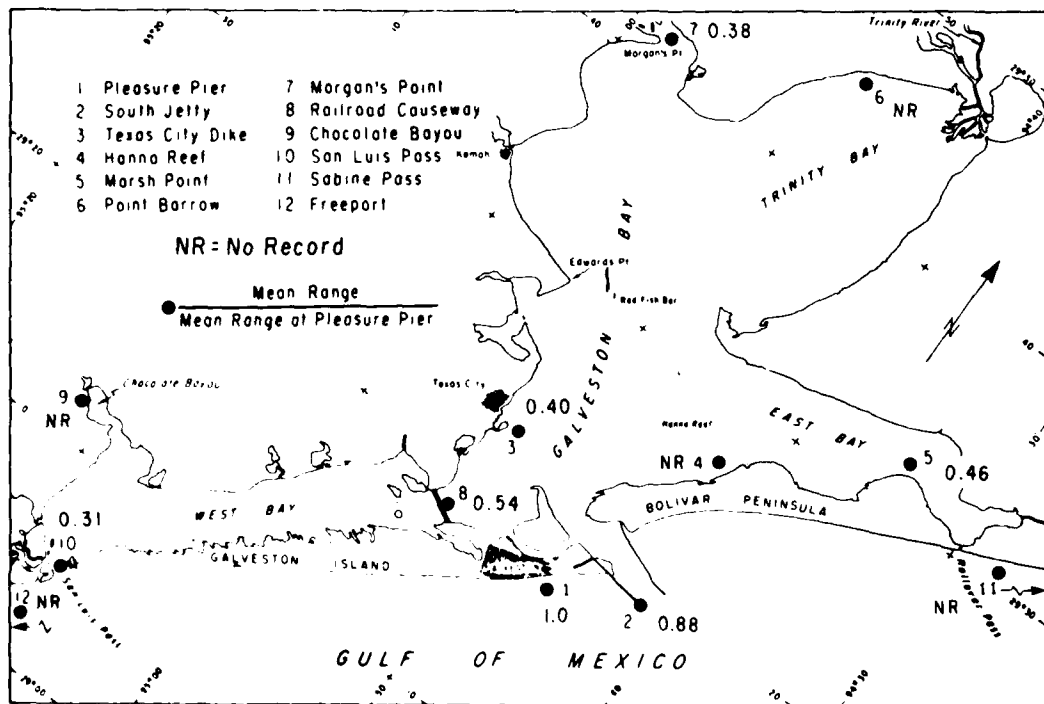


Figure 55. Galveston Bay tidal range distribution, June 1937.

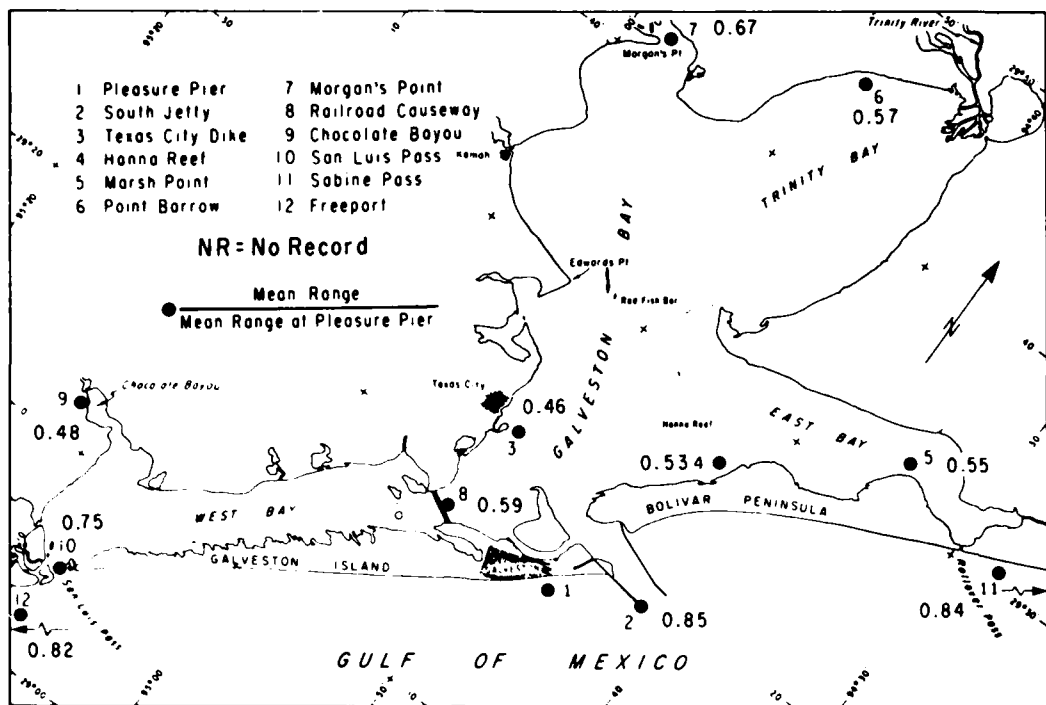


Figure 56. Galveston Bay tidal range ratio distribution, average annual, 1974.

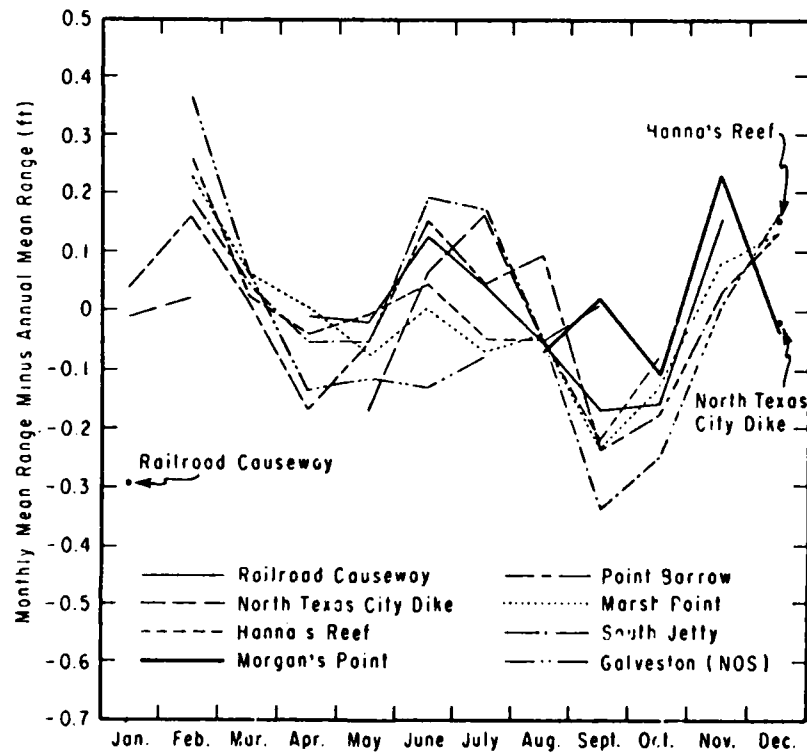


Figure 57. Galveston Bay monthly mean tidal range variability, 1974.

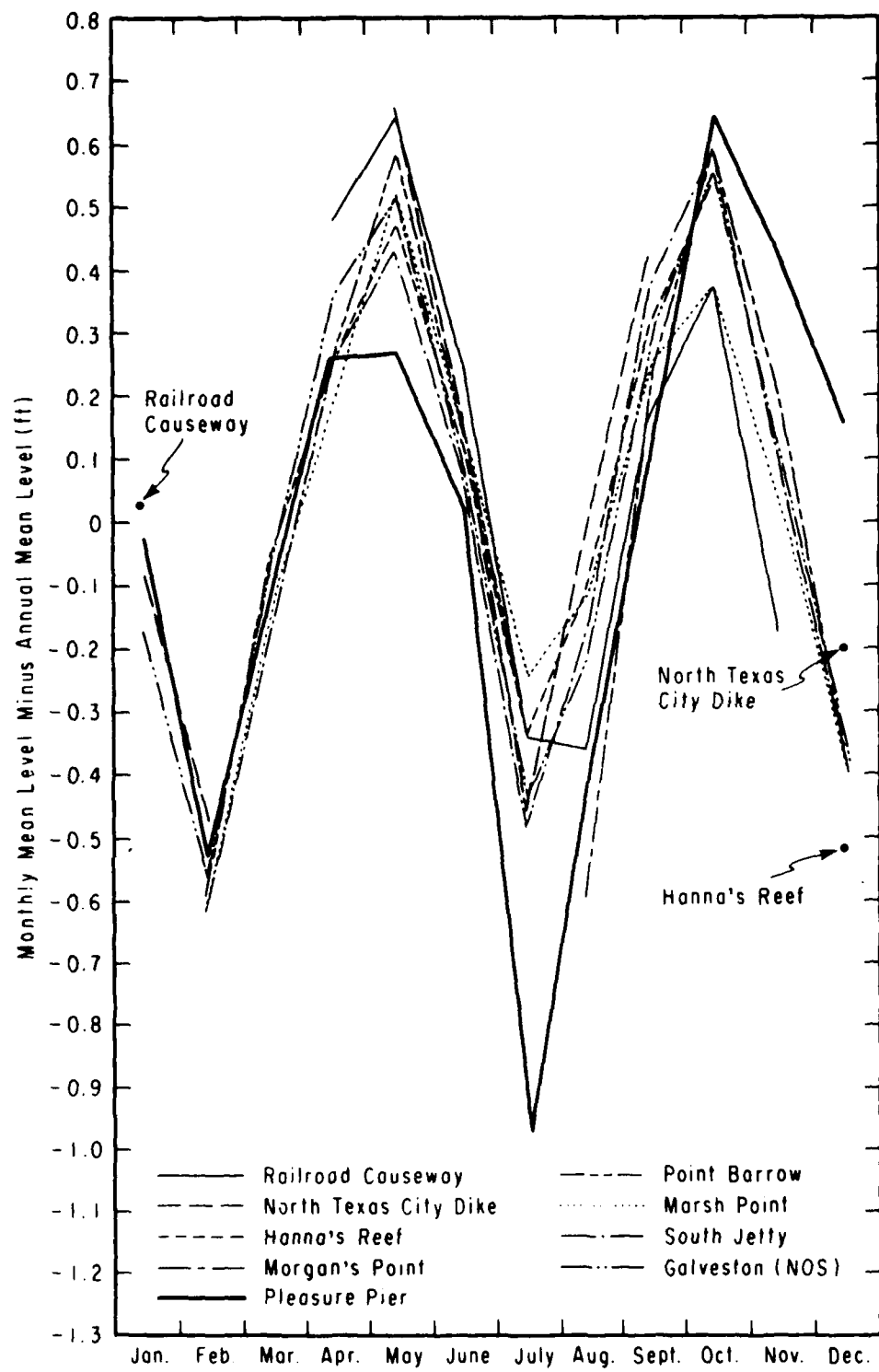


Figure 58. Galveston Bay monthly mean water level variability, 1974.

Table 6. Galveston Bay entrance hydraulic characteristics.

Date	Tide condition	Tidal prism (ft <sup>3</sup> x 10 <sup>9</sup> )	Minimum cross- sectional area (ft <sup>2</sup> x 10 <sup>5</sup> )	$\bar{V}$ <sup>1</sup> (ft/s)	$\bar{V}_{max}$ <sup>2</sup> (ft/s)
1877	Mean range	7.6	1.4	1.22	1.92
1891	Diurnal	10.7	1.6	1.50	2.36
	Mixed	3.7		1.1	1.75
1895	Mean range	6.0	1.6	0.84	1.33
1900-15	Hurricanes	196.0	---	---	---
1936	Diurnal	13.0	1.7	2.5 <sup>3</sup>	4.0 <sup>3</sup>
	Norther	41.0	---	1.7 <sup>4</sup>	2.7 <sup>4</sup>
1962	Diurnal	10.6	1.9	2.34	3.64

<sup>1</sup>Computed from  $\bar{V} = \frac{P}{A_c(T/2)}$  where T is tidal period, P tidal prism, and  $A_c$  cross-sectional area.

<sup>2</sup>Computed from  $\bar{V}_{max} = \frac{\pi}{2} \bar{V}$ .

<sup>3</sup>Measured.

<sup>4</sup>Predicted.

<sup>5</sup>Period unknown.

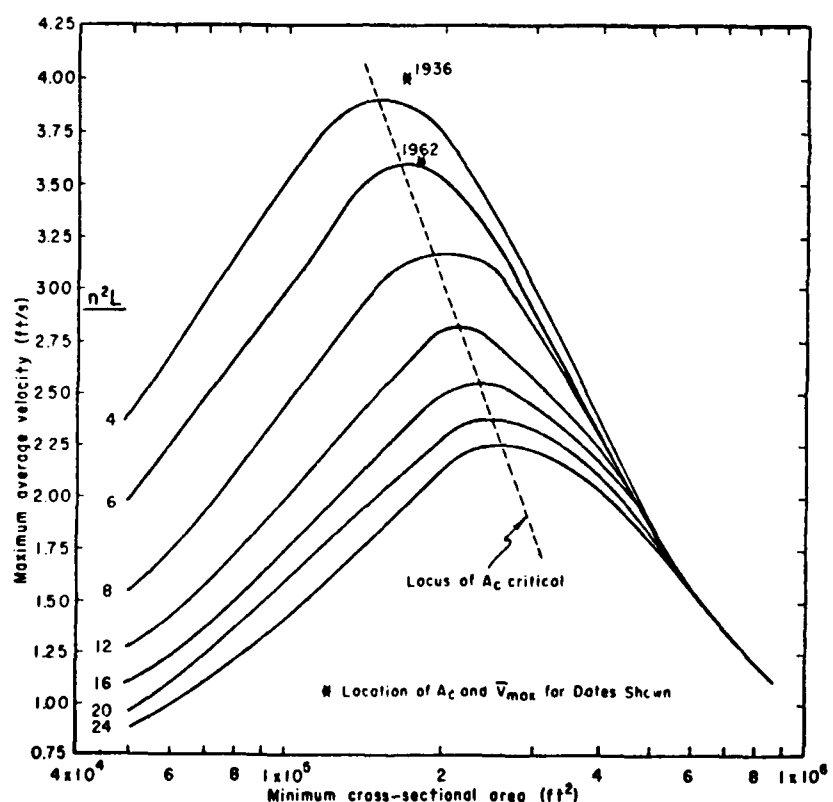


Figure 59. Average maximum velocity versus minimum cross-sectional area, Galveston Bay entrance, Texas.

value of 0.025 for Manning's  $n$ , these curves represent deposition lengths of between 6,400 and 38,400 feet. Note that the actual values of  $\bar{V}_{max}$  and  $A_c$  critical fall above the curve  $n^2 L = 6$ . Thus for  $n = 0.025$ , the predicted deposition length is less than 19,200 feet; the actual length is about 35,000 feet. Thus, the theoretical stability does not match actual conditions, perhaps because of the jetty's effect on longshore sediment transport into the inlet.

d. Summary. In its natural state, Galveston entrance was a typical downdrift offset inlet, similar to most inlets on the upper Texas coast. Jetty construction caused extensive changes in the ebb tidal delta, with a tripartite pattern of downdrift deposition offshore and in the fillet, and erosion between these zones, and updrift deposition. This entrance appears to effectively block any net westward transport to the beaches on Galveston Island; longshore sediment transport is directed toward the inlet from both the north and south sides. However, extensive sand deposits in the south fillet and along the inside of the south jetty could be dredged and pumped or hauled to nourish Galveston beaches.

After a period of relative stability, the minimum cross-sectional area of the entrance increased about 30 percent between 1933 and 1974 which, with an essentially constant width, increased the hydraulic radius by about the same amount. Most of this change presumably resulted from dredging, although construction of the Texas city dike (see Fig. 44) may have changed the ebb flow direction sufficiently to increase the throat area. Limited data indicate that, contrary to expectations, the tidal prism did not increase proportionately.

#### 4. Rollover Pass.

a. Historical Review. Rollover Pass (Fig. 56), an artificial pass connecting Rollover Bay to the Gulf of Mexico about 22 miles northeast of Galveston, was constructed by the Texas Parks and Wildlife Department to enhance fish migration into East Bay and improve bay water quality and salinity. A number of reports have been published on the characteristics and behavior of Rollover Pass, the three most comprehensive being those by U.S. Army Engineer District, Galveston (1958), Prather and Sorensen (1972), and Lockwood, Andrews, and Newnam, Inc. (1974). The following brief historical review is quoted from the latter report:

"Engineering and ecological studies prior to 1954 established the feasibility and desirability of a tidal inlet at this location. The pass was constructed between October 1954 and February 1955. It had an 80-foot bottom width and an 8-foot depth. Sloping earthen sides were constructed except for the southwest side which was protected by a steel sheet pile bulkhead.

"Unusually high tides during 1955 resulted in extensive erosion of the pass. The Gulf entrance widened to about 500 feet and the depth of water under Highway 87 bridge increased to 30 feet. In November 1955, in an effort to stop erosion, a steel sheet pile wall (sill) was constructed across the pass 40 feet south of the Highway bridge. Alternate sheet piles of this sill were driven 2 feet below mean sea level (MSL) to permit some water flow through the pass. A short steel sheet

pile groin was constructed about 350 feet northeast of the inlet centerline on the Gulf side to stop further erosion of beach front and to protect nearby summer homes.

"The Pass remained partially closed until July 1958 while the Corps of Engineers was preparing recommendations for its stabilization. Their report was published in April 1958. The report proposed constructing steel sheet pile bulkheads along both sides of the pass, north and south of the highway bridge, installation of a second sill across the Gulf entrance, and periodic deposition of sand on the Gulf beach area southwest of the pass to replace material lost through littoral drift processes. These recommendations were implemented between July 1958 and May 1959, with the exception of beach nourishment.

"The Pass has remained open since 1959 in a relatively stable condition to this date. Anticipating the gradual weakening of the steel bulkheads through corrosion, Texas Parks and Wildlife Department constructed a concrete retaining wall behind the southwest steel bulkhead in 1966. A similar concrete wall was installed behind the southeast bulkhead in 1972. These concrete walls extend from the highway bridge to a point 600 feet south."

b. Beach Changes. Between 1882 and 1974, beaches within about 10 miles north and 7 miles south of the pass eroded at a rate of about 5 feet per year (Morton, 1975); however, erosion rates since the pass was created have been greater, although estimates differ. Morton (1975) found that rates varied between 15 and 25 feet per year; rates developed for the Galveston County Shore Erosion Study being conducted by the Galveston District varied between 7 and 14 feet per year. The volume losses associated with this erosion were established from the following analysis of beach profiles.

Profiles near Rollover Pass were published by Lockwood, Andrews, and Newnam, Inc. (1974), and profiles for the High Island area by the U.S. Army Engineer District, Galveston (1975). The annual rates of volumetric change per longshore foot of beach were plotted from a planimeter of the area between the earliest profile and the latest profile at each station (Fig. 60). At High Island, the average rate of volume change between 1967 and 1973 was 2.3 cubic yards per foot per year. The rate for the two profiles just updrift of Rollover Pass was about 1.5 cubic yards per foot per year. If an average rate of about 2 cubic yards per foot per year is assumed to represent the noninlet-related beach erosion, profile data show that higher rates occur downdrift at least as far west as station 2000W (see Fig. 60). Although no profile data between stations 2000W and 14000W were available, the plot of shoreline recession rates shows that erosion can be assumed to decrease linearly toward station 14000W. Thus, the shaded area in Figure 60 represents the annual volume loss from the longshore transport system due to inlet processes, i.e., about 26,000 cubic yards.

c. Tide Characteristics.

(1) Summary of Hydraulic Data Collection. The earliest tide measurements in the vicinity of Rollover Bay were reportedly obtained between 1887 and 1890 but were not published (U.S. Army Engineer District, Galveston, 1942). Since other preinlet data were available, no attempt was made to locate these measurements.

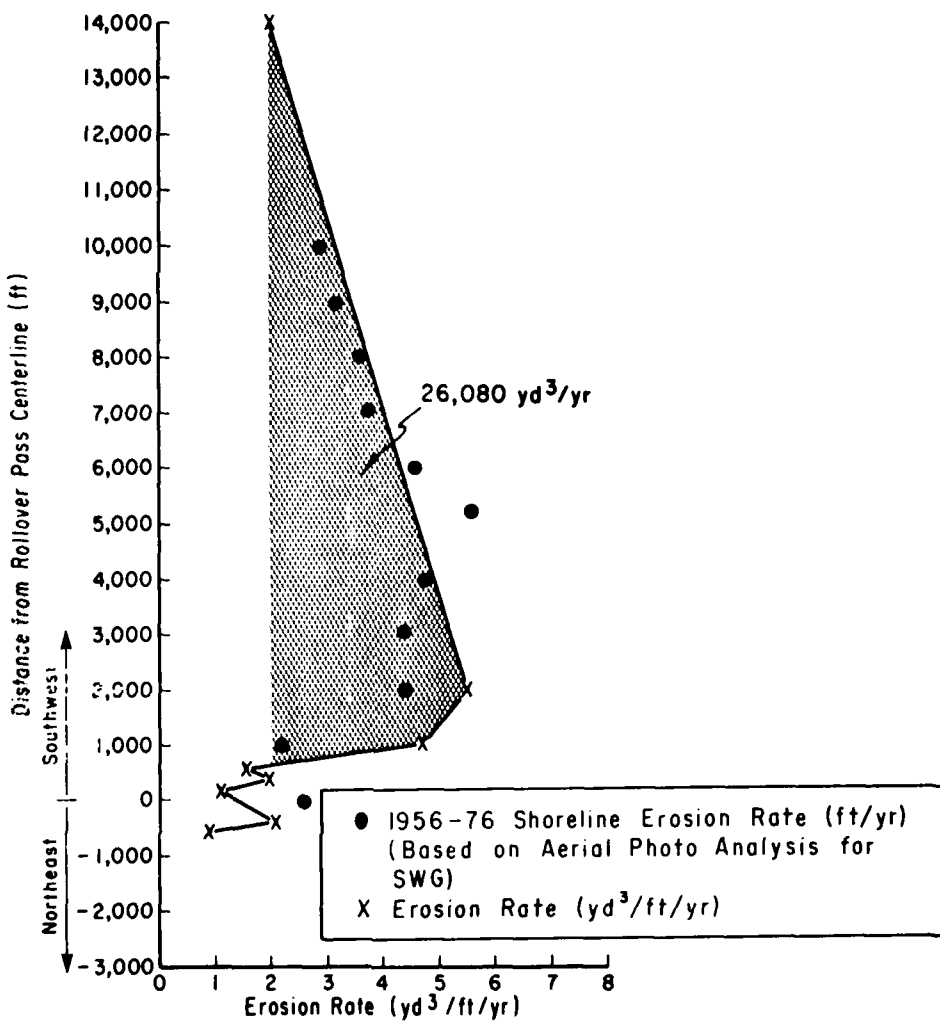


Figure 60. Comparison of beach profile and aerial photo erosion rates.

Tide data were collected in Rollover Bay between September 1936 and October 1937 by the Galveston District as part of a comprehensive measurement program. The first tidal data collected after Rollover Pass opened in 1955 were obtained from May 1956 to April 1957 from an SWG gage located in Mud Bayou, about 10 miles east of Rollover Pass. Between 21 November 1956 and 19 February 1957 gages were also operated in the Gulf of Mexico at Gilchrist and in Rollover Bay. Gages usually provide an excellent record of the hydraulics of a bay; however, the tide curves in the U.S. Army Engineer District, Galveston (1958) revealed a serious malfunction in the Rollover Bay gage, making the bay data unusable. In October 1962, the Galveston District began a comprehensive tide gaging program to continuously monitor water levels at many coastal locations. Tide data from the SWG South Jetty and Marsh Point (East Bay) gages are complemented by NOS data collected at Gilchrist (East Bay) in March and April 1965.

Tidal currents were measured in the pass on 4 and 5 May 1965 by the Galveston District in connection with a physical modeling program of a

hurricane protection system. Simultaneous tidal data are available for the SWG South Jetty and Marsh Point gages.

Between November 1971 and February 1972 Prather and Sorensen (1972) operated tide gages in Rollover Bay, and at selected times measured current speeds in the pass. Tide data are plotted in the report, but no current data were published.

(2) Data Analysis and Results. The present-day hydraulics of Rollover Pass were defined, and preconstruction and postconstruction data were compared to determine any effect of inlet construction on the bay's hydraulics. Tables 7 and 8 summarize the available information on tidal ranges and lags in the vicinity of Rollover Pass. Before the pass was constructed, Rollover Bay was filled entirely by water entering the Galveston entrance. Tidal lags were about 1.3 hours longer than postconstruction conditions, and bay tidal ranges were about 23 percent less than in 1965. In comparing two postconstruction conditions (1965 and 1974) the bay tidal ranges were greater for the earlier years, and the tidal lags were shorter, indicating that the efficiency of the pass to fill the bay decreased. Another indication was the lag between the Gilchrist and Marsh Point gages. In 1965, this time difference was 0.35 hour, while in 1971-72 Prather and Sorensen (1972) computed the difference to be about 0.8 hour. Their study also discussed the propagation of the tide into East Bay. They found that high and low waters occurred first in Rollover Bay, then at Marsh Point, and finally at Hanna Reef, indicating that East Bay tides were influenced primarily from flow through Rollover Pass, an unusual condition in view of the pass's small effect on tidal range. To evaluate this conclusion, tidal lags between Marsh Point and Hanna Reef were calculated for the period 16 July to 9 September 1974. On the average, tide extremes at Hanna Reef lagged those at Marsh Point by about 0.3 hour. However, many times the reverse was true, and it appeared that the direction of tide propagation was influenced by at least two factors--bay water level and wind effects. Figure 61 is a plot of the tidal lag between Marsh Point and Hanna Reef versus the average daily water level at Marsh Point, computed as the mean of the diurnal high and low. Note that for levels greater than +1 foot MSL, tide extremes usually occur at Marsh Point first, while for lower levels they are evenly distributed.

Seasonal variability in tide level and tidal range is plotted in Figures 62 and 63, respectively, for Marsh Point and Galveston South Jetty gages in 1974. Note the close correspondence in level variation. Range variability is also similar except during June and July, when tidal ranges were below normal at Marsh Point.

d. Tidal Hydraulics. Tide and current data collected in 1965 by the Galveston District were compared with 1971 data by Prather and Sorensen (1972). The 1965 velocity measurements were made from the bridge channel centerline at three depths, between 0530 hours, 4 May and 1300 hours, 5 May 1965. A plot of the average velocity variation is shown in Figure 64. Also plotted are the tidal curves for the Galveston South Jetty and Marsh Point locations. Note the strong predominance of flood currents (flood prism =  $3.8 \times 10^8$  cubic feet, ebb prism =  $6.7 \times 10^7$  cubic feet), due to 15- to 20-mile-per-hour winds from the south during the entire measurement period. Table 9 summarizes the 1965 measurements. Using the velocity and tidal

Table 7. Tidal ranges and tidal lags, Rollover Pass.

Date	Location	Tidal range (ft)	Ratio of ranges, Jetty	Average ratio
Nov. 1936	South Jetty	1.97	1.0	
	Rollover Bay	1.23	0.62	0.57
June 1937	South Jetty	2.07	1.0	
	Rollover Bay	1.08	0.52	
Mar. 1965	South Jetty	1.74	1.0	
	Gilchrist	1.16	0.67	
	Marsh Point	1.21	0.70	
Apr. 1965	South Jetty	1.54	1.0	
	Gilchrist	1.13	0.73	
	Marsh Point	1.12	0.73	
1974	South Jetty	1.91	1.0	
	Marsh Point	1.20	0.63	
	Hanna Reef	1.16	0.61	0.63

Table 8. Tidal lags, Rollover Pass.

Date	Location	Tidal lags (hr from reference station)			
		High water	Low water	Average	
Reference station: South Jetty					
1936-1937	Rollover Bay				
Nov. 1936		4.31	5.7	4.0	4.95
June 1937		3.7	4.20		
1965	Rollover Bay				
	Gilchrist (Bay)				
Mar. 1965		3.0	4.5	2.65	3.75
Apr. 1965		2.3	3.0		
1965	Marsh Point				
Mar. 1965		3.3	4.8	2.95	4.15
Apr. 1965		2.6	3.5		
Reference station: Gilchrist (Bay)					
Mar.-Apr. 1965	Marsh Point	0.3	0.4	0.35	
Nov. 1971-Feb. 1972		---	---	0.8	
Nov. 1971-Feb. 1972	Hanna Reef	---	---	1.7	
Reference station: Marsh Point					
Nov. 1971-Feb. 1972	Hanna Reef	----	----	0.9	
16 July-9 Sept. 1974		0.22	0.36	0.29	

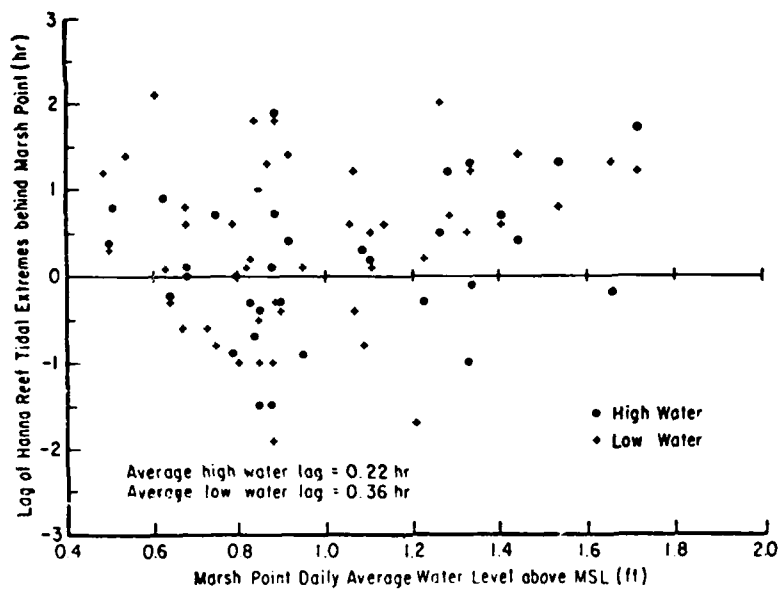


Figure 61. Tidal lags versus water level,  
16 July-9 September 1974.

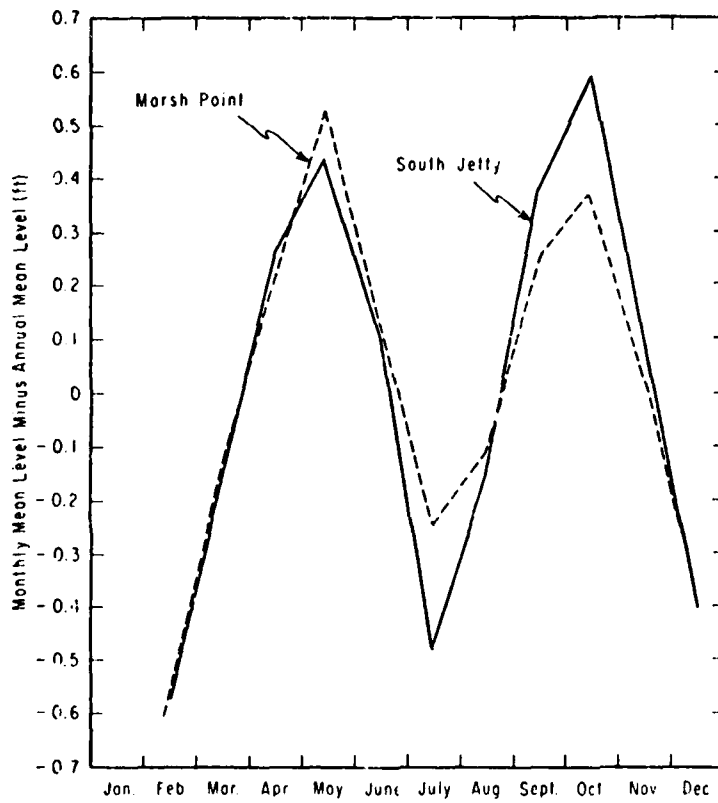


Figure 62. Rollover Pass monthly mean tide level variability, 1974.

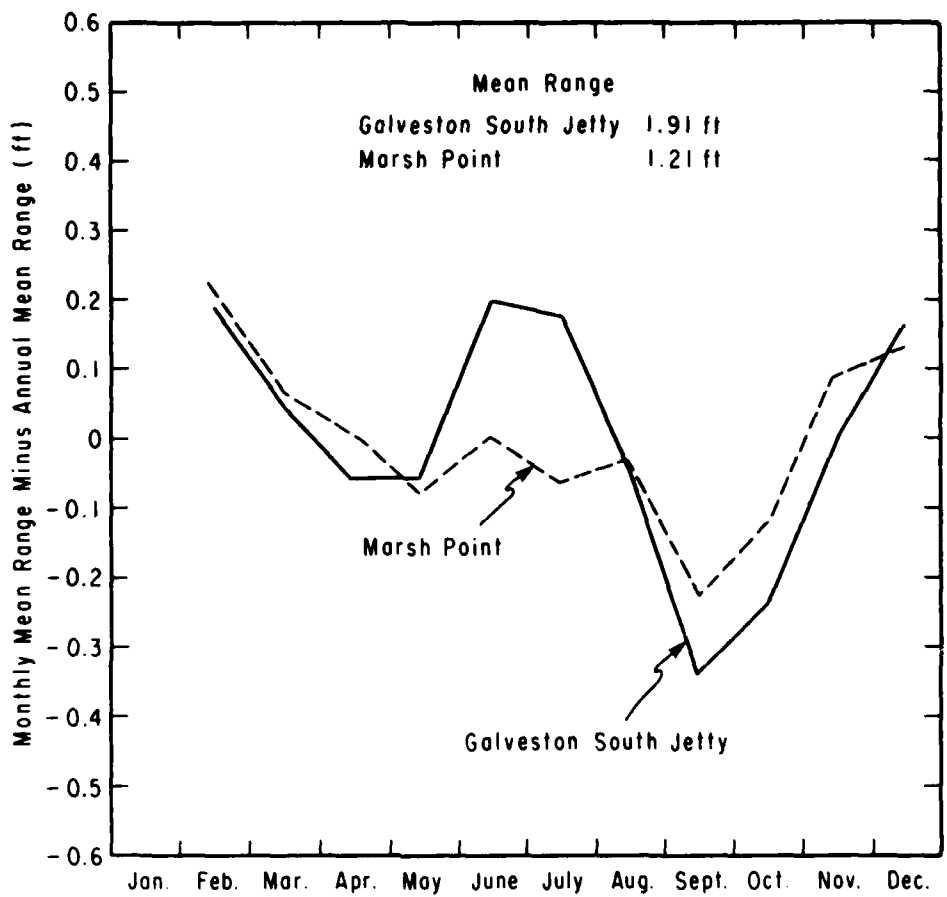


Figure 63. Rollover Pass monthly mean tidal range variability, 1974.

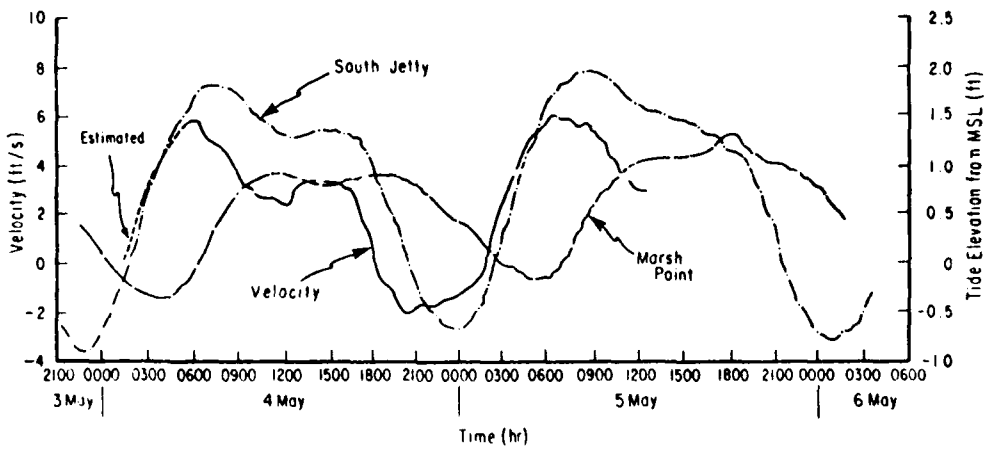


Figure 64. Tides and currents at Rollover Pass, 4 and 5 May 1965.

Table 9. Summary of Rollover Pass hydraulic data.

Tidal data by date	Flow area (ft <sup>2</sup> )	Average head differential (ft)	Average velocity (ft/s)	Maximum average velocity (ft/s)	Tidal prism (ft <sup>3</sup> )
4 and 5 May 1965	1,900				
Flood		0.67	3.26	6.02	3.8 x 10 <sup>8</sup>
Ebb		0.80	1.22	1.95	6.7 x 10 <sup>7</sup>
1971					
One tidal cycle (Prather and Sorensen, 1972)	1,130	1.5	2.71	4.23	----- 1
Nov. 1971-Feb. 1972	1,290	0.67	3.1 <sup>2</sup>	-----	1.8 x 10 <sup>8</sup> 2
			0.67	-----	3.8 x 10 <sup>7</sup> 3

<sup>1</sup>Unknown.<sup>2</sup>Predicted from 1965  $\bar{V}$  versus  $\Delta H$ .<sup>3</sup>Predicted by Prather and Sorensen (1972).

differential data, the total friction loss through the inlet during the 1965 measurements was determined. Manning's friction coefficient is given by

$$n = \frac{1.49R^{2/3} \Delta H^{1/2}}{\bar{V} L^{1/2}} \quad (9)$$

where

R = hydraulic radius

 $\Delta H$  = head differential between bay and gulf $\bar{V}$  = average velocity through the pass

L = inlet length

Throughout the tidal cycle, L, n, and R are assumed to remain constant which means  $\bar{V}$  varies as a function of  $\Delta H^{1/2}$ . To find the function, all instantaneous values of  $\bar{V}$  and  $\Delta H^{1/2}$  were plotted (Fig. 65). A line was best fit to the points using a linear regression analysis, and the slope of the line was substituted into equation (9), using values of R = 6.5 feet and L = 1,200 feet. The resulting value of n was 0.032, which includes the resistance due to the weir.

Velocity measurements by Prather and Sorensen (1972) were made 500 feet north of the bridge at two depths at eight locations across the channel. Although instantaneous current data were not published, the data were calculated from plotted discharge values and the assumed average cross-sectional area of 1,130 square feet. In plotting the data in Figure 65, note that although the best-fit line does not pass close to the origin, the slope of the line is almost exactly the same as that for 1965, indicating the same value of Manning's n of 0.032. Table 9 summarizes the 1971 hydraulic parameters by Prather and Sorensen (1972) for both their tidal cycle measurements and their predicted long-term averages. Note also that because of their average velocity versus head difference relationship, their long-term average tidal prism was only one-tenth of the 1965 prism, and only about one-fifth of the prism calculated using their average differential and the 1965 relationship. In view of commonly reported high-velocity conditions in the pass, it is

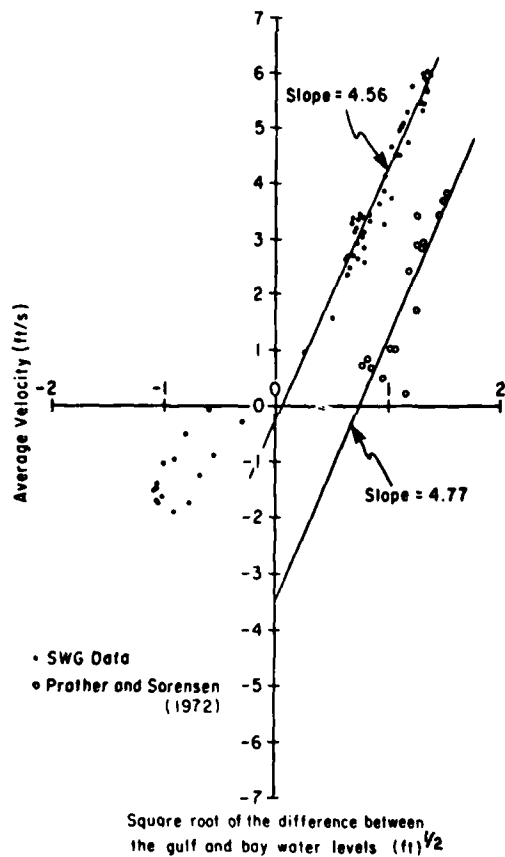


Figure 65. Relationship between average velocity and head difference, Rollover Pass.

concluded that the actual average velocities are closer to the 3.1 feet per second predicted using the 1965 relationship than to the 0.66 calculated by Prather and Sorensen (1972).

e. Inlet Stability.

(1) Observed. Rollover Pass, when first built, was in an extremely unstable erosion condition. However, with the artificial stabilization of the banks by sheet pile and the cross-channel weir, velocities were reduced and further erosion was halted. Figure 66 shows the variation in cross-sectional area at four locations since 1957. The minimum cross-sectional area, always located at station 500S (see Fig. 66), has been constant since 1963; however, Prather and Sorensen (1972) showed that between 1968 and 1971 the deepest part of the channel south of the weir moved from the east to the west side. In addition, a deep scour hole just south of the weir in 1968 shoaled extensively by 1971, reducing the maximum depths from 28 feet to only about 12 feet (Fig. 67). This shoaling, combined with a possible increase in the inlet length due to deposition in Rollover Bay, may be the cause of the decreased efficiency of the pass (i.e., lower bay ranges and longer lags) which occurred between 1965 and 1971.

(2) Theoretical. O'Brien and Dean's (1972) stability method was used to predict the response of Rollover Pass to sedimentation. The most difficult

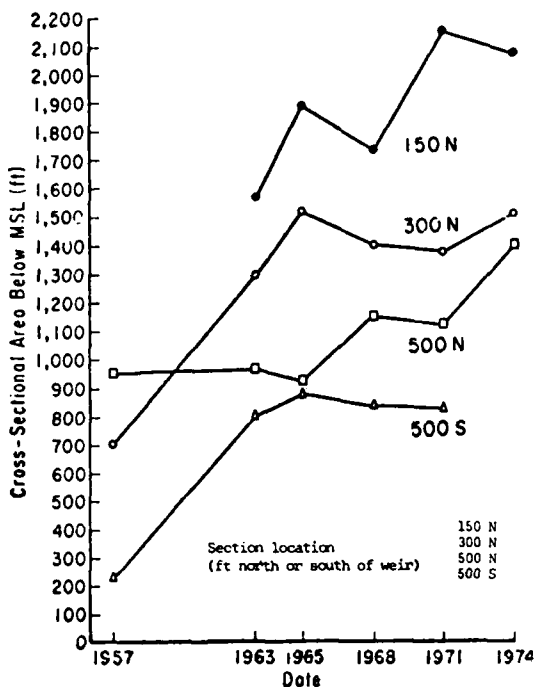


Figure 66. Time history of cross-sectional area changes by section location (in feet north or south of weir, e.g., 150 N) Rollover Pass, 1957-74.

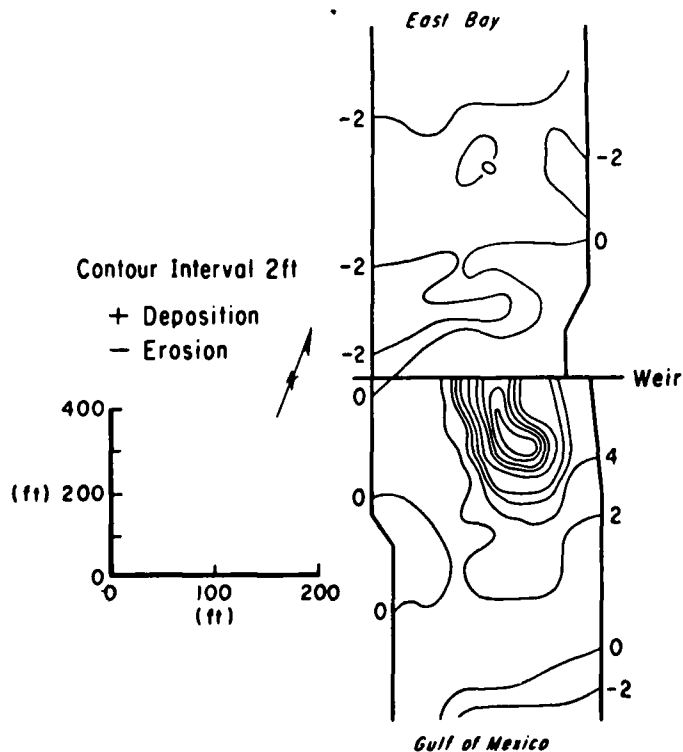


Figure 67. Depth changes, Rollover Pass, Texas, July 1968-winter 1971-72 (after Prather and Sorensen, 1972).

parameter to determine for Rollover Pass was the effective bay area, since East Bay fills both from the pass and from Galveston entrance. Before the inlet was cut, the ratio of Rollover Bay tidal range to Galveston South Jetty gage was 0.57. In 1971, this ratio was 0.63. Therefore, it is assumed that the difference is due to flow through Rollover Pass, or that the effective range due to this flow equals (0.63 minus 0.57) times the South Jetty range. From continuity, the effective bay area is equal to the tidal prism divided by the effective range. Using the 1971 average prism of  $1.8 \times 10^8$  cubic feet and an effective range of 0.06 (2) = 0.12 foot, an effective area of  $1.5 \times 10^9$  square feet is found, which is exactly the same as the measured area of East Bay.

Letting the minimum inlet width remain constant at 200 feet (i.e., letting the hydraulic radius vary directly with  $A_c$ ), values of the maximum average velocity and minimum cross-sectional area are plotted in Figure 68 for an inlet length of 1,200 feet, bay area of  $1.5 \times 10^9$  square feet, tidal period of 89,400 seconds, and Manning's  $n$  of 0.032. Also plotted are measured values of  $\bar{V}_{max}$  and  $A_c$  min. Note that the theoretical curve does not agree with actual values. Better agreement could be achieved if the curve was developed using a much smaller bay area. For instance, if the bay range was assumed to result only from flow through Rollover Pass, then the effective bay area filled by this flow would be about  $4 \times 10^8$  square feet. This would produce a stability curve, shown as the dashline in Figure 68, which exactly fits the field data. In either case, the pass is on the unstable side of the critical cross-sectional area.

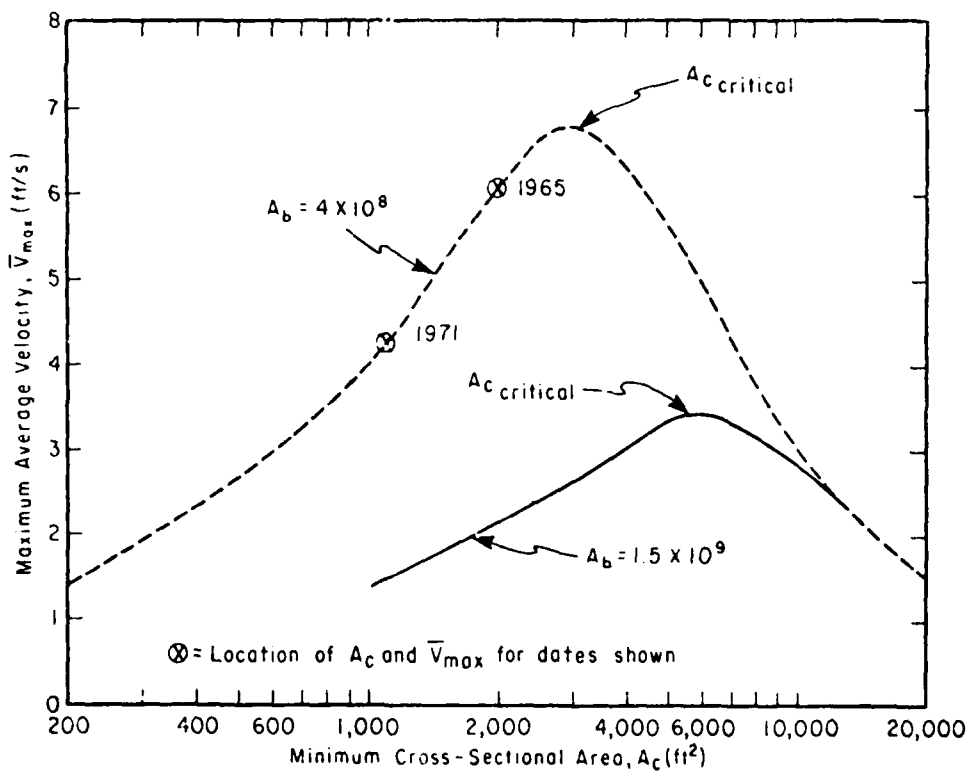


Figure 68. Average maximum velocity versus cross-sectional area, Rollover Pass, Texas.

Jarrett's (1976) relationship between equilibrium cross-sectional area and tidal prism gives an equilibrium area of 4,400 square feet for the 1971 tidal prism, which is considerably larger than the minimum area has ever been at the pass. Thus, without the weir section in the throat, the inlet could be expected to resume its initial unstable scour mode.

f. Summary. The construction of Rollover Pass has affected the adjacent downdrift beach, producing a deficit of about 26,000 cubic yards per year in the net longshore sediment transport rate. The minimum cross-sectional area, about 875 square feet, has remained relatively constant, although the seaward part of the pass experienced extensive deposition in recent years. Unfortunately, the lack of long-term velocity data in the pass precludes determining the predominance of flood or ebb flows, as well as an accurate portrayal of the current speed characteristics. Limited sand-size distribution data indicate that material deposited in Rollover Bay is probably finer than that on the gulf beaches. Additional samples should be taken if nourishment of adjacent beaches with bay shoal material is contemplated.

##### 5. Sabine Pass.

a. Historical Review. Sabine Pass, on the Texas-Louisiana border, is a tidal inlet about 7 miles long and 2,000 to 5,000 feet wide, connecting Sabine Lake to the Gulf of Mexico. The Sabine and Neches Rivers empty into the north end of Sabine Lake, contributing an average of 14,650 cubic feet per second of freshwater to the system. During storms, discharges exceed 200,000 cubic feet per second. Unlike the other inlets considered, where sand bottoms predominate, the ebb tidal delta and offshore areas at Sabine Pass are comprised of thick layers of mud. Net longshore transport is to the west. Figure 69 shows the longshore and shore-normal components of the monthly resultant winds for the Sabine Pass (Port Arthur) shoreline orientation for 1973. Note the strong westward longshore component which agrees with the net longshore sediment transport direction.

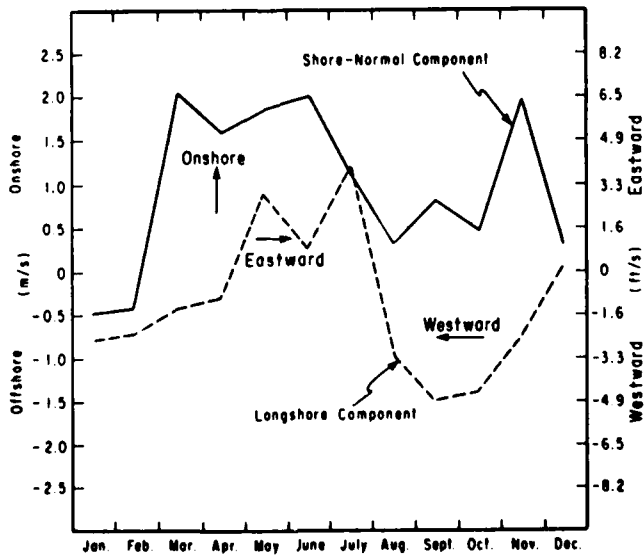


Figure. 69. Longshore and shore-normal components of monthly resultant wind, Sabine Pass (Port Arthur), Texas, 1973.

The first USC&GS chart of Sabine Pass, made in 1840 (Fig. 70,a), indicates that the controlling depth was less than 6 feet, with a small, symmetrical ebb tidal delta. Under the original improvement plan, an entrance channel 12 feet deep, 150 feet wide, and 2.5 miles long, was to be maintained through the bar. However, yearly dredging between 1876 and 1881 failed to maintain the desired channel dimensions. Construction of two jetties began in 1883, and by 1885 they had extended 13,000 feet gulfward (Fig. 70,b). Between 1840 and 1885 (Fig. 71,a) extensive deposition occurred in the nearshore zone on the west (downdrift) side, and in an updrift fillet adjacent to the toe of the east jetty. Over the years, the jetties were extended, raised, and repaired, reaching their present lengths in 1929, with an 1,800-foot width at their gulfward ends. Jetty construction has not produced the scouring action necessary for enhanced self-maintenance, and dredging has been required almost yearly since 1893.

Following jetty construction, large fillets (1.7 million and 5.8 million cubic yards) formed on both the west and east sides of the entrance, respectively, with extensive offshore deposition (5.1 million cubic yards) west of the jetty ends (Fig. 71,b). Erosion occurred seaward of the fillet on the east side and between the fillet and deposition zone on the west. Blackman (1938) attributed the west-side deposition to two principal causes. First, longshore currents carrying very fine suspended material can more readily retain it in suspension and carry it around and past the jetty ends for deposit in the quieter waters west of the jetties. Second, much dredge spoil has been deposited adjacent to the west jetty. More recent nearshore changes (1966 to 1974) have been minor (Fig. 72)--a small area of deposition updrift of the jetties and about 12,000 feet offshore.

b. Tide Characteristics.

(1) Summary of Hydraulic Data Collection. The first SWG tide measurements at Port Arthur began on 29 December 1934 and continue to date. NOS installed a control station tide gage in the pass in June 1958; the gage has also operated continuously. SWG installed a continuously operating, permanent gage on the southwest jetty in May 1965. Locations of these and other tide and current measurement points are shown in Figure 73.

Between June 1960 and April 1961, NOS operated a gage near the end of the southwest jetty. This station was reestablished with a portable NOS gage between 22 July and 26 August 1962, in connection with extensive current measurements taken by NOS between 17 and 23 July. A temporary NOS gage was also operating at Mesquite Point between 18 July and 9 August. In July 1966, SWG installed a gage at the north end of Sabine Lake; the gage has operated continuously since then.

Tide data for the representative year (1974) at other locations were incomplete for the Port Arthur gage, so 1973 data were used to examine variability in the tidal ranges and levels at four stations in the Sabine Pass-Lake system. Unfortunately, the NOS pass gage was operational only between March and August 1973.

Finally, results of recent hydraulic studies were obtained from Ward and Johnston (1977) and Ward and Chambers (1978).

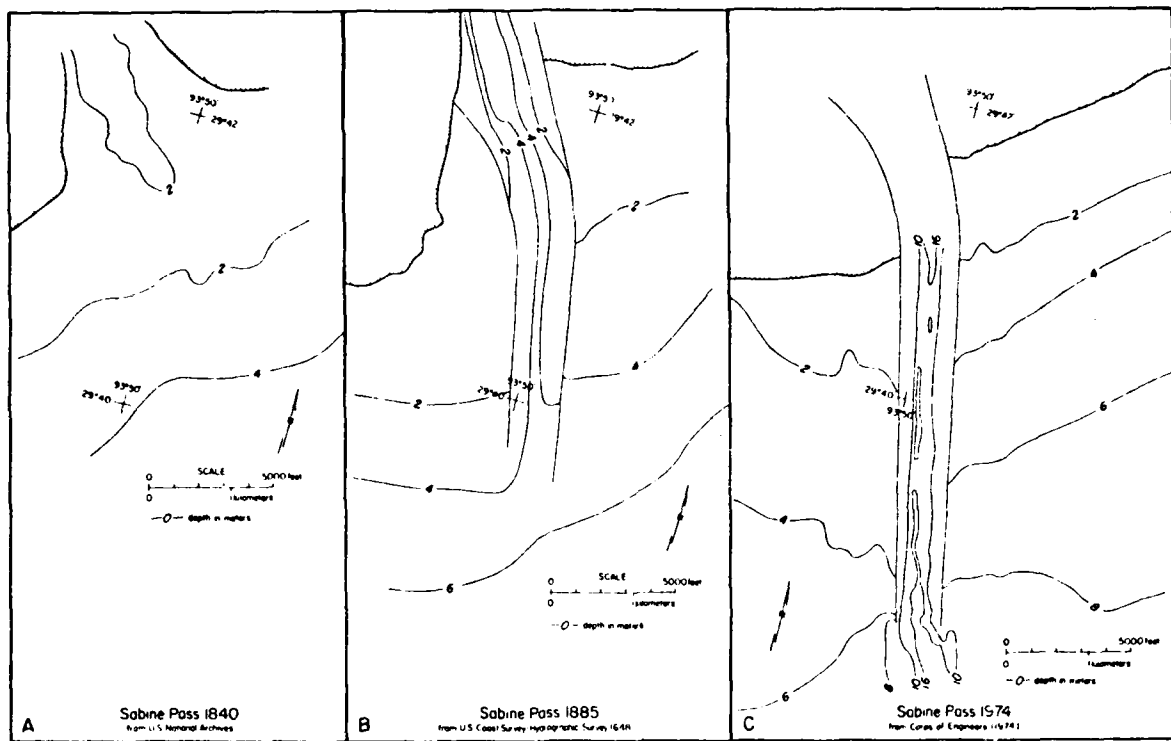


Figure 70. Bathymetry, Sabine Pass (after Morton, 1977).

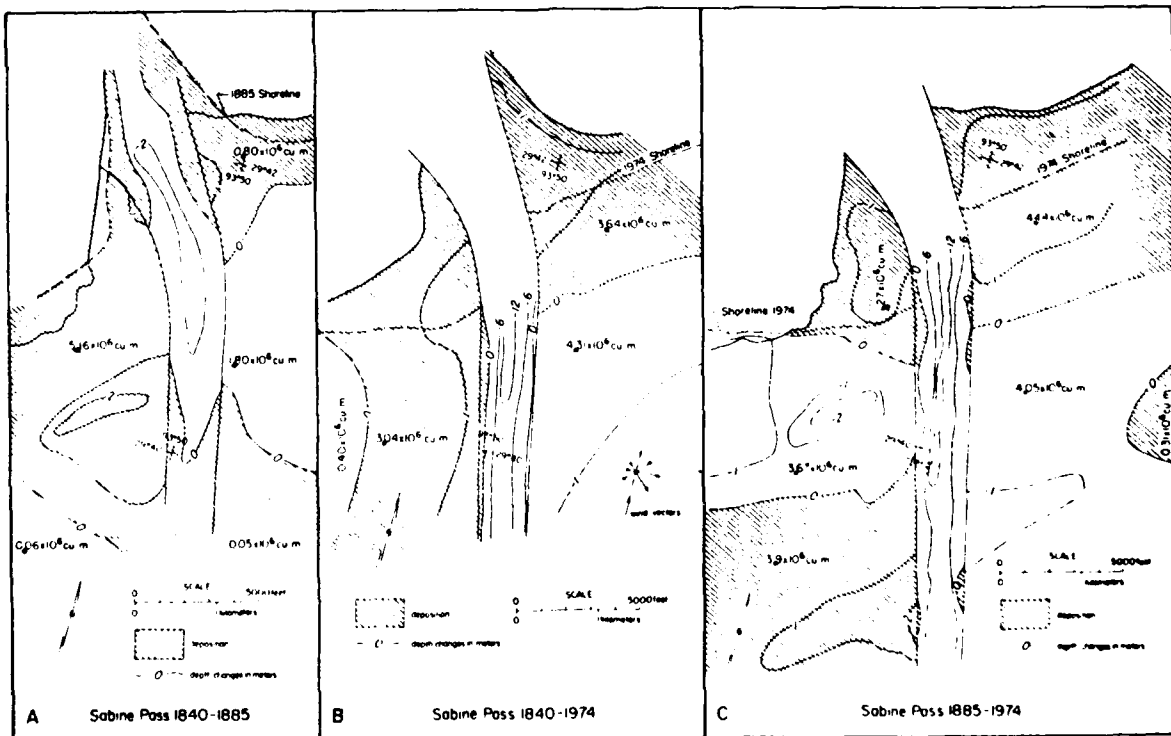


Figure 71. Nearshore changes, Sabine Pass (after Morton, 1977).

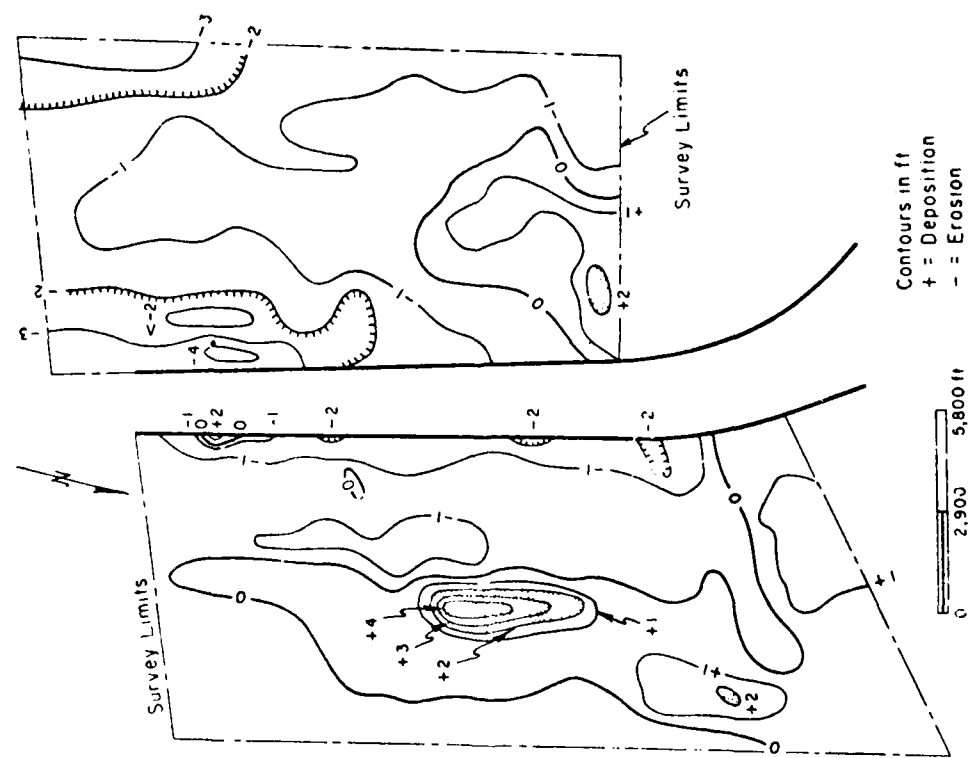
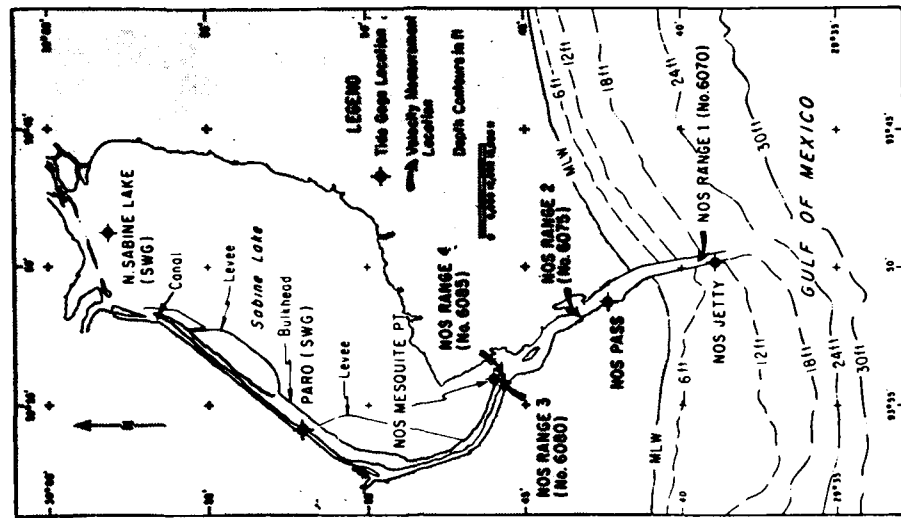


Figure 72. Sabine Pass fill and scour, 1966-74.

Figure 73. Tide gage locations, Sabine Pass, Texas.

(2) Data Analysis and Results.

(a) Tidal Ranges and Levels. Table 10 summarizes the available information on tidal ranges throughout the inlet-bay system. Long-term averages indicate that the tidal range at the Sabine Pass southwest jetty is about 95 percent of the range at the Galveston Pleasure Pier, and that the pier range is reduced another 10 percent midway through the pass. At Mesquite Point, the entrance to Sabine Lake, the tidal range during the short period record was about half that of the range at the jetty. However, long-term averages from other gages indicate that the Mesquite Point range usually exceeds 60 percent of the jetty range.

Table 10. Tidal ranges, Sabine Pass, Texas.

Date	Location and gage	Diurnal range (ft)	Ratio of ranges		
			Pier	Jetty	Pass
1936	Port Arthur (SWG)	0.94	----	----	----
June 1960-Apr. 1961 (excluding Jan.)	Galveston Pleasure Pier (NOS)	2.01	1.0	----	----
	Jetty (NOS)	2.30	1.14	1.0	----
	Pass (NOS)	1.80	0.90	0.78	1.0
23 July-9 Aug. 1962	Galveston Pleasure Pier (NOS)	2.12	1.0	----	----
	Jetty (NOS)	1.95	0.92	1.0	----
	Pass (NOS)	1.54	0.73	0.79	1.0
	Port Arthur (SWG)	0.83	0.39	0.43	0.54
	Mesquite Point (NOS)	1.03	0.49	0.53	0.67
Mar.-Aug. 1973	Galveston Pleasure Pier (NOS)	2.27	1.0	----	----
	Jetty (NOS)	2.18	0.96	1.0	----
	Pass (NOS)	1.90	0.84	0.87	1.0
	Port Arthur (SWG)	1.10	0.43	0.50	0.58
	North Sabine Lake (SWG)	0.91	0.40	0.42	0.48
1974	Galveston Pleasure Pier (NOS)	2.18	----	----	----
	Pass (NOS)	1.83	0.86	----	----

As shown previously in Figure 2, monthly tidal range variability at Sabine Pass (NOS gage) closely approximates that of other Texas locations. Incomplete data for 1973 (Fig. 74) indicate that the Port Arthur and north Sabine Lake gages respond similarly but differ in range characteristics from the NOS pass gage. In 1936, the Port Arthur gage data exhibited a different pattern of range variability (Fig. 75). Over the past 20 years, the pattern of annual mean range variability at Sabine Pass has differed significantly from that at Galveston and Freeport (Fig. 7). Thus, it appears that over the long term, minor variations in tidal range are caused by differing local meteorological conditions in the lake (wind, rainfall, etc.) rather than astronomical forces on gulf tides. Both short- and long-term patterns of tide level variability (Figs. 3, 4, and 76) are similar for all stations within the pass system.

(b) Tidal Phases. Average phase lags were computed from available data for the NOS Sabine Pass and jetty gages and for the SWG Port Arthur gage (Table 11). As expected, extremes occur at about the same times at the jetties and in the pass, while at Port Arthur they occur much later.

c. Tidal Hydraulics.

(1) Tidal Currents. NOS made extensive current measurements at the four ranges shown in Figure 73 between 17 and 22 July 1962. The data were

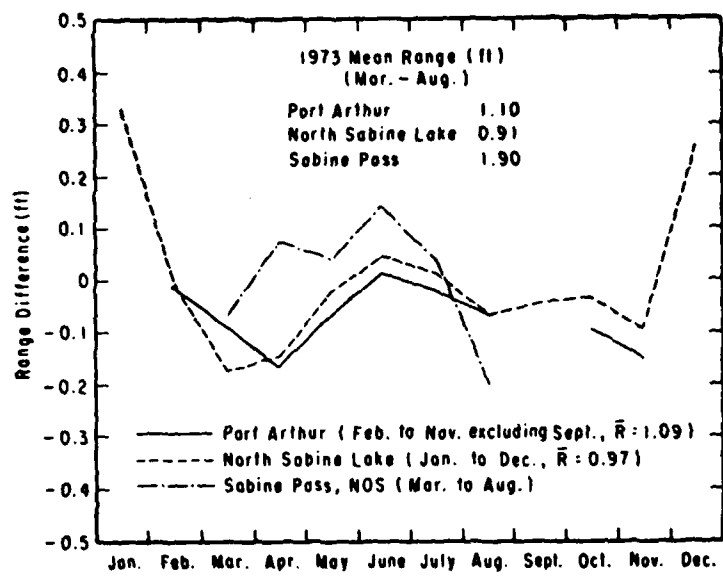


Figure 74. Sabine Lake monthly mean tidal range variability, 1973.

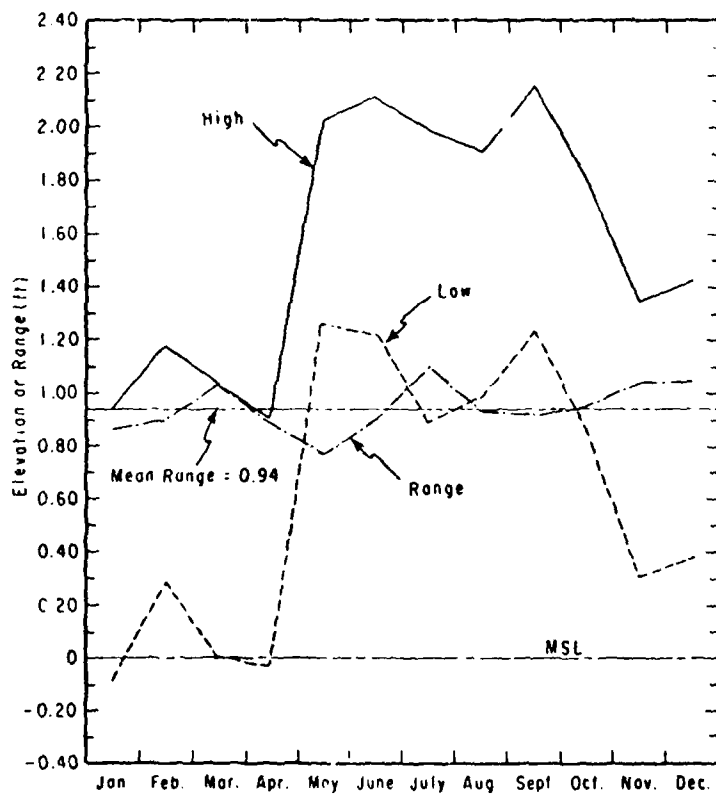


Figure 75. Mean monthly highs, lows, and ranges, Port Arthur canal SWG gage, 1936.

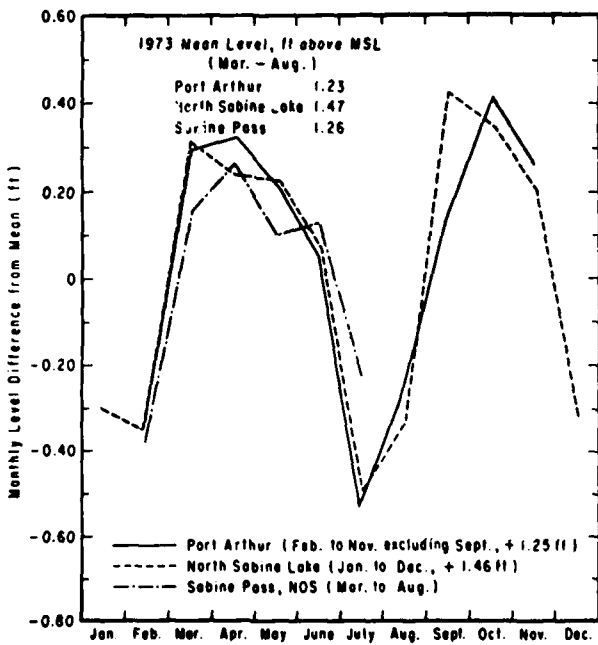


Figure 76. Sabine Lake monthly mean tide level variability, 1973.

Table 11. Tidal lags in Sabine Pass system, 23 July-5 August 1962.

Location	Tidal lag	
	High water (hr)	Low water (hr)
Sabine jetty	0.0	0.0
Sabine Pass	0.11	0.05
Port Arthur	3.5	2.7

taken at three depths (surface, middepth, and bottom) at each station; the stations were located near the center of the channel. Winds during the survey period were less than 10 miles per hour and variable in direction. Freshwater discharges from the Sabine and Neches Rivers were about 2,300 cubic feet per second, well below the 1961-65 average of 14,650 cubic feet per second. A plot of the surface currents is shown in Figure 77.

(2) Tidal Discharges and Prisms. Discharges through each range (see Fig. 73 for locations) were computed as follows: Cross-sectional profiles for NOS ranges 2, 3, and 4 were obtained from NOS chart 517 dated 12 February 1968, and for range 1 from dredging surveys made in 1962. For each ebb or flood phase, the areas under the velocity-time curves were planimetered. Because of the crudeness of the cross-sectional profiles at ranges 3 and 4, the discharge through each range was taken to be the product of the total cross-sectional area and the average of the three integrated areas under the velocity curve. At range 1, however, the current meter positions were plotted on each profile, and horizontal lines were drawn across the profile midway between the meter positions. The area within each of the three sections was

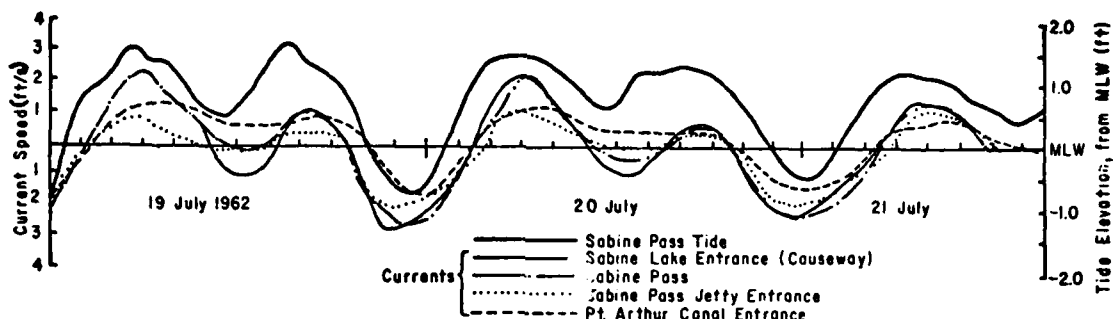


Figure 77. Tides and surface currents, Sabine Pass, Texas, 19-21 July 1962.

measured, and the discharge through the section was the product of that area and the integrated velocity-time area. The total discharge is the sum of the three discharges.

This same procedure was attempted at range 2, using a crude profile obtained from NOS chart 517. However, a quick comparison of discharges showed that range 2 values were considerably lower than range 1, apparently due to an incorrect cross-sectional area. Therefore, an "effective" cross-sectional area for range 2 was determined as follows: First, the average ebb-to-flood discharge ratio at range 1 was 1.24; the ratio at range 2 was very close to unity. This indicates some of the flood tidal prism apparently enters the pass landward of the jetty range, while all the ebb discharge passes through both ranges 1 and 2. Thus, the effective cross-sectional area of range 2,  $A_{c2}$  was obtained for ebb flow only:

$$Q_{\text{ebb}} = A_{c2} \sum_{n=1}^3 \int V_{2n} dt = A_{c1} \sum_{n=1}^3 \int V_{1n} dt \quad (10)$$

where

$Q_{\text{ebb}}$  = instantaneous ebb tidal discharge

$A_{c1}$  = cross-sectional area of range 1

$\int V_{2n} dt$  = area under velocity-time ebb curve for one of the current meters (numbered 1 to 3) on range 2

$\int V_{1n} dt$  = area under velocity-time ebb curve for one of the current meters on range 1

or

$$A_{c2} = A_{c1} \frac{\sum_{n=1}^3 \int V_{2n} dt}{\sum_{n=1}^3 \int V_{1n} dt} \quad (11)$$

Averaging values for each of the ebb prisms gave an effective area of 35,250 square feet, which was then used to obtain corrected discharges through range 2. Tables 12 and 13 show the discharges and phase predominance for the four ranges for flood and ebb phases between 18 and 23 July 1962.

Table 12. Discharges through Sabine Pass ranges, 18-23 July 1962.

Date	Tidal phase	Discharge by range locations (ft <sup>3</sup> x 10 <sup>8</sup> )			
		Range 1 (entrance)	Range 2 (pass)	Range 3 (lake entrance)	Range 4 (canal)
18 July	Flood	+18.91	+25.00	----- <sup>1</sup>	-----
	Ebb	-0.76	-1.68	-----	-----
	Flood	+3.41	+2.43	-----	-----
18-29 July	Ebb	-29.70	-33.00	-----	-13.30
19 July	Flood	+11.70	+24.10	-----	+10.70
	Ebb	-1.72	-0.45	-3.10	+4.10
	Flood <sup>2</sup>	+4.70	+9.50	+5.60	+7.00
19-20 July	Ebb <sup>2</sup>	-30.50	-27.50	-18.30	-10.20
20 July	Flood <sup>2</sup>	+20.20	+22.50	+15.40	+8.70
	Ebb	-----	-1.34	-2.42	+3.40
	Flood <sup>2</sup>	+4.54	+5.54	+2.80	+3.40
20-21 July	Ebb <sup>2</sup>	-28.70	-25.10	-15.70	-11.00
21 July	Flood <sup>2</sup>	+18.00	+16.40	+10.00	+5.50
	Ebb	-3.74	-4.69	-----	+6.56
	Flood	+6.98	+8.18	-----	-----
21-22 July	Ebb	-21.90	-19.40	-----	-7.56
22 July	Flood	+14.80	+14.70	-----	+5.90
	Ebb	-9.00	8.90	-----	-1.73
	Flood	+6.70	+7.50	-----	+3.85
23 July	Ebb	-10.40	-11.50	-----	-1.75
	$\Sigma Q_E$	$136 \times 10^8$	$134 \times 10^8$	-----	-----
	$\Sigma Q_F$	$110 \times 10^8$	$136 \times 10^8$	-----	-----
	$Q_E/Q_F$	1.24	0.98	1.17	0.58

<sup>1</sup>No data available.<sup>2</sup>Data used to compare pass discharge with sum of canal and lake discharges.

Table 13. Tidal prisms through Sabine Pass, 18-23 July 1962.

Depth of limits of section	$\Sigma Q_{Flood}$ (ft <sup>3</sup> x 10 <sup>9</sup> )	$\Sigma Q_{Ebb}$ (ft <sup>3</sup> x 10 <sup>9</sup> )	$\frac{\Sigma Q_{Ebb}}{\Sigma Q_{Flood}}$
Surface to 11.6 feet	4.76	6.66	1.4
11.6 to 23.4 feet	4.83	4.22	0.87
23.4 feet to bottom	4.01	2.47	0.62

As mentioned previously, ebb discharges predominate between the gulfward jetty ends at range 1. Thus, about 24 percent of the flood prism enters the inlet through the small-boat passes and perhaps the jetty stones. On ebb flow, the channel through the barrier island and the jetties confine the flow, and all the ebb prism passes through range 1. This ebb flow predominance promotes self-maintenance of the jetty channel, keeping shoaling rates below what they would be if the flow were balanced.

Flood and ebb flows at range 2 were evenly balanced, since river discharge was far below normal during the measurement period. Nonetheless, its effect on flow distribution in the pass can be determined by comparing the discharges through each vertical section of this range. Table 13 shows that ebb flows predominate in the usually fresher upper layer, while floodflows predominate in the denser bottom layer. Temperature, salinity, and current data taken in 1974-75 more clearly illustrate this condition (Ward and Johnston, 1977).

At range 4 (Port Arthur canal entrance), peculiar circulation patterns develop. Note that on 19, 20, and 21 July 1962, while certain ebb flows were occurring at all other ranges, floodflow was passing through this range. As a result, flood discharges predominated by about 1.7:1. This also is evident in Figure 77 which shows that water flowed into the canal while it flowed out of the lake and pass.

At range 3 (Sabine Lake entrance), ebb flows predominate for two reasons: First, freshwater from Sabine and Neches Rivers exits here. Second, floodflow predominance through the Port Arthur Canal must also leave Sabine Lake (i.e., there is a net clockwise circulation through the canal and lake).

During the simultaneous measurements at all four locations (19 to 21 July), the accuracy of the discharge calculations was checked by summing the values from ranges 3 and 4 and comparing them to those of range 2. For the six tidal phases in which the flow directions were always in agreement (footnote 2 values in Table 12) the average difference was only 7 percent and in all but one case the sum of the two channels exceeded the pass discharge. This small error adds confidence to the estimate of the effective cross-sectional area of range 2 determined earlier in this report.

An attempt was made to verify the tidal discharges by calculating the tidal prism as the product of bay area and bay tidal range. However, the only bay tide data were from the Port Arthur SWG gage, and these data were not compatible with discharges through Sabine Pass, since the canal receives water (i.e., floods) during parts of ebb flow in the pass.

Rathbun and Goodwin's (1976) data reported in Ward and Johnston (1977) are plotted in Figures 78 to 81. Note the same pattern exhibited in the 1962 data: floodflow into Port Arthur canal, ebb flows from Sabine Lake. The two measurement periods (1974 and 1975) were during diurnal tides; the 1962 discharges were semidiurnal. Therefore, the more recent average tidal cycle discharges are about twice those of 1962 (Table 14).

d. Theoretical Stability Analysis. O'Brien and Dean's (1972) stability method was again used to predict the response of this jettied entrance to sedimentation. The 1973 tide data indicated that the Sabine Lake tidal range was about 0.41 the jetty range which, from Figure 37, yields a K value

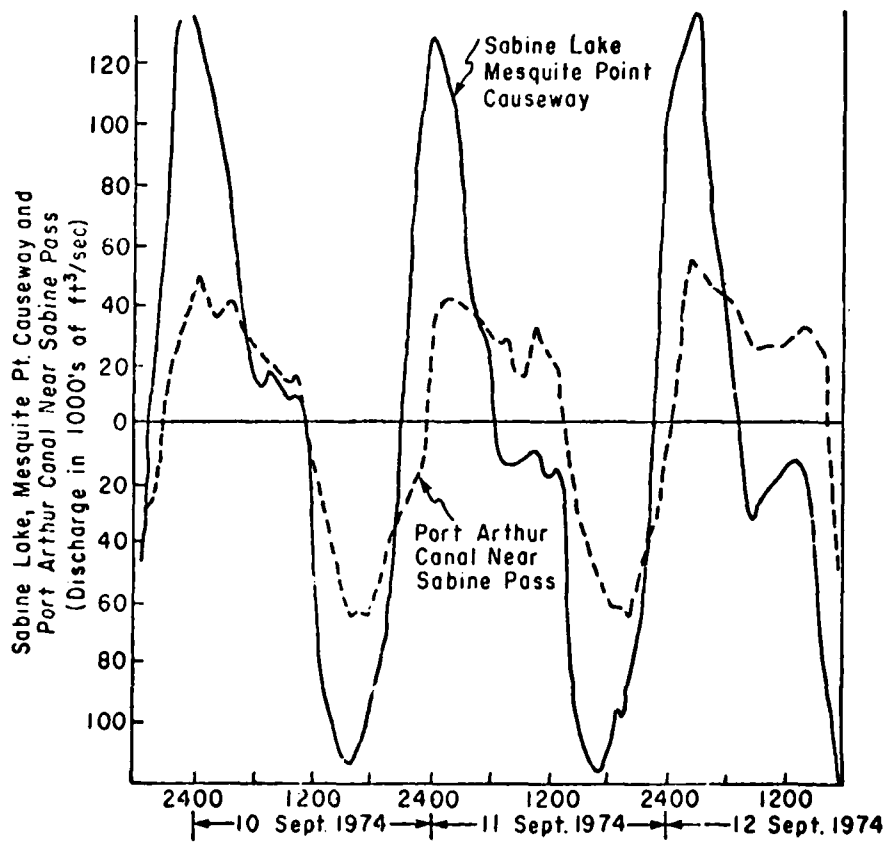


Figure 78. Sabine Pass discharges, 10-12 September 1974  
(after Ward and Johnston, 1977).

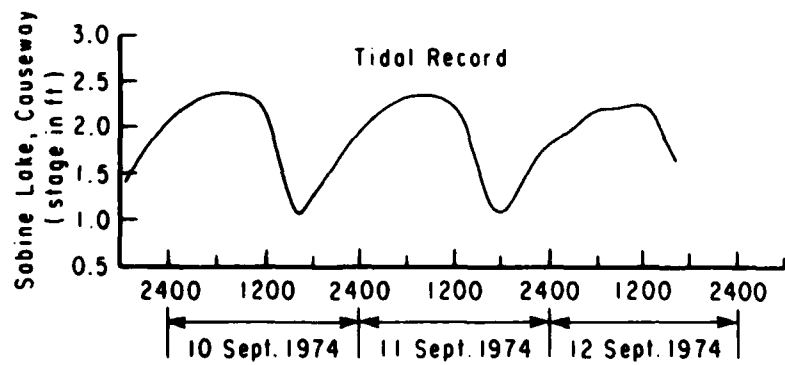


Figure 79. Sabine Pass stage, 10-12 September 1974  
(after Ward and Johnston, 1977).

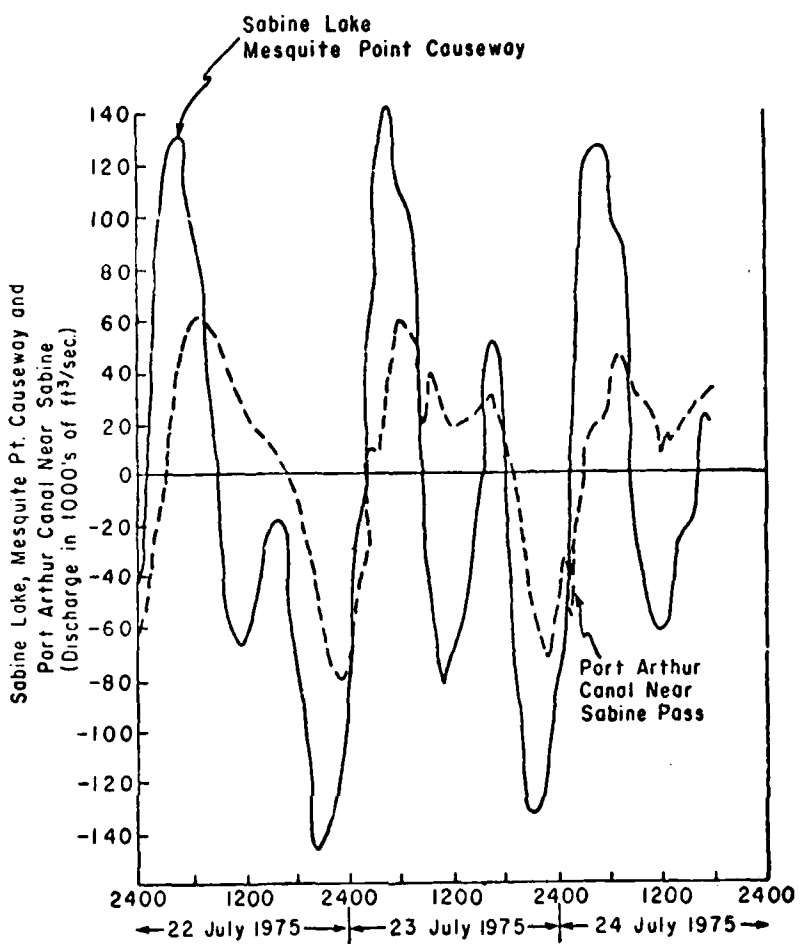


Figure 80. Sabine Pass discharges, 22-24 July 1975  
(after Ward and Johnston, 1977).

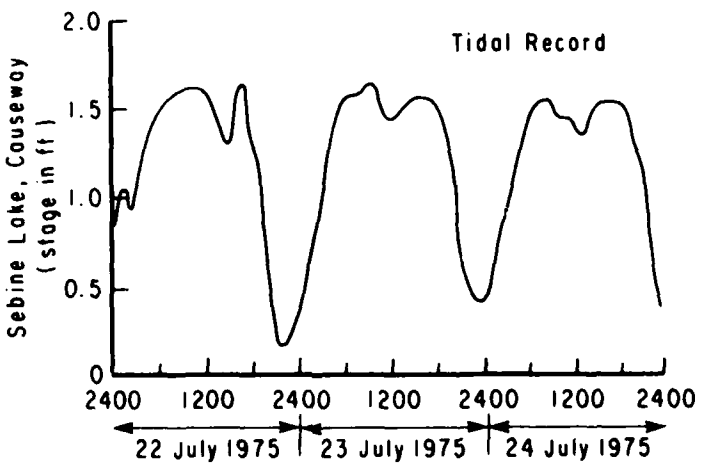


Figure 81. Sabine Pass stage, 22-24 July 1975  
(after Ward and Johnston, 1977).

Table 14. Tidal prisms at Sabine Lake and Port Arthur Canal entrances.

Date	Tidal phase	Tidal prism ( $\text{ft}^3 \times 10^8$ )	
		Lake entrance	Canal
1974			
10 Sept.	Flood	3.53	1.71
	Ebb	2.74	1.74
10-11 Sept.	Flood	2.55	1.44
11 Sept.	Ebb	3.36	1.68
11-12, Sept.	Flood	2.65	1.88
1975			
22 July	Flood	2.69	1.74
22-23 July	Ebb	4.40	1.60
23 July	Flood	2.35	1.74
	Ebb	1.18	----
	Flood	0.53	----
23-24 July	Ebb	2.52	1.18
24 July	Flood	2.46	----
	Ebb	1.00	----
	$\bar{Q}_F$	2.79	1.70
	$\bar{Q}_E$	3.55	1.55

of 0.44. For Sabine Pass, the most difficult parameter to determine was the friction factor,  $f$ . Substituting the values listed below into equation (1) gave an  $f$  value of 0.0145 ( $n = 0.018$ ), which is considerably lower than the previously assumed value of 0.025 but may be realistic due to the mud bottom at Sabine.

$$A_c = 35,250 \text{ square feet}$$

$$A_b = 2.6 \times 10^9 \text{ square feet}$$

$$L = 43,000 \text{ feet}$$

$$R = 17.6 \text{ feet}$$

$$T = 89,000 \text{ seconds}$$

Letting the minimum inlet width remain constant (i.e., letting  $R$  vary directly with  $A_c$ ), values of maximum average velocity and cross-sectional area are plotted in Figure 82 for various deposition lengths. Note that the 1962 area and velocity plot very close to the locus of critical  $A_c$ 's for a deposition length about three-fourths the actual length, and that  $\bar{V}_{\max}$  is about 3 feet per second at the critical area.

Comparing Sabine Pass to Jarrett's (1976) stability relationship for other dual-jettied inlets,  $A_c = 3.76 \times 10^{-4} P$ , the predicted equilibrium area is 26,917 square feet. This equilibrium area is probably close to that of the original unjettied entrance, but less than the present area and the critical

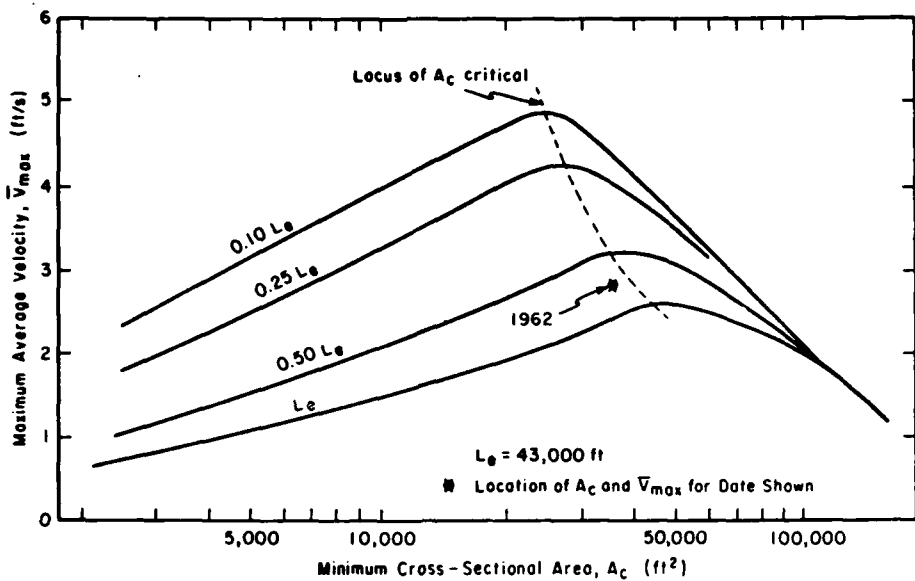


Figure 82.  $\bar{V}_{\max}$  versus  $A_c$  stability curves, Sabine Pass, Texas.

area predicted by Figure 82. Thus, O'Brien and Dean's (1972) method shows Sabine to be near equilibrium; Jarrett's (1976) method indicates that the channel should be shoaling.

e. Summary. Sabine Pass is an anomalous inlet compared to the other inlets in the study area. Sediments in the inlet and on the adjacent beaches are very fine silts and mud; freshwater outflow affects the vertical distribution of flood and ebb currents and may produce density currents which influence depositional patterns. Although the Sabine and Neches Rivers probably transport sand-sized material to their mouths, Sabine Lake acts as a filter and prevents this sediment from reaching gulf beaches. Even with this difference in sediment, changes following jetty construction followed the same pattern as at Galveston: downdrift deposition offshore and in the fillet, with erosion in between, and updrift deposition. Unfortunately, the lack of sufficient survey data precluded analysis of changes in the cross-sectional area at Sabine Pass. However, it appears that construction of the jetties with small-boat passes has increased the natural scouring capacity of tidal currents by establishing an ebb flow predominance between the jetties. This scouring is particularly accentuated during the passage of northerns, when instantaneous discharges three times those of normal diurnal tides produce ebb currents in excess of 6 feet per second (Ward and Chambers, 1978).

#### IV. SUMMARY

##### 1. Tide Characteristics.

Tide data from a number of SWG and NOS gages throughout the upper Texas coast revealed the following characteristics:

- (a) Long-term variability in monthly mean tidal range and water level is uniform throughout the area, with two maximums and two minimums per year. Annual variability in range is small (16 percent),

but mean monthly water levels can vary by as much as 0.9 foot during the year as a result of astronomical and meteorological influences. The variability of the predicted tidal range is less than that actually measured.

(b) Mean monthly range variability in 1974 was greater than normal (about 25 percent), and mean monthly levels varied as much as 1.4 feet. Thus, considerable variation in tidal prisms can be expected, which impacts not only on the natural scouring capacity of the inlets, but also on the exchange rate of gulf and bay waters.

(c) Hicks (1972) showed that the trend in sea level rise between 1940 and 1970 at Galveston was 0.014 foot per year. This rate is less than that shown in Figure 8 for 1900 to 1970 (about 0.018 foot per year), and an order of magnitude less than the post-1970 rates of as much as 0.15 foot per year at Freeport and Galveston. The annual mean water levels at Freeport and Galveston should be monitored to determine whether these present trends continue. Continuation of the SWG tide gage network is also recommended to document localized trends in interior waters.

(d) In the mid-1970's mean annual tidal ranges have been at a minimum in the 19-year cycle (Fig. 9). However, ranges within the following decade will increase about 20 percent, reaching a maximum between about 1986 and 1988. If the mean annual water level remains at the 1975 value, by 1986 bay tides will penetrate to areas which are as much as 1 foot above high water values in 1970. More importantly, if the present trend in sea level rise continues, this penetration between 1986 and 1988 could reach areas that are more than 2.5 feet above 1970 high waters.

## 2. Freeport Entrance.

a. Bathymetric Changes. Since 1946, the areas offshore of Freeport (Figs. 12 and 13) have generally been eroding (Seelig and Sorensen, 1973; Morton, 1977). Most of the downdrift offshore change to the west is attributed to erosion of the former Brazos River delta. Between 1960 and 1975, shoreline recession on the east side of the entrance occurred at about twice the rate as on the west side. This difference may have resulted from the protection afforded the west side by the relic delta and by the wave shadow zone created by the jetties. However, the actual causes of this erosion are difficult to determine due to the lack of definitive process data.

b. Tides and Hydraulics. Lack of prototype data also hindered analysis of the Freeport entrance hydraulics. In the absence of current measurements, the long-wave equation is assumed to be the most applicable model for prediction of entrance channel currents. However, a harbor resonance model shows that amplification of long wave amplitudes in the harbor and currents in the entrance channel will be reduced if the harbor is expanded as planned.

c. Stability. The offshore part of the Freeport navigation channel is plagued with rapid sedimentation, particularly between 3,000 and 4,000 feet gulfward of the jetty ends. Between the jetties, currents are apparently too weak to scour the bottom, and deposition also occurs. In view of the lack of

buildup of dredged disposal material in the offshore dumping zone, and the low rate of offshore erosion versus annual dredging rates (600,000 versus 1,450,000 cubic yards per year, respectively), further studies are required to determine the major source of channel deposits. Consideration should also be given to monitoring the current flow and circulation in Freeport Harbor, particularly the effects of cooling water withdrawal by Dow Chemical Company.

### 3. San Luis Pass.

a. Bathymetric Changes. The present site of San Luis Pass has been open since at least 1834. This equilibrium condition is exemplified by the fact that only minor changes in sediment volumes occurred on the ebb and flood tidal deltas between 1853 and 1933. However, the inlet cross-sectional area and width have generally been increasing since 1853, which agrees with O'Brien and Dean's (1972) theoretical stability analysis indicating San Luis Pass to be on the unstable side of the critical cross-sectional area.

The shoulders of the inlet (within the influence of the ebb tidal delta) show frequent short-term changes, but the present trend is one of accretion on the west shoulder and erosion on the east. The deepest part of the inlet throat has always been on the west (downdrift) side; the outer part of the channel has usually been oriented at about 90° to the shoreline trend.

Both the ebb and flood tidal deltas contain sufficiently large volumes of sand to serve as beach nourishment borrow areas. Dredging of material from the relatively protected landward edge of an east coast ebb tidal delta has been accomplished in recent years by the U.S. Army Engineer Division, South Atlantic. Similar operations are feasible at San Luis Pass, but sand samples should be obtained from throughout the inlet complex to determine the locations of optimally sized sediment.

b. Tides and Hydraulics. Tides at the San Luis Pass bridge, although in phase with those at the Galveston Pleasure Pier, exhibit only about 75 percent of the pier's range. Bay tidal ranges are slightly more than 50 percent of the bridge range and show greater than expected phase lags. The average tidal prism was  $1.65 \times 10^9$  cubic feet, and it was found that computations of the prism using the bay tidal range and bay area relationship given by equation (6) agreed well with the discharge method. Measured mean currents through the inlet throat were about 2 feet per second, although higher currents will occur during diurnal tides. Slight increases in the tidal prism will occur in future years if the predictions of increased inlet cross-sectional area and maximum velocity are correct.

### 4. Galveston Bay Entrance.

a. Bathymetric Changes. Extensive changes to adjacent beaches and the entrance channel have occurred since construction of the Galveston entrance jetties. On the updrift side, sediment has been depositing at a relatively constant rate of about 430,000 cubic yards per year. On the downdrift (south) side, an adjustment of the ebb tidal delta to the altered wave and current conditions resulted in a tripartite pattern of deposition offshore and in the fillet, and erosion between these zones; this pattern was apparently completed by 1933. Subsequent changes to the south side have been minor, although the shoreline slowly moved gulfward between 1933 and 1965. The minimum width of

the entrance has remained relatively constant since 1850 at about 9,500 feet, but the cross-sectional area and hydraulic radius have increased from 13,000 to 19,000 feet and 14 to 21 feet, respectively.

As at San Luis Pass, the large deposition volumes at Galveston could be used for beach nourishment, particularly the southwest fillet and the adjacent spit extending eastward into the channel. Located only a few miles from the Galveston Beach groin field, the sand has little functional importance in its present state, and it is probably the most economical borrow site, both in terms of grain-size characteristics and transportation costs.

b. Tides and Hydraulics. Tidal ranges in Galveston Bay increased about 12 percent between 1936 and 1974, and are presently about 0.56 that of the Galveston Pleasure Pier. This increase is considerably less than might be expected, based on the observed 25-percent increase in minimum cross-sectional area. The average diurnal tidal prism is about  $11 \times 10^9$  cubic feet, but ebb discharges during northerns were more than three times as great and must contribute significantly to natural maintenance of the channel.

#### 5. Rollover Pass.

The history of this small manmade inlet offers an object lesson in proper inlet design considerations. First, numerical or physical model studies of proposed plans should be performed to determine the effects of any inlet on the bay system, and to predict the flow characteristics through the inlet. Creation of Rollover Pass increased the East Bay tidal ranges by about 10 percent and currents were extremely rapid, due to initially low frictional resistance. Subsequent installation of a weir and growth of a flood tidal delta increased friction to a Manning's *n* value of 0.032. Second, inlet stability should be assessed: Will the planned inlet be unstable, i.e., in scour or deposition modes, or will it be in harmony with the local tide and wave regimes? Third, inlets typically act as sediment sinks, removing material from the longshore transport regime through development of fillets and ebb and flood tidal deltas. Removal of this material and the resulting deficit in available littoral material typically produces downdrift beach erosion. At Rollover Pass, the excess volume removed from the beaches was almost exactly equal to the volume deposited in the inlet.

#### 6. Sabine Pass.

a. Bathymetric Changes. Although the material comprising the present nearshore and channel bottoms is much finer than that of other Texas coast inlets, Sabine Pass postconstruction bathymetric changes closely parallel those at Galveston--updrift, deposition in a fillet with offshore erosion; downdrift, a tripartite pattern of deposition-erosion-deposition (Fig. 73). Lack of sufficient survey data precludes calculation of the total amounts of material which accumulated near the pass, but within the data limits there was a net accretion of 900,000 cubic yards on the updrift side and 2 million cubic yards on the downdrift side between 1885 and 1974.

b. Tides and Hydraulics. Available tide data indicate that the annual mean bay tidal range has remained constant at about 50 percent of the pass range since 1936, although the pattern of seasonal variability in range differs greatly. The mean pass range between 1960 and 1975 was 1.85 feet. Ebb flows predominate between the jetties (1.24:1, ebb:flood) due to freshwater

discharge from the Sabine and Neches Rivers, and from the fact that apparently the jetties are quite porous, allowing relatively uniform inflow of flood-tides but constraining the ebb discharge to the channel. A discharge imbalance also prevails in the Port Arthur Canal, where floodflows predominate (1.7:1, flood:ebb), which may produce increased deposition in this part of the system. Net ebb flows also predominate at the Sabine Lake entrance; the excess flood discharge from the system into the canal must exit here.

c. Stability. The necessity for continued dredging of Sabine Pass indicates that the entrance is unstable. However, the stability is undoubtedly enhanced by frequent strong ebb discharges which occur during the passage of winter frontal systems. O'Brien and Dean's (1972) stability analysis revealed that the 1962 channel dimensions were only slightly less than the critical cross-sectional area required for stability. Therefore, maximum natural maintenance of the channel is probably being achieved.

AD-A101 902

COASTAL ENGINEERING RESEARCH CENTER FORT BELVOIR VA  
HYDRAULICS AND STABILITY OF FIVE TEXAS INLETS. (U)  
JAN 81 C MASON  
CERC-MR-81-1

F/6 8/8

UNCLASSIFIED

NL

2  
2  
4-C-090

END  
DATE FILMED  
8-81  
DTIC

#### LITERATURE CITED

BEHRENS, E.W., WATSON, R.L., and MASON, C., "Hydraulics and Dynamics of New Corpus Christi Pass, Texas: A Case History, 1972-73," GITI Report 8, U.S. Army, Corps of Engineers, Coastal Engineering Research Center, Fort Belvoir, Va., and U.S. Army Engineer Waterways Experiment Station, Vicksburg, Miss., Jan. 1977.

BLACKMAN, B., "Report of Jetties," U.S. Army, Corps of Engineers, Beach Erosion Board, Washington, D.C., unpublished, 1938.

DEAN, R.G., and WALTON, T.L., Jr., "Sediment Transport Processes in the Vicinity of Inlets with Special Reference to Sand Trapping," *Proceedings of the Second Estuarine Research Conference*, 1973.

ESCOFFIER, F.F., "The Stability of Tidal Inlets," *Shore and Beach*, 1940, pp. 114 and 115.

GALVIN, C.J., "Wave Climate and Coastal Processes," *The Water Environment and Human Needs*, Massachusetts Institute of Technology, Department of Civil Engineering, Boston, Mass., 1971, pp. 44-78.

HAYES, M.O., GOLDSMITH, V., and HOBBS, C.W., "Offset Coastal Inlets," *Proceedings of the 12th Coastal Engineering Conference*, American Society of Civil Engineers, Vol. 2, 1970, pp. 1187-1200.

HERBICH, J.B., and HALES, Z.L., "Remote Sensing Techniques Used in Determining Changes in Coastlines," Technical Report RSC-16, COE-134, Texas A&M University, College Station, Tex., 1970.

HICKS, S.D., "On the Classification and Trends of Long Period Sea Level Series," *Shore and Beach*, 1972, pp. 20-23.

IPPEN, A.T., and GODA, Y., "Wave-Induced Oscillations in Harbors, the Solution for a Rectangular Harbor Connected to the Open Sea," Report R63-36, Massachusetts Institute of Technology, Department of Civil Engineering, Boston, Mass., 1963.

JARRETT, J.T., "Tidal Prism-Inlet Area Relationships," GITI Report 3, U.S. Army, Corps of Engineers, Coastal Engineering Research Center, Fort Belvoir, Va., and U.S. Army Engineer Waterways Experiment Station, Vicksburg, Miss., Feb. 1976.

JOHNSTON, W.A., and WARD, G.R., *Galveston Bay Comprehensive Inflow/Exchange Survey Data Report*, Espey, Huston, & Associates, Inc., Austin, Tex., 1976.

KEULEGAN, G.H., "Tidal Flow in Entrances Water-Level Fluctuations of Basins in Communication with Seas," Technical Bulletin 14, U.S. Army, Committee on Tidal Hydraulics, Vicksburg, Miss., 1967.

LEE, H.T., "Passes of the Texas Coast," Internal Report, Texas Parks and Wildlife Department, unpublished, 1966.

LOCKWOOD, ANDREWS, and NEWNAM, INC., "Localized Erosion at Rollover Fish Pass, Bolivar Peninsula, Texas," Houston, Tex., 1974.

MARMER, H.A., "Tidal Datum Planes," Special Publication No. 135, U.S. Coast and Geodetic Survey, Washington, D.C., 1951.

MATHEWSON, C.C., and MINTER, L.L., "Impact of Water Resource Development on Coastal Erosion, Brazos River, Texas," TR-77, Texas Water Resource Institute, Texas A&M University, College Station, Tex., 1976.

MORTON, R.A., "Shoreline Changes Between Sabine Pass and Bolivar Roads," Circular 75-6, Bureau of Economic Geology, University of Texas, Austin, Tex., 1975.

MORTON, R.A., "Nearshore Changes at Jettied Inlets, Texas Coast," *Proceedings of Coastal Sediments '77*, American Society of Civil Engineers, New York, 1977.

O'BRIEN, M.P., and DEAN, R.G., "Hydraulics and Sedimentary Stability of Coastal Inlets," *Proceedings of the 13th Coastal Engineering Conference*, Vancouver, British Columbia, 1972, pp. 761-780.

PRATHER, S.H., and SORENSEN, R.M., "An Investigation of Rollover Pass, Bolivar Peninsula, Texas," Sea Grant Publication No. TAMU-SG-72-202, Texas A&M University, College Station, Tex., 1972.

PRICE, W.A., "Equilibrium of Form and Forces in Tidal Basins of Coasts of Texas and Louisiana," *Bulletin of the American Association of Petroleum Geologists*, Vol. 31, No. 9, Sept. 1947, pp. 1619-1663.

PRICE, W.A., "Reduction of Maintenance by Proper Orientation of Ship Channels Through Tidal Inlets," *Proceedings of the Second Coastal Engineering Conference*, Council on Wave Research, Houston, Tex., Nov. 1951, pp. 243-255.

PRICE, W.A., "Patterns of Flow and Channeling in Tidal Inlets," *Journal of Sedimentary Petrology*, Vol. 33, No. 2, June 1963, pp. 279-290.

RATHBUN, I.G., and GOODWIN, J.J., "Provisional Data, Sabine-Neches Inflow Studies," USGS Draft Report to Texas Water Development Board, Austin, Tex., 1976.

SEELIG, W.N., and SORENSEN, R.M., "Investigation of Shoreline Changes at Sargent Beach, Texas," Sea Grant Publication TAMU-SG-3-212, Texas A&M University, College Station, Tex., 1973.

SEELIG, W.N., HARRIS, D.L., and HERCHENRODER, B.E., "A Spatially Integrated Numerical Model of Inlet Hydraulics," GITI Report 14, U.S. Army, Corps of Engineers, Coastal Engineering Research Center, Fort Belvoir, Va., and U.S. Army Engineer Waterways Experiment Station, Vicksburg, Miss., Nov. 1977.

THOMPSON, E.F., "Wave Climate at Selected Locations Along U.S. Coasts," TR 77-1, U.S. Army, Corps of Engineers, Coastal Engineering Research Center, Fort Belvoir, Va., Jan. 1977.

U.S. ARMY, CORPS OF ENGINEERS, "Annual Report of the Chief of Engineers," Washington, D.C., 1868.

U.S. ARMY ENGINEER DISTRICT, GALVESTON, "Report on Galveston Bay, Texas, for the Reduction of Maintenance Dredging," Galveston, Tex., 1942.

U.S. ARMY ENGINEER DISTRICT, GALVESTON, "Report on Beach Erosion Control Cooperative Study of the Gulf Shore of Bolivar Peninsula, Texas," Galveston, Tex., 1958.

U.S. ARMY ENGINEER DISTRICT, GALVESTON, "Texas Coast Inlet Studies," Galveston, Tex., 1975.

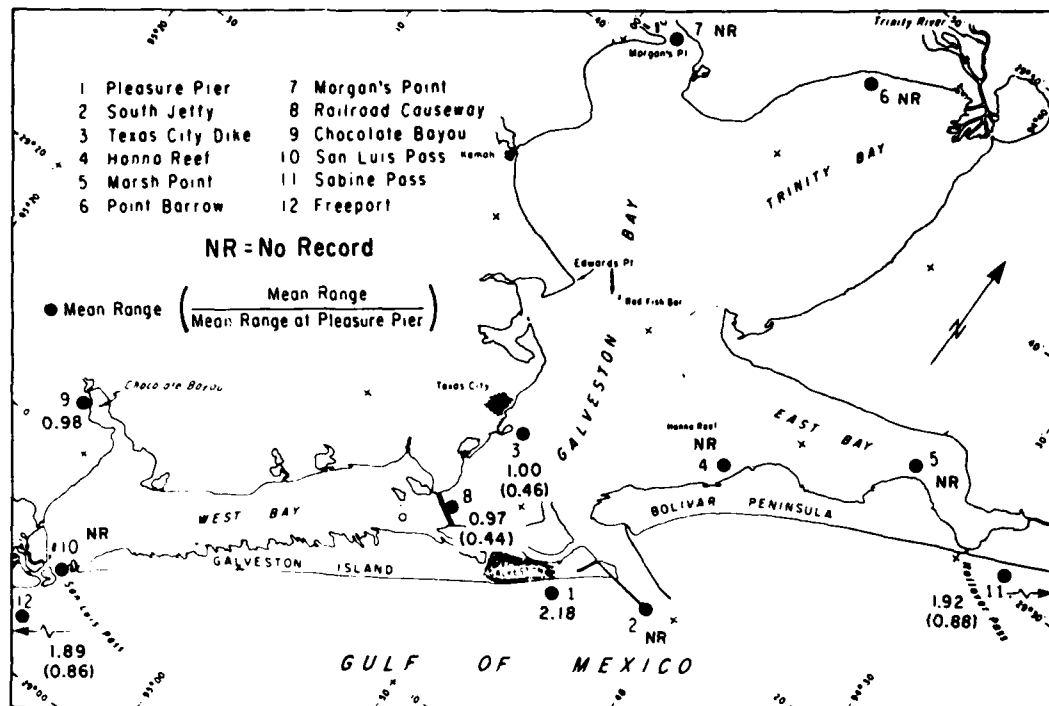
WARD, G.H., Jr., and CHAMBERS, C.L., *Meteorologically Forced Currents in Upper Sabine Pass, Texas*, Espey, Huston & Associates, Inc., Austin, Tex., 1978.

WARD, G.H., Jr., and JOHNSTON, W.A., *Hydrographic Survey of Upper Sabine Pass, Texas*, Espey, Huston & Associates, Inc., Austin, Tex., 1977.

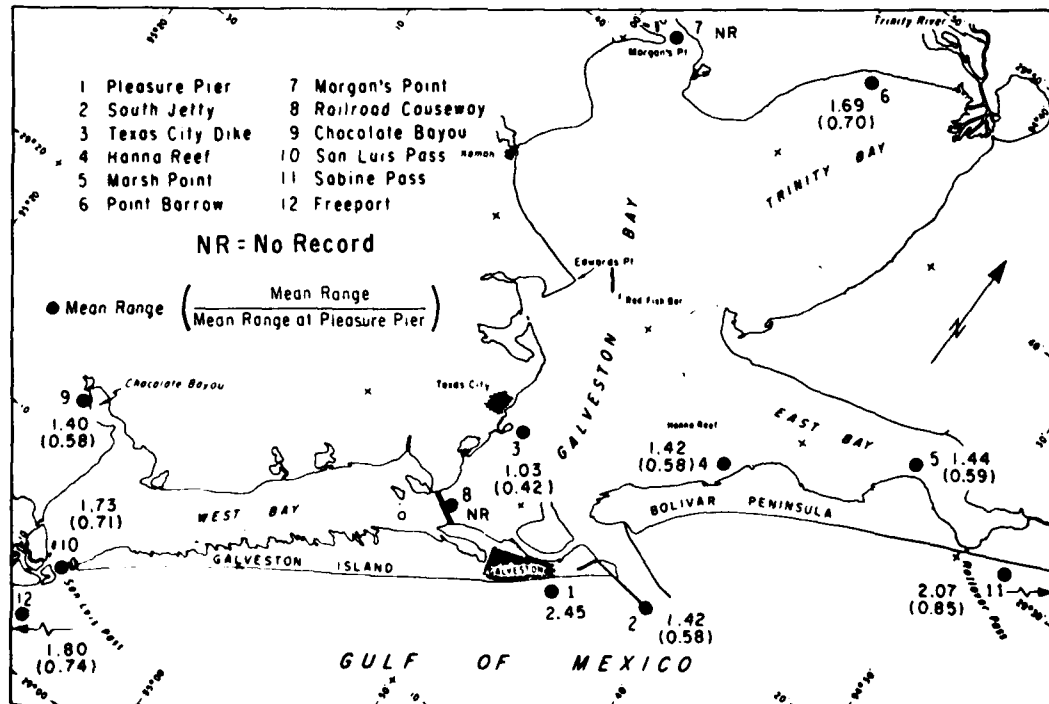
APPENDIX

MONTHLY TIDAL RANGE DISTRIBUTION,  
GALVESTON BAY, 1974

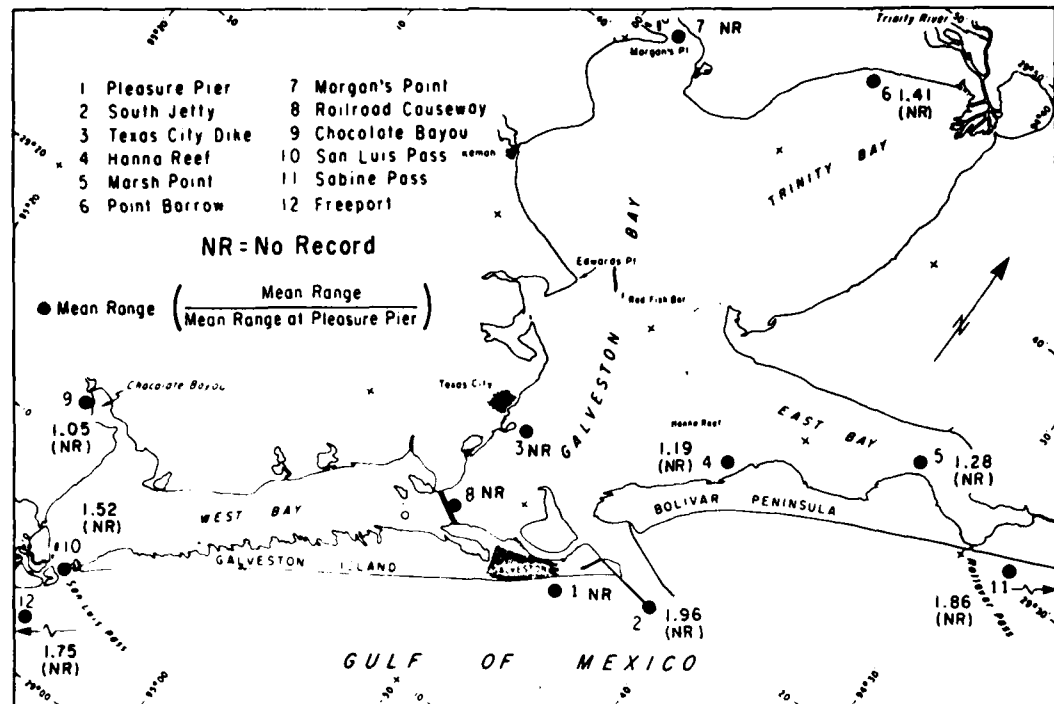
PRECEDING PAGE BLANK-NOT FILMED



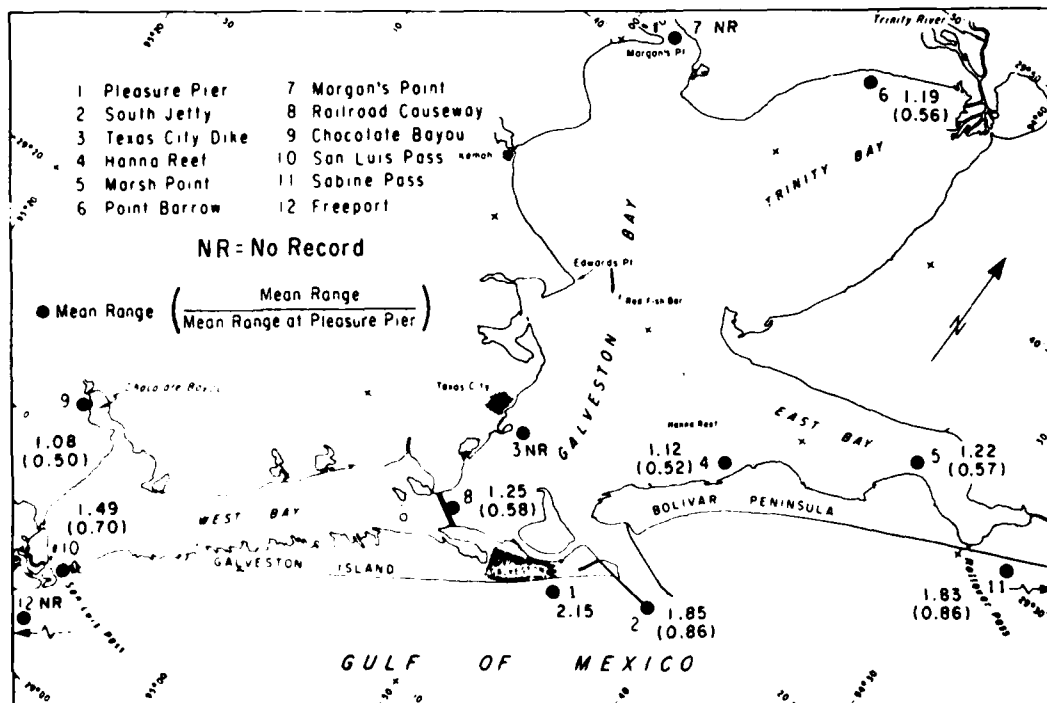
January 1974



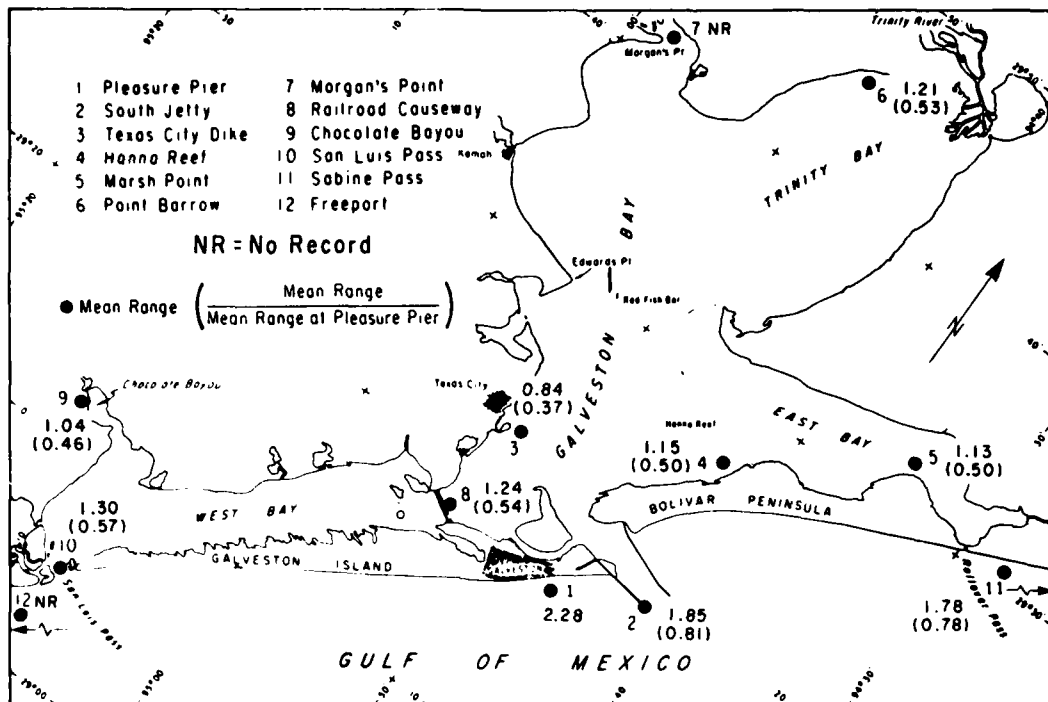
February 1974



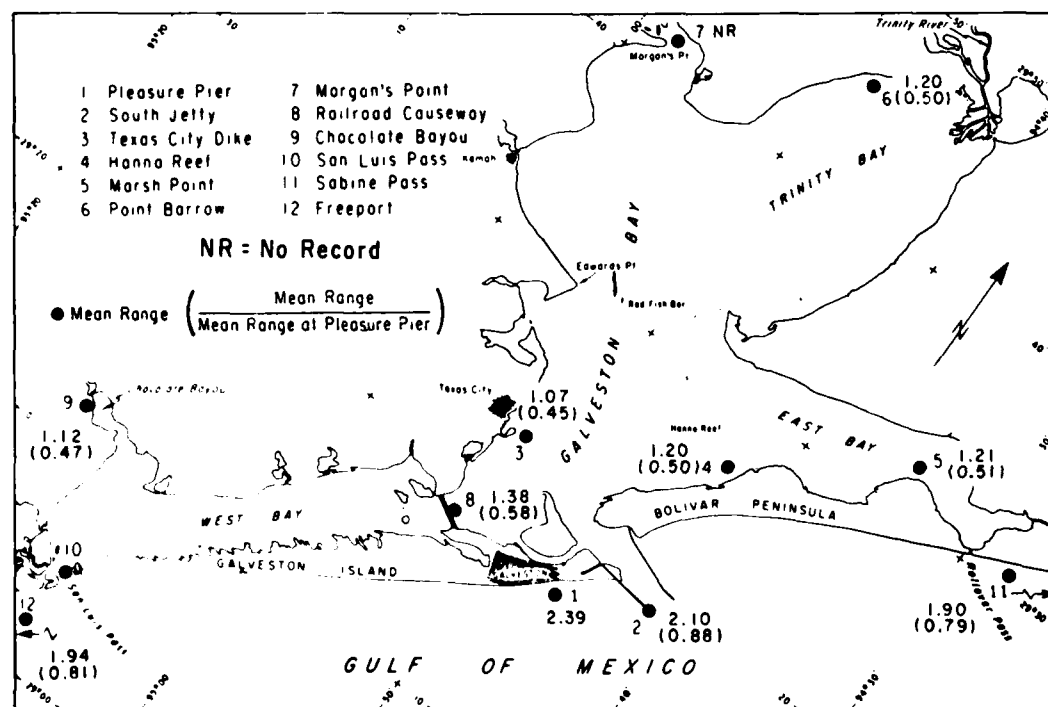
March 1974



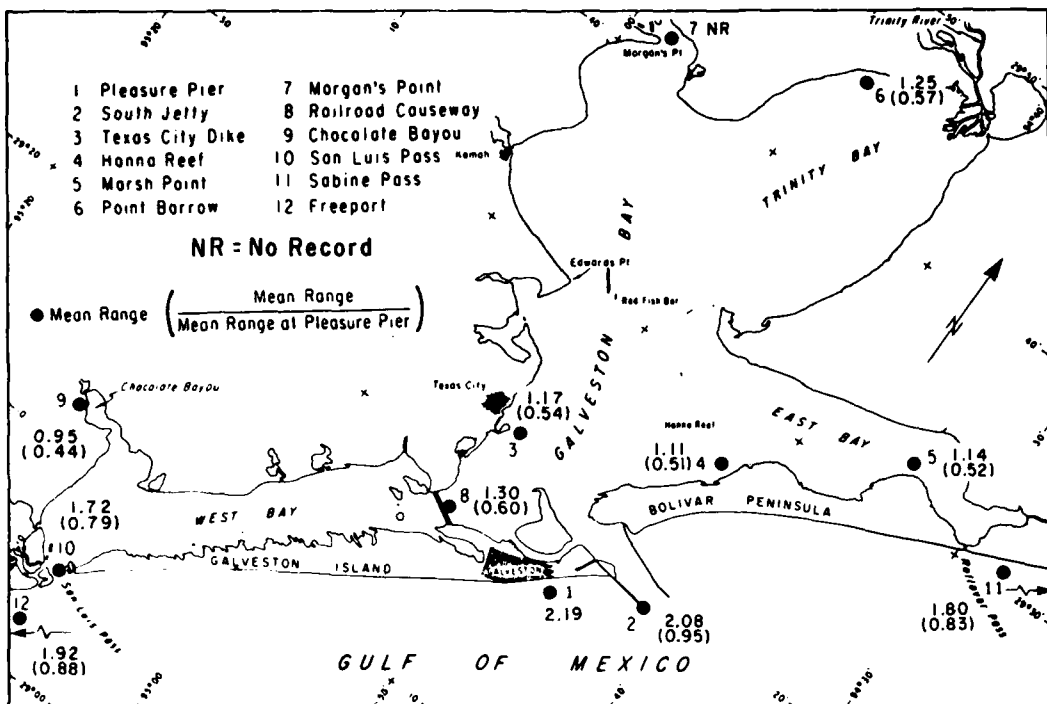
April 1974



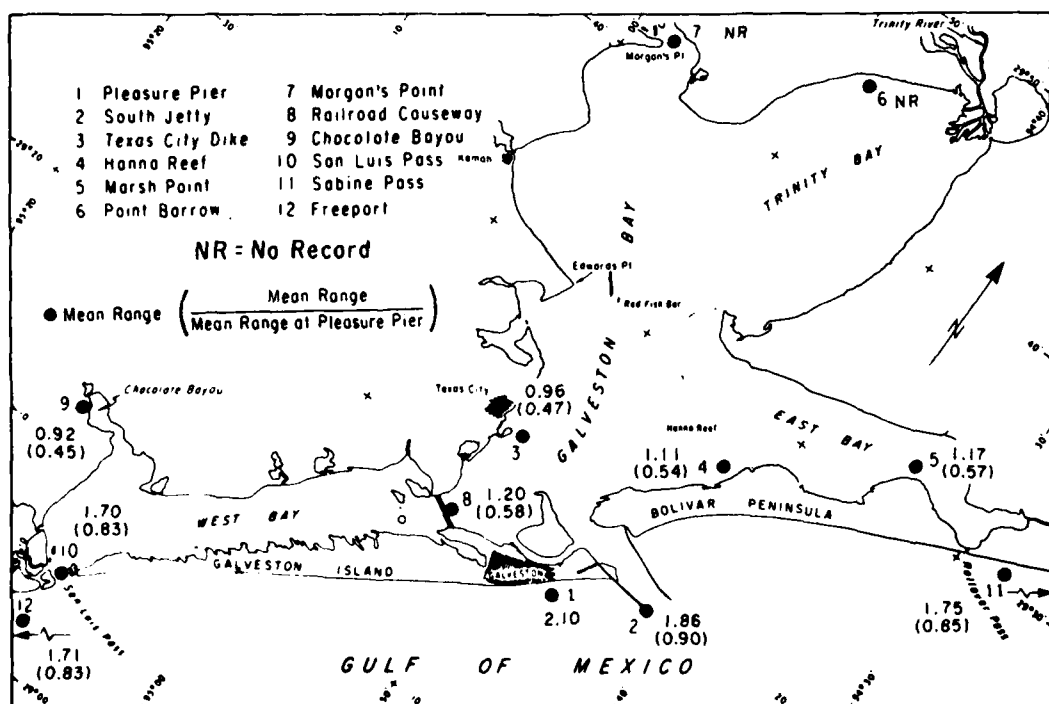
May 1974



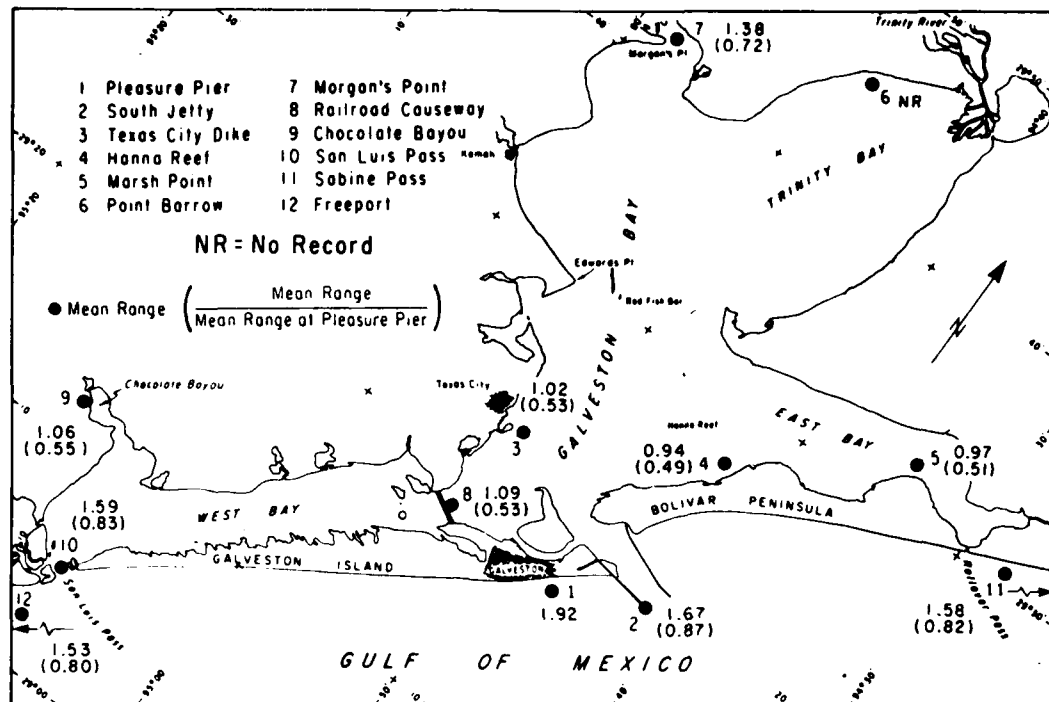
June 1974



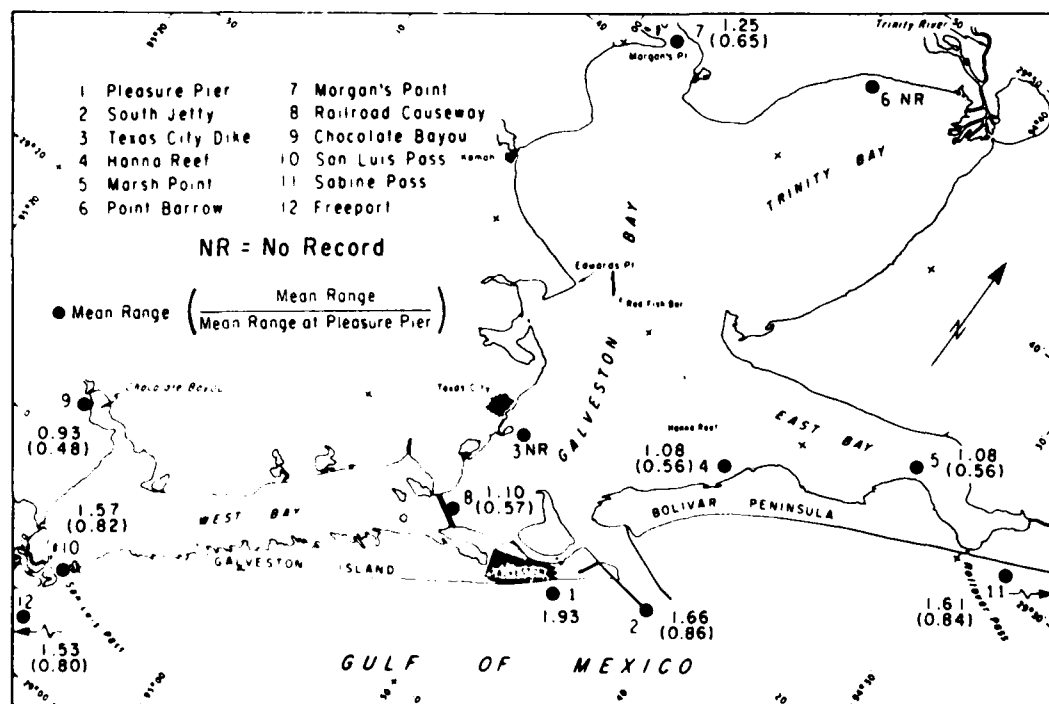
July 1974



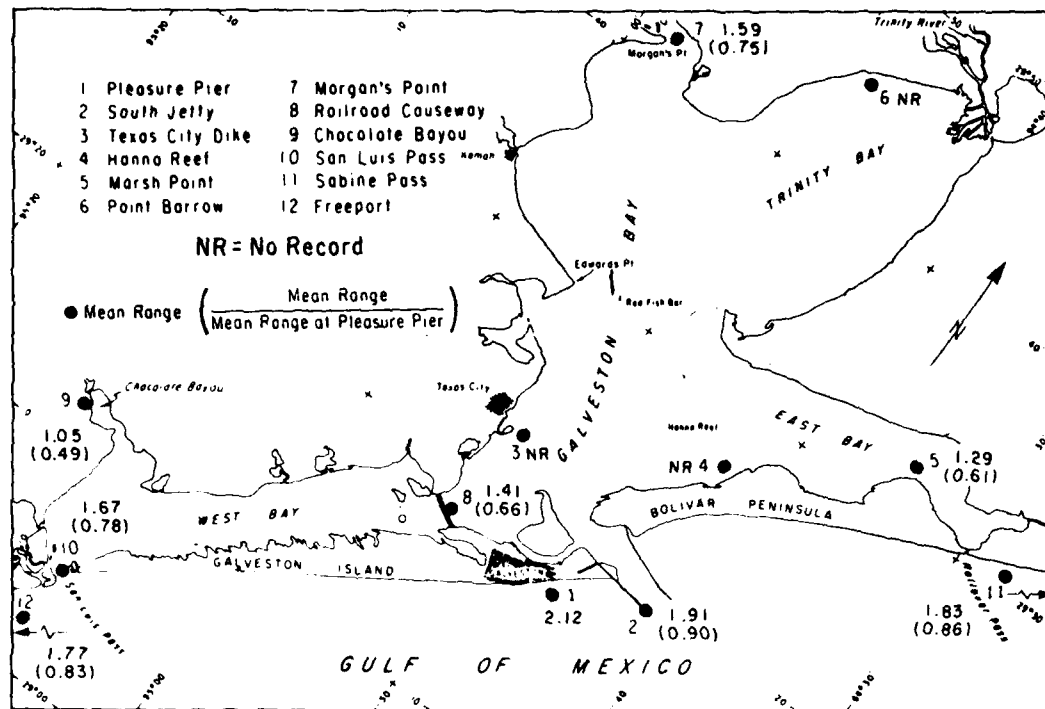
August 1974



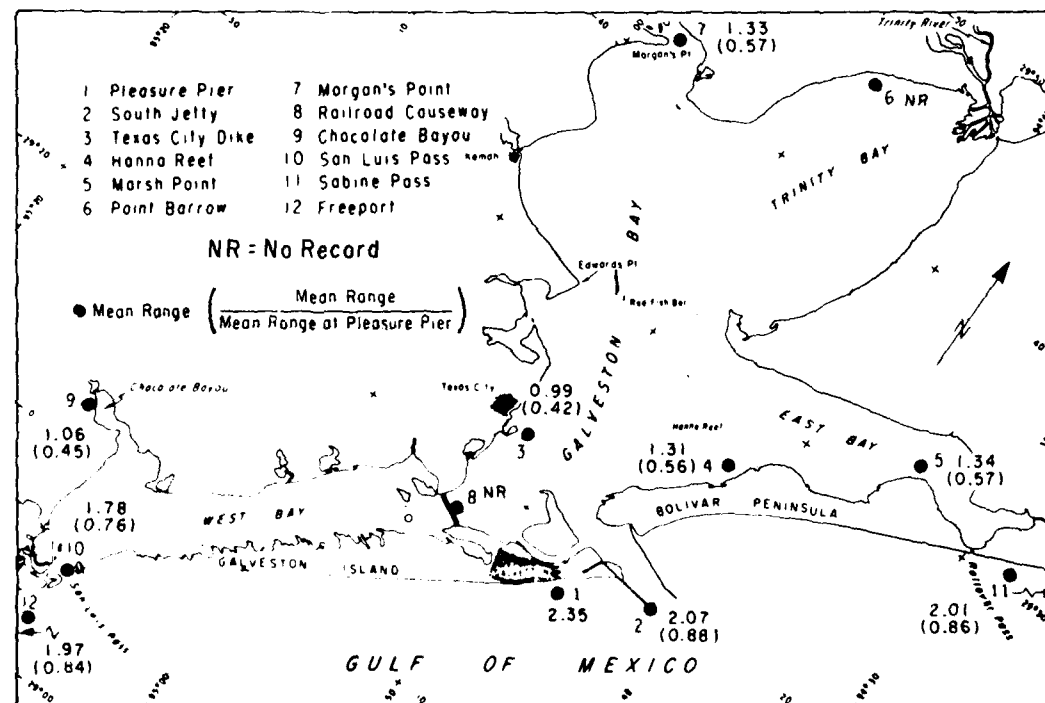
September 1974



October 1974



November 1974



December 1974

Mason, Curtis

Hydraulics and stability of five Texas inlets / by Curtis Mason. --  
Fort Belvoir, Va. : U.S. Coastal Engineering Research Center ;  
Springfield, Va. : available from National Technical Information  
Service, 1981.  
[105] p. ill. : 27 cm. -- (Miscellaneous report -- U.S. Coastal  
Engineering Research Center ; no. 81-1)  
Includes bibliographical references.  
This report provides improved planning and design information on  
the hydraulic characteristics, stability, and effect on the longshore  
transport regime and adjacent beaches of five inlet-bay systems  
(Freeport Harbor, San Luis Pass, Galveston Bay, Rollover Pass, and  
Sabine Pass) on the upper Texas coast.  
1. Hydraulics. 2. Inlets. 3. Tidal inlets. I. Title. II. Series:  
U.S. Coastal Engineering Research Center. Miscellaneous report no.  
81-1.

TC203 .U581mr no. 81-1 627

Mason, Curtis

Hydraulics and stability of five Texas inlets / by Curtis Mason. --  
Fort Belvoir, Va. : U.S. Coastal Engineering Research Center ;  
Springfield, Va. : available from National Technical Information  
Service, 1981.  
[105] p. ill. : 27 cm. -- (Miscellaneous report -- U.S. Coastal  
Engineering Research Center ; no. 81-1)  
Includes bibliographical references.  
This report provides improved planning and design information on  
the hydraulic characteristics, stability, and effect on the longshore  
transport regime and adjacent beaches of five inlet-bay systems  
(Freeport Harbor, San Luis Pass, Galveston Bay, Rollover Pass, and  
Sabine Pass) on the upper Texas coast.  
1. Hydraulics. 2. Inlets. 3. Tidal inlets. I. Title. II. Series:  
U.S. Coastal Engineering Research Center. Miscellaneous report no.  
81-1.

TC203 .U581mr no. 81-1 627

Mason, Curtis

Hydraulics and stability of five Texas inlets / by Curtis Mason. --  
Fort Belvoir, Va. : U.S. Coastal Engineering Research Center ;  
Springfield, Va. : available from National Technical Information  
Service, 1981.  
[105] p. ill. : 27 cm. -- (Miscellaneous report -- U.S. Coastal  
Engineering Research Center ; no. 81-1)  
Includes bibliographical references.  
This report provides improved planning and design information on  
the hydraulic characteristics, stability, and effect on the longshore  
transport regime and adjacent beaches of five inlet-bay systems  
(Freeport Harbor, San Luis Pass, Galveston Bay, Rollover Pass, and  
Sabine Pass) on the upper Texas coast.  
1. Hydraulics. 2. Inlets. 3. Tidal inlets. I. Title. II. Series:  
U.S. Coastal Engineering Research Center. Miscellaneous report no.  
81-1.

TC203 .U581mr no. 81-1 627

Mason, Curtis

Hydraulics and stability of five Texas inlets / by Curtis Mason. --  
Fort Belvoir, Va. : U.S. Coastal Engineering Research Center ;  
Springfield, Va. : available from National Technical Information  
Service, 1981.  
[105] p. ill. : 27 cm. -- (Miscellaneous report -- U.S. Coastal  
Engineering Research Center ; no. 81-1)  
Includes bibliographical references.  
This report provides improved planning and design information on  
the hydraulic characteristics, stability, and effect on the longshore  
transport regime and adjacent beaches of five inlet-bay systems  
(Freeport Harbor, San Luis Pass, Galveston Bay, Rollover Pass, and  
Sabine Pass) on the upper Texas coast.  
1. Hydraulics. 2. Inlets. 3. Tidal inlets. I. Title. II. Series:  
U.S. Coastal Engineering Research Center. Miscellaneous report no.  
81-1.

TC203 .U581mr no. 81-1 627